Dynamic Network Modeling for Spaceflight Logistics with Time-Expanded Networks

by

Koki Ho

B.E., Aeronautics and Astronautics, The University of Tokyo (2009)
M.E., Aeronautics and Astronautics, The University of Tokyo (2011)

Submitted to the Department of Aeronautics and Astronautics
in partial fulfillment of the requirements for the degree of

Doctor of Philosophy

at the

MASSACHUSETTS INSTITUTE OF TECHNOLOGY

June 2015

© Koki Ho, MMXV. All rights reserved.

Author . . . .
Department of Aeronautics and Astronautics
May 20, 2015

Certified by . . . .
Olivier L. de Weck
Professor of Aeronautics and Astronautics and Engineering Systems
Thesis Supervisor

Certified by . . . .
Jeffrey A. Hoffman
Professor of the Practice, Department of Aeronautics and Astronautics
Thesis Committee Member

Certified by . . . .
Robert Shishko
Principal Systems Engineer/Economist, NASA Jet Propulsion Laboratory,
California Institute of Technology
Thesis Committee Member

Accepted by . . . .
Paulo C. Lozano
Associate Professor of Aeronautics and Astronautics
Chair, Graduate Program Committee

Dynamic Network Modeling for Spaceflight Logistics with Time-Expanded Networks

by

Koki Ho

Abstract

This research develops a dynamic logistics network formulation for high-level lifecycle optimization of space mission sequences in order to find an optimal space transportation architecture considering its technology trades over time. The proposed methodology is inspired by terrestrial logistics analysis techniques based on linear programming network optimization. A new model with a generalized multi-commodity network flow formulation and a time-expanded network is developed for dynamic space logistics optimization. The developed methodology is applied to three case studies: 1) human exploration of Mars; 2) human exploration of a near-Earth object (NEO); 3) their combination (related to the concept of the Flexible Path). The results reveal multiple dynamic system-level trades over time and provide recommendations for an optimal strategy for human space exploration architecture. The considered trades include those between in-situ resource utilization (ISRU) and propulsion technologies as well as orbit and depot location selection over time. The numerical results show that using specific combinations of propulsion technologies, ISRU, and other space infrastructure elements effectively, we can reduce the initial mass in low-Earth orbit (IMLEO) by 45-50% compared with the baseline architecture. In addition, the analysis results also show that we can achieve 15-20% IMLEO reduction by designing Mars and NEO missions together as a campaign compared with designing them separately owing to their common space logistics infrastructure pre-deployment. This research serves as a precursor for eventual permanent settlement and colonization of other planets by humans, thus transforming us into a multi-planet species.

Thesis Supervisor: Olivier L. de Weck
Title: Professor of Aeronautics and Astronautics and Engineering Systems

Acknowledgments

I have a lot of people to thank for their support during my four-year Ph.D. study at MIT.

First of all, I cannot thank enough my advisor, Prof. Olivier de Weck. Without his insight and guidance, I could not have made it this far. He has taught me not only the technical details of aerospace systems engineering but also the attitude of an independent academic researcher.

In addition, I would like to acknowledge my other committee members, Prof. Jeffrey Hoffman and Dr. Robert Shishko. Jeff has provided me with inspiring advice since my first semester through supervising my class and research projects. Bob has spent a lot of time to review my thesis and provided me with numerous valuable comments and suggestions.

I am also grateful to Prof. Richard Larson, Prof. Amedeo Odoni, and Prof. Arnold Barnett. Thanks to them, I had a chance to TA the class 16.76 Logistical and Transportation Planning Method. This TA opportunity was a wonderful experience for me and has motivated me to pursue a university faculty career.

I also deeply appreciate the financial support from the Funai Foundation for Information and Technology through a graduate student scholarship. Particularly, Prof. Takashi Masuda at Funai Foundation encouraged me to study in the U.S., which turns out to be the best decision I have ever made.

I would also like to thank my friends at the Strategic Engineering Research Group (SERG) and Space Systems Lab (SSL) for working together with me throughout my graduate student life. Particularly, I would like to thank Takuto Ishimatsu. He has been the best supporter of my research and private life since my first day at MIT. I have learned so much from him.

My Japanese friends in and outside of MIT have made my Boston life wonderful and memorable. Despite its cold weather and heavy snow, Boston is and will always be one of the most favorite cities of mine in the world.

Last but not least, I would like to thank my mother, grandparents, and relatives who encouraged my life at MIT. Their love and support have been the major driving force of my Ph.D. study.

Contents

List of Figures

List of Tables

Nomenclature

Symbols

$\mathcal{A}$	set of directed arcs
$\boldsymbol{B}$	transformation matrix
$\boldsymbol{B}^d$	transformation rate coefficient matrix
$\boldsymbol{C}$	concurrency matrix
$\mathcal{G}$	directed network graph
I	subset of time windows $(\in W)$
I_{sp}	specific impulse
$\mathcal{J}$	objective function
$\mathcal{N}$	set of nodes
W	set of time windows
$\boldsymbol{X}$	node/arc aggregated flow variable vector
$\boldsymbol{b}$	demand/supply vector
$\boldsymbol{c}$	unit cost vector
e	arc index for multi-graph
g_0	standard gravity $(= 9.80665 \text{ m/s}^2)$
i	node index $(\in \mathcal{N})$
j	node index $(\in \mathcal{N})$
(i, j)	arc from node i to node j $(\in \mathcal{A})$
(i, j, e)	eth arc from node i to node j $(\in \mathcal{A})$
k	number of types of commodities
l_C	maximum number of concurrency constraints on each arc
m	number of directed arcs
n	number of nodes

$\boldsymbol{p}$	constant vector for concurrency constraints
t	time step (integer)
t_d	departure time step (integer)
t_a	arrival time step (integer)
v	time window index
w	time window index
$\boldsymbol{x}$	flow variable vector
$\boldsymbol{x}'$	node/arc restricted flow variable vector
Δt	time length (real number)
Δt_{ije}	length of arc (i, j, e) (integer)
ΔV	change in velocity
α_d	dry mass degradation rate
α_r	resource depletion rate
β	resource generation or loss rate
η	factor of proportionality in concurrency constraints
ϕ	propellant mass fraction

Superscripts and Subscripts

$(\cdot)^+$	outflow from tail node
$(\cdot)^-$	inflow into head node
$(\cdot)^\pm$	both outflow and inflow
$(\cdot)^{\mathrm{T}}$	transpose
$(\cdot)^a$	node/arc aggregation
$(\cdot)^r$	node/arc restriction
$(\cdot)_i$	node i
$(\cdot)_j$	node j
$(\cdot)_{ij}$	arc (i, j)
$(\cdot)_{ije}$	arc (i, j, e)
$(\cdot)_{ijt_dt_ae}$	arc (i, j, e) departing at t_d and arriving at t_a

Chapter 1

Introduction

1.1 Background and Motivation

Since the first man-made satellite, Sputnik 1, orbited Earth in 1957, space has been a new frontier for us. An enormous number of spacecraft have been launched and many unmanned or manned missions have been conducted in space. There are also numerous potential programs and projects that promote human space exploration with robotic assistance collaboratively or competitively by multiple countries, organizations, and companies [8].

Just as other frontiers humans have explored, space is still a hostile environment for us; surviving in such a world involves tough challenges.

Logistics is one of the toughest challenges that humans have faced in our exploration history. When we explore a new world, we need to examine what we carry, what we predeploy, or what we get resupplied by other groups. When the Antarctic was one of the common exploration destinations in the early 20th century, a number of expeditions had to suspend their exploration due to logistics issues. In the Nimrod Expedition led by Sir Ernest H. Shackleton in 1907-09, for example, food shortages due to uncertain weather conditions prevented the team from becoming the first humans to reach the South Pole [9]. Through these experiences, it has been known that logistics considerations play an important role in exploration of an uncertain world.

In space exploration, however, logistics has not been the main topic of research so far. This is because most space exploration campaigns up to now have not been complex enough to require network considerations. For example, in the Apollo program that sent humans to the lunar surface, all missions transported everything they needed by themselves (i.e., carry-

along strategy). This was possible because all these missions were so short (e.g., 2 weeks) that they required only a small amount of consumables and equipment. Another example of representative human space exploration missions is the International Space Station (ISS) program. In this program, astronauts have stayed in space over the long term (since 2000 up to now), but the facility is located so close to Earth that resupply vehicles can transport consumables regularly and even rotate the crew members (i.e., resupply strategy). As can be seen in these examples, conventional space programs have not explored destinations at interplanetary distances over the long term and therefore simple logistics strategies have been sufficient.

However, our next destination, whether Mars or a near-Earth object (NEO), is not close to Earth and the journey will not be short; therefore a pure carry-along or resupply strategy might not be the most efficient paradigm. We need a new framework to find an optimal logistics strategy to achieve long-term human exploration of Mars and a NEO with proper robotic assistance.

The logistics design for long-term space exploration can be even more critical with consideration of how to combine existing or emerging technologies dynamically. Numerous technologies have been developed to support long-term space exploration. These include in-situ resource utilization (ISRU) technologies for harvesting local resources on the Moon, Phobos, Deimos, and Mars [10–13], on-orbit propellant storage depots coupled with temperature control technologies [14–17], and novel rocket propulsion technologies such as nuclear thermal rockets (NTR), high-power solar electric propulsion (SEP) systems, and advanced chemical propulsion systems [18–20]. Most of these technologies have been developed in isolation, and there has been little research about how to optimally combine them. In actual space exploration missions, these technologies interact with each other both positively and negatively, which makes the logistics design a complex systems engineering problem. We need a system-level integrated method that considers those trades and can find an optimal combination of each technology at each stage of the mission.

In addition, given the tight budget in today's space exploration enterprise, it is not efficient anymore to consider each space mission separately. Instead, multiple space exploration missions need to be coupled as a *campaign*, and optimized over its entire lifecycle. For example, lunar missions can help prepare for future Mars exploration through technology demonstration or prepositioning of ISRU plants. Such a campaign-level analysis can

provide more efficient solutions where multiple space exploration missions are concurrently optimized.

Motivated by the above backgrounds, this research develops a dynamic logistics network formulation that can be used for lifecycle optimization of space mission sequences. This formulation can be used to find an optimal transportation architecture including its technology selection so that more efficient space exploration can be achieved. Note that although space exploration missions are considered for case studies in this research, the methodology developed here can be applied to any network optimization problem that contains resource transformation and interaction as well as dynamic infrastructure deployment over time.

1.2   Problem Statement

This research aims to develop a dynamic network optimization formulation, which can be applied to space logistics flows with resource gains, losses, and type conversions. In space launch campaigns, the system aims to minimize the initial mass in low-Earth orbit (IMLEO) to satisfy constant or time-dependent demands at the destinations over a time horizon. During the campaign, resources can be generated at intermediate locations via ISRU in addition to those at the supply origin. At the same time, resources can also be consumed or lost due to external factors (e.g., propellant boiloff). Development and demonstration of a dynamic network formulation that considers all the above factors is an important purposes of this research. Together with commercial linear programming software such as CPLEX, this research provides a general tool for space logistics design as well as other dynamic network optimization problems containing resource interaction.

This research considers Mars exploration, NEO exploration, and their combination (related to the concept of the Flexible Path) as the three case studies to demonstrate the applicability of the proposed methods as well as to find an innovative long-term space exploration strategy from a logistics network perspective. With mathematical rigor, this research identifies the *hidden* technology and trajectory trades that need to be considered, which can then be used to provide recommendations and technology development roadmaps for space missions in the next decades.

21

1.3   Thesis Overview

The rest of this thesis is organized as follows: Chapter 2 provides a literature review of the research. Chapter 3 introduces the mathematical theories behind this thesis as well as the proposed methods. Chapter 4 applies the developed methods to space exploration. Chapters 5 - 7 show three case studies: 1) human exploration of Mars; 2) human exploration of a NEO; 3) their combination (in spirit of the Flexible Path). Chapter 8 concludes the thesis with key contributions and recommendations for future work. A thesis roadmap is shown in Figure 1-1.
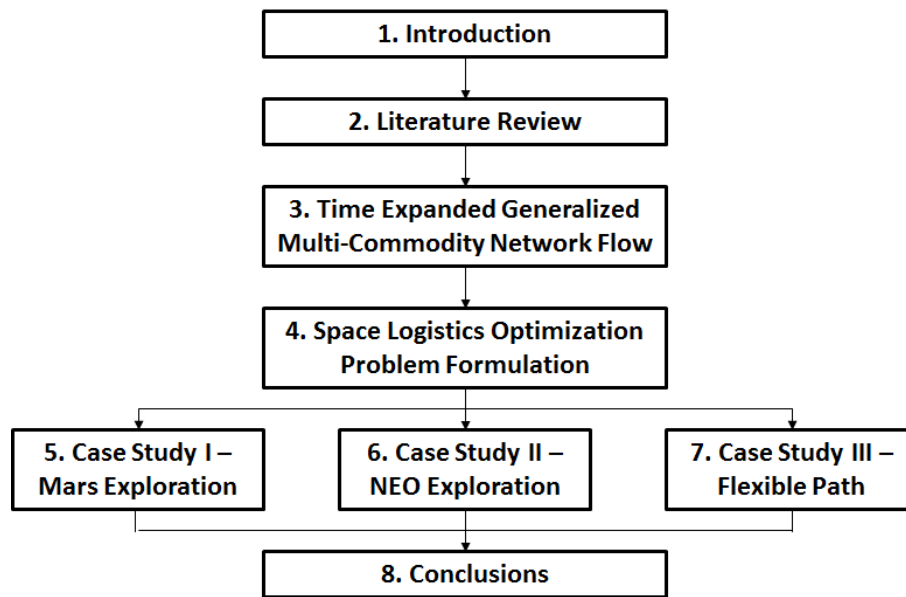
Figure 1-1: Thesis Roadmap.

Chapter 2

Literature Review

2.1 Space Logistics Infrastructure and Modeling

This research aims to provide a new dynamic space logistics modeling methodology, and part of the main contribution is in the space logistics research field. This section reviews past space logistics research briefly.

Space Logistics is defined as "the theory and practice of driving space system design for operability and managing the flow of materiel, services, and information needed throughout the system lifecycle" by the American Institute of Aeronautics and Astronautics (AIAA) Space Logistics Technical Committee [21]. The main purpose of space logistics research is to find an efficient way to plan and manage logistics in space throughout the mission lifetime. In particular, this research focuses on the resource economy in space logistics. The typical objective function is to minimize initial required mass or maximizing delivered mass. Research in this field includes efficient deployment of in-space infrastructure as well as its efficient use. This section reviews the literature on space logistics and its infrastructure that can contribute to a future space resource economy.

2.1.1 Overview of Space Logistics

Despite the long history of terrestrial logistics research, space logistics is a relatively new field. Recent rapid technology advances in space engineering have provided us with increased potentials for resource-intensive human exploration of the Moon, Mars, NEOs, or other planets. The further the destinations are, the more complex the required systems and

logistics are. Therefore, for human missions to distant destinations like Mars, logistics considerations must be part of the tradespace from which the design solution emerges.

It has been shown that terrestrial logistics research cannot be directly applied to space logistics because the latter requires additional challenges. Ishimatsu listed the following challenges of space logistics that rarely appear in terrestrial logistics design [5]. (The fourth one was not explicitly mentioned, but was implied in his model.)

- Infrequent launch windows
- Long transport durations
- Minimal cargo capacity
- Transformation of resources during transportation

These four factors represent special features of space exploration, which make terrestrial logistics research less applicable to space. First, infrequent launch windows are caused by orbital mechanics. This makes the required propellant mass and transport duration dependent on when the spacecraft departs. In addition, long transport durations lead to large consumption of resources such as water, air, and spares, which makes the consumption during transportation non-negligible. Also, minimal cargo capacity equals a large propellant ratio. This, again, makes traditional modeling formulations less applicable because the flows are not conserved. Finally, in space transportation, resources are not only consumed, but can also be transformed into other types. For example, the crew consumes water and food during transportation and these resources are converted into waste. This is also an additional challenge in space logistics.

However, there is another large difference between space and terrestrial logistics that has been relatively overlooked:

- A long and high-cost infrastructure deployment phase

This is a special feature in space exploration due to its high cost and long duration. For example, the ISS required about 13 years (1998-2011) for its assembly, and is only operated for about 15 years (2011-2024) as a complete state (though this can be extended) [22]. Conventional space logistics modeling methods have only focused on the operational phase, assuming that the necessary infrastructure elements such as ISRU plants already exist or can be built instantaneously compared with the length of the operational phase. As a result, the system is only optimized for a snapshot of the operational phase. However, in order to find a sustainable space logistics design solution, the system should be optimized for its

entire lifecycle including the assembly or deployment phase and the operational phase. To this end, this research proposes a new formulation that enables efficient integrated planning of space logistics.

2.1.2   Space Logistics Infrastructure

In past human space exploration missions, a spacecraft transported everything the crews needed in space from Earth. The commodities that the spacecraft transported include propellants, food, gases, water, science equipment, and structure mass to support all of them. Even though environmental control and life support system (ECLSS) technologies have improved [23], thus reducing crew consumables demands significantly, other commodities still need to be launched from Earth.

The largest fraction of the mass launched to space is rocket propellant. Of the gross launch mass of the rocket Saturn V that launched the Apollo spacecraft to the Moon, 98.5% was for its propellant and propulsion system, and the actual payload part is only 1.5% of the total mass [24]. This is due to the deep gravity well around Earth as shown in Figure 2-1, which fact makes space launches expensive and inefficient particularly for large-scale space exploration projects.
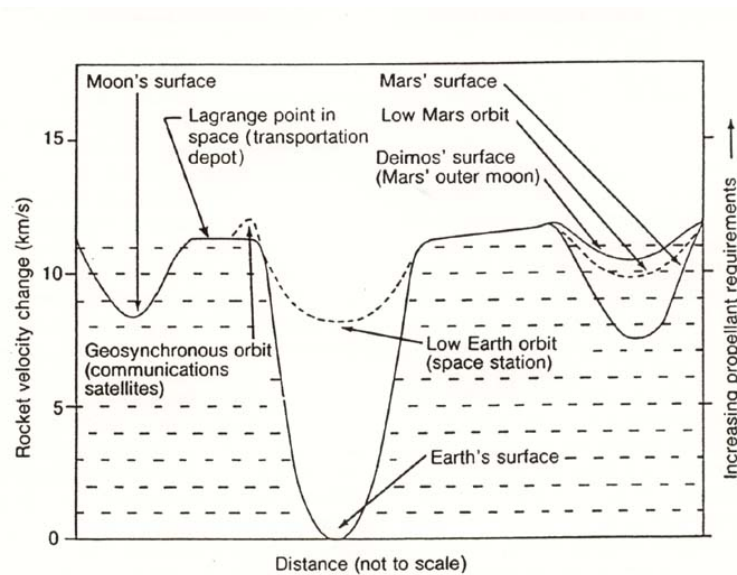
Figure 2-1: The gravity well of Earth [1].

In order to deal with this issue, many types of space logistics infrastructure have been proposed that can be located at the outside of the Earth's gravity well. One of them is

25

the concept of on-orbit propellant depots. Propellant depots can be used as gas stations in space so that rockets or spacecraft can carry less propellant. Depots can be located in a low-Earth orbit (LEO), at a Earth-Moon Lagrangian point (EML), or in other locations depending on the architecture. Numerous architectures have been proposed about how to use on-orbit propellant depots from both technological aspects [14–16] and economical aspects [25–27], most of which showed that propellant depots can provide design flexibility to future large-scale space missions.

On-orbit propellant depots have an important constraint in that they need to be refilled before they provide service to spacecraft. These refill tasks can be performed either by resupply from Earth, by reuse of residual propellant, or by ISRU. First, propellant resupply from Earth corresponds to dedicated missions that transport propellant from Earth to the depot [14, 24, 28, 29]. In addition, reuse of residual propellant has also been proposed for multiple mission campaigns in the recent literature [17]. In that concept, the vehicle docks with the propellant depot on the way back from every mission and leaves the residual propellant in the depot so that later missions can use it. Finally, ISRU plants generate propellant from in-situ resources on moons or planets, and the generated propellant is carried to the depot by propellant tankers and is used for subsequent missions [27, 30].

It can be expected that ISRU gives the largest advantage if its technologies mature. Various concepts of ISRU have been proposed and some literature provides good reviews of them [10–13].

The proposed lunar ISRU processes for oxygen generation include hydrogen reduction, methane carbothermal reduction, and electrowinning. The chemical reactions for each of these processes are shown in Eqs. (2.1) - (2.3) respectively, where MOx represents generic metal oxide in the notation. All of these processes extract oxygen from lunar regolith, which contains 42% oxygen by mass. A tradespace exploration and optimization based on these three processes was performed by Chepko [2]. The functional decomposition used by Chepko is shown in Figure 2-2. Recently, Schreiner has performed a more detailed system-level ISRU plant sizing analysis for the molten regolith electrolysis process, one type of electrowinning [31]. In addition to these methods, volatile extraction and polar water extraction (if any) have also been proposed for lunar surface ISRU [12].

$$FeTiO_3 + H_2 \longrightarrow Fe + TiO_2 + H_2O \quad (2.1a)$$

$$2\,H_2O \longrightarrow 2\,H_2 + O_2 \tag{2.1b}$$

$$MOx + CH_4 \longrightarrow CO + 2\,H_2 + M \tag{2.2a}$$

$$CO + 3\,H_2 \longrightarrow CH_4 + H_2O \tag{2.2b}$$

$$2\,H_2O \longrightarrow 2\,H_2 + O_2 \tag{2.2c}$$

$$2\,FeO \longrightarrow 2\,Fe + O_2 \tag{2.3a}$$

$$SiO_2 \longrightarrow Si + O_2 \tag{2.3b}$$

$$2\,Al_2O_3 \longrightarrow 4\,Al + 3\,O_2 \tag{2.3c}$$
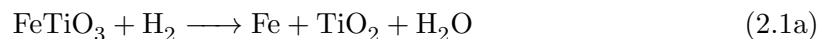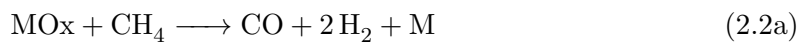
On the Martian surface, on the other hand, the Sabatier reaction has been the main focus, whose chemical equations are shown in Eq. (2.4). In addition, other proposed methods have also been proposed such as solid oxide electrolysis, reverse water gas shift reaction, and cold plasma CO_2 dissociation. Currently, the Mars Oxygen ISRU Experiment (MOXIE) is under development aiming to conduct the first in-space hardware demonstration of the solid oxide electrolysis process on the Mars 2020 rover by NASA Jet Propulsion Laboratory [32]. Finally, Phobos and Deimos [33] have also been proposed as potential locations for ISRU, as well as NEOs [34].

$$CO_2 + 4\,H_2 \longrightarrow 2\,H_2O + CH_4 \tag{2.4a}$$

$$2\,H_2O \longrightarrow 2\,H_2 + O_2 \tag{2.4b}$$

Although no ISRU plant has been actually launched to space yet, a vast body of research has suggested a high potential of ISRU. The analysis in this research assumes that ISRU technologies are mature enough to be utilized, but even if ISRU is less efficient than expected or if its performance improvement over time is slow, the proposed methodology can still be used.

27
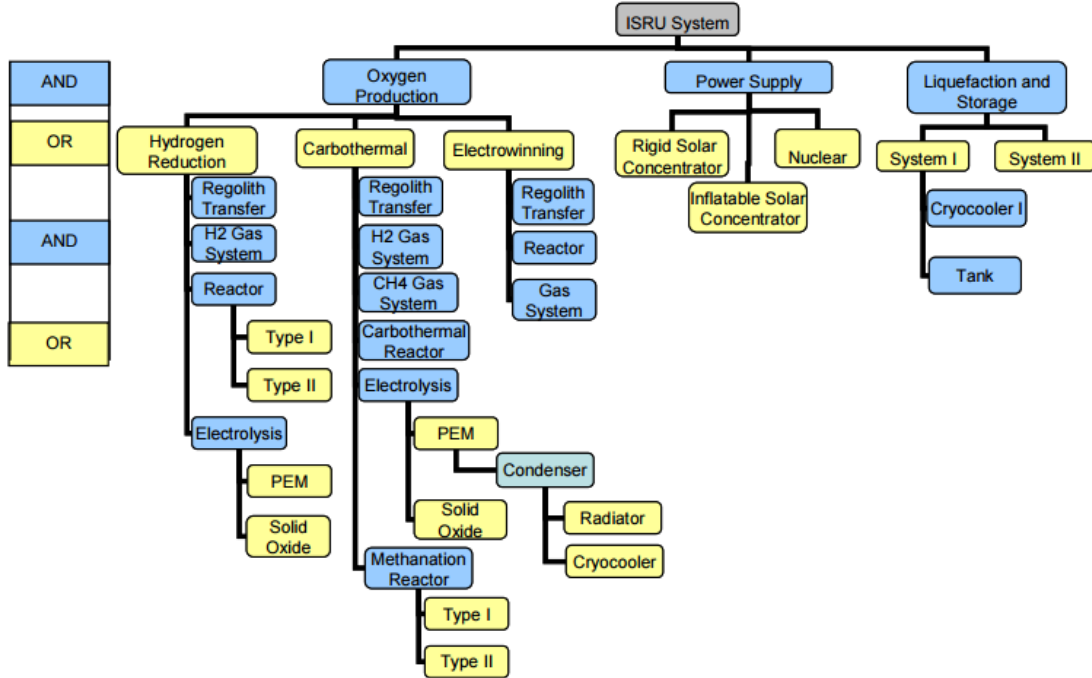
Figure 2-2: ISRU oxygen system functional decomposition by Chepko [2].

2.1.3 Space Logistics Modeling

With ISRU and propellant depot infrastructure available, space logistics network design is not simply deciding on the relative amount of prepositioning, carry-along, or resupply. Instead, more sophisticated modeling methods are necessary for tradespace exploration and optimization. This section provides a literature review about space logistics modeling.

In the space logistics research field, Massachusetts Institute of Technology (MIT) has been one of the main players since 2004. The MIT Strategic Engineering Research Group (SERG) launched the Space Logistics Project in coordination with NASAs Constellation Program to study interplanetary supply chain management and logistics [4]. The Space Logistics Project proposes the following four steps for an integrated space logistics design.

- Terrestrial supply chain analogies
- Space logistics network analysis
- Exploration demand-supply modeling with uncertainties
- Interplanetary supply chain architecture: trade studies

One of the important research projects regarding terrestrial supply chain analogies includes the NASA Haughton-Mars Project (HMP) [35]. This project developed a base in

the high Arctic (75N 90W) whose environment is functionally equivalent to a Martian base. MIT participated in the HMP expedition in 2005 and conducted experiments about asset management in space, network modeling, and extra vehicular activities (EVA) logistics. One of the results from the HMP was formulation of a formal class of supply (COS) multi-level structure to enable trades between transportation modes and the critically of commodities to be transported [36].

Another large contribution of the Space Logistics Project, particularly related to this research, was network modeling of space logistics. With sophisticated technologies and logistics infrastructure, an efficient mathematical modeling tool is required in order to analyze interplanetary supply chain. Sustainable space exploration with low life-cycle cost cannot be achieved without strategic planning on how to use existing technologies. To this end, the Space Logistics Project has been involved in developing several modeling tools for space logistics.

As part of the project, Taylor et al. extended terrestrial logistics modeling tools for space transportation applications [37, 38]. In their formulation, a spacecraft is divided into the payload part, the structural part, and, if necessary, the propellant part in order to express dynamics and requirements that do not exist in terrestrial logistics problems. A network-based approach with nodes and arcs is used for space logistics modeling, where the nodes correspond to different physical destinations or potential locations for staging or mass transfer in space (e.g., planets, moons, orbits), and the arcs connect pairs of nodes. The transit time of each arc is defined as its arc length. The static physical network is also extended for dynamic cases using a time-expanded network. (The details of time-expanded networks and their utilization for dynamic modeling are reviewed in Section 2.3.)

This formulation was substantially upgraded by Gralla et al. into a more integrated space logistics modeling software that enables simulation of interplanetary logistics as well as its results visualization and evaluation [39, 40]. In order to evaluate the results of each scenario, measures of effectiveness (MOEs) were developed as quantitative metrics. Examples of MOEs include Crew Surface Days, Exploration Mass Delivered, or Total Launch Mass, Upmass Capacity Utilization, or Exploration Capability [41].

All these efforts were integrated into an open-source space logistics simulation software tool: SpaceNet. SpaceNet enables integrated interplanetary supply chain management and space logistics planning. With its graphical user interface (GUI) supported by a spread-

sheet database for inputs, SpaceNet enables users to simulate and evaluate discrete-event logistics campaign scenarios easily and intuitively. SpaceNet 1.3 was released in 2007 on the MATLAB platform [41], and has been frequently upgraded and refined. The most recent version, SpaceNet 2.5r2 [42, 43], was written in JAVA under a GNU public license, and is available from [44].

SpaceNet has four main blocks: Network Model, Mission Model, Manifest Model, and Analysis (Visualization) as shown in Figure 2-3. The Network Model includes all nodes and arcs over time using time-expanded networks, and the Mission Model defines the mission sequence for each mission such as transportation, rendezvous, or exploration. The Manifest Model performs the demand analysis. SpaceNet then automatically manifests the required resources to the vehicles and checks for logistical feasibility. SpaceNet has been used extensively for simulation of space logistics. Grogan et al. used SpaceNet to simulate multiple cases including ISS, lunar expedition, and Mars exploration to demonstrate its usefulness [3, 45, 46]. Yue used SpaceNet to show an efficient combination of human and robotic mission concepts for Martian system exploration [47]. Grogan et al. also compared the usability of SpaceNet with that of a spreadsheet-based tool, and provided feedback for its future upgrades [48].
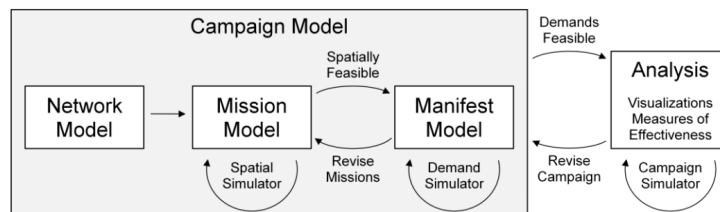
Figure 2-3: Campaign modeling and analysis in SpaceNet [3].

One of the purposes of the Space Logistics Project was to find a method to optimize commodity flows in space, which is also the main focus of this research. Taylor et al. proposed a heuristic optimization algorithm in support of their space logistics modeling [37,38]. The proposed algorithm is based on a multi-commodity combinatorial optimization problem. The problem is divided into three stages: selection of commodity routing path, assignment of commodities to non-propulsive vehicle elements, and assignment of propulsive vehicle elements to each arc in the path. This approach has several limitations in that it is not applicable to the cases where ISRU or other resource generation nodes are available,

and it is also computationally inefficient. There were some other optimization methods proposed in the Space Logistics Project, but they had similar issues as above [41, 49–52].[1]

Recently, there has been a proposal to use a graph-theoretic approach to perform space architecture tradespace exploration [53]. This approach is similar as the network modeling of space logistics reviewed above, but it also considers the order of system sizing, or the *system hierarchy*, using topological sorting. The resulting method is powerful in rapid tradespace exploration, but it explores only a limited tradespace due to its lack of feedback in its system hierarchy.

In order to deal with these difficulties in the past space logistics modeling efforts, Ishimatsu proposed a generalized multi-commodity network flow (GMCNF) formulation for space logistics modeling [5]. This formulation transforms space logistics problems including resource generation nodes (e.g., ISRU) into linear programming (LP) problems so that commercial software such as CPLEX can solve them efficiently. However, the original GMCNF formulation has some problems due to oversimplification, particularly in terms of dynamic behaviors, and this research aims to improve the GMCNF and make it even more general.

2.2 Generalized Multi-Commodity Network Flows (GMCNF)

As mentioned above, this research extends the space logistics modeling formulation GMCNF. Before introducing this formulation, the relevant literature about the classical modeling of network flows in terrestrial logistics is reviewed. Network flow modeling has been one of the common topics in the LP literature. There have been numerous formulations developed to model different types of network flows.

One of the most classical general network optimization formulations is the minimum cost flow formulation. In this formulation, a cost and capacity are assigned for each arc, and a demand or supply are assigned for the appropriate nodes. For those nodes without a demand or supply, the flows are conserved; in other words, the sum of inflow into a node is equal to the sum of outflow from that node. For those nodes with a demand or supply, the gap between inflow and outflow is equal to their demand or supply. The objective function is to minimize the total cost of the flows. Typical network optimization textbooks provide the mathematical formulation and algorithms to solve this type of problem [54, 55].

---

[1]The space logistics network optimization function used to be implemented in SpaceNet 1.3, but was removed from SpaceNet 2.5 due to its computational inefficiency.

This classical formulation cannot be applied to the problems where the flows are not conserved. For example, water reservoir models should consider evaporation or rainfall, which changes the amount of water in it. This case cannot use the above classical formulation directly. In space application, also, propellant is consumed as the spacecraft performs the required propulsive burns over an arc, which makes the above classical formulation inapplicable.

In order to deal with the flows that include gains or losses, the generalized flow problem formulation was developed. In this formulation, every arc has an additional component of gain/loss in the form of a mass ratio. When the flows are transported across an arc, the total mass is multiplied by a predetermined ratio, which expresses the expected gain or loss. In this way, the flows are not conserved across the arcs, although they are still conserved at the nodes. This generalized problem formulation is powerful and has been applied to multiple applications such as water distribution systems with losses [56], cash management problems [57], and copper refining processes [58].

Although the generalized flow formulation can be used for many problems that the classical formulation could not, there are some other problems that require further generalization of the network formulation. One example where the classical formulation cannot be applied is a network in which multiple types of commodities (resources) are transported. This type of problem is called a multi-commodity flow problem and requires a new formulation to solve.

For that sake, the multi-commodity transportation problem formulation was proposed. In this formulation, the flows on each arc composed of multiple types, each of which represents the flow of a single commodity. If there are no interactions between commodities, the problem for each single commodity can be solved separately. However, this is not true in many cases. For example, in a problem of global transportation of different varieties of grains to different destinations, multiple commodities share a common capacity on the arcs, in which case the multi-commodity flow formulation becomes powerful due to the shared capacity constraints. There are numerous applications for multi-commodity flows such as distribution networks [59] or railroad crew scheduling networks [60], among many others [54, 55, 61].

Unfortunately, however, in space logistics network problems as well as some terrestrial applications, the flows are not conserved and there are interactions among commodities at

the same time. Propellant can be consumed and water and food can be converted into waste on each arc. For these types of systems, the conventional generalized flow formulation or multi-commodity flow formulation is not applicable; a new formulation is required.

Ishimatsu proposed such a new formulation, the generalized multi-commodity network flows, or GMCNF [5]. This formulation combines both ideas of generalized flows and multi-commodity flows, where resource flows over the arcs are modeled as matrix multiplications. Also, self-loops are introduced to cope with resource generation nodes such as ISRU, and the concept of multi-graphs is proposed to incorporate trades between technology options along the same arcs or at the same nodes.

In this way, the GMCNF can formulate a campaign-level space logistics network problem with resource generation nodes (e.g., ISRU) as an LP problem. Incorporating ISRU into space logistics modeling is a large advantage that no other proposed formulation has been able to achieve. The GMCNF also improves the computational efficiency of space logistics optimization largely because LP problems can be solved rapidly using commercial software such as CPLEX or similar open source solvers.

However, there is a large drawback in this approach: the proposed GMCNF by Ishimatsu only solves static problems (i.e., the time dimension is not considered). This feature of the static GMCNF can lead to time inconsistencies (or time paradoxes) and thus can result in infeasible dynamic network flows when the arc transit times are positive. Such time inconsistencies have also been observed in conventional static network optimization problems [62], but the static GMCNF has additional issues due to existence of flow generating loops and multi-commodity interactions. The following lists some of the limitations in the static GMCNF:

- The static GMCNF results can contain a time paradox in a network containing resource generation. An example is shown in Figure 2-4, which shows a loop between two nodes. The arcs connecting node i and j involves consumption of 50 [kg] of propellant, and node j has a potential for ISRU, where 10 [kg] of propellant can be generated per kg of ISRU plant. Node i has a 10 [kg] supply of ISRU plant and node j has a 10 [kg] demand of ISRU plant. Without external propellant, this 10 [kg] of ISRU plant at node i cannot flow into node j to satisfy the demand, but in the static GMCNF, this time paradox can happen because, without consideration of the time dimension, the propellant generated by the ISRU plant can be used to deploy that

plant itself. In other words, the static GMCNF cannot ensure that the resources are not used before they are generated, which erroneously allows the optimizer to "count chickens before they hatch" [5].
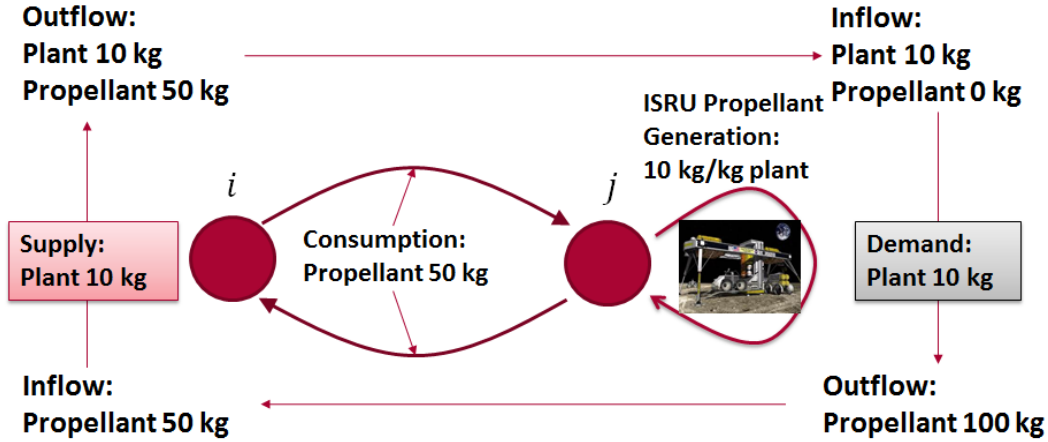
Figure 2-4: Time Paradox in the static GMCNF due to resource generation.

- The static GMCNF results can also contain a time paradox in a loop network due to interactions between multiple commodities. An example is shown in Figure 2-5, which shows a loop between two nodes. The arcs in the loop require both hydrogen (150 [kg]) and oxygen (850 [kg]). Each node only has either a hydrogen supply (300 [kg] at node i) or oxygen supply (1700 [kg] at node j), and therefore in reality this flow is not allowed without an additional external supply. In the static GMCNF, however, commodities can flow in this loop between two nodes in the way that Figure 2-5 shows because the mass balance equations are satisfied for both nodes. This time paradox is also because the static GMCNF only ensures the mass balance and does not consider the timing of the inflow and outflow for each commodity.

- The static GMCNF does not consider properly the concept of *stock* and the related concepts such as ISRU or on-orbit propellant depots. In the static GMCNF, self-loops are used to express the *stock*, but lack of the time dimension can lead to an unrealistic situation where a large inflow and outflow exist over a self-loop that do not originate from any source node. At the ISRU node, for example, a large plant mass can exist in both inflow and outflow of the ISRU self-loop to generate a large amount of propellant, but the plant mass inflow and outflow cancel each other in the mass

34
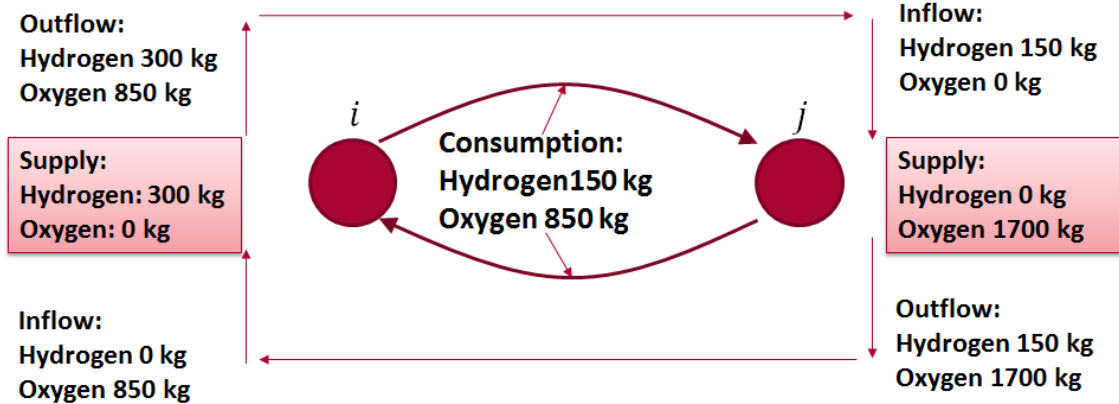
Figure 2-5: Time Paradox in the static GMCNF due to multi-commodity interaction.

balance constraint of the static model and may not require any plant mass supply from Earth. This flow is feasible in the static model because the constraints are satisfied, but does not happen in reality. Ishimatsu uses some creative tricks in order to avoid such problems (e.g., ISRU plant mass "disappears" after its utilization [5]), but these tricks are not generally applicable to all problems.

- The static GMCNF only considers the overall campaign-level mass flows instead of the flows in each mission; therefore it cannot consider the interdependency of the flows in different missions. In the space logistics case, particularly, the network *grows* over time because not all commodities are demanded; rather some of the commodities stay in the network and can be reused (e.g., propellant depot). For example, the structure mass is only used to support transportation of the payload or crew, and after the payload or crew is demanded, part of it can be reused for other purposes. This dynamic network growth itself is also part of the important results but is not considered in the static GMCNF.

- The static GMCNF cannot cope with a time-dependent supply or demand at the nodes; it only considers the cumulative or aggregated demand. This includes the launch window from the Earth/Cis-lunar system to the Martian system or NEOs.

All the above issues are critical in the actual space logistics design, but cannot be considered in a purely static formulation. Coping with these issues by a dynamic formulation is an important contribution of this research.

35

2.3 Dynamic Network Flows

As stated in the previous section, a static network flow formulation cannot capture various features that are important in the actual space logistics design; instead a dynamic network flow formulation is necessary. This section provides a literature review of dynamic aspects of network flow problem formulation.

There are a couple of methods proposed to introduce the time dimension in the network optimization, for which a number of review papers have been published [63–65]. Practically, many network flows are discrete-time events or can be decomposed into discrete-time events. For the space logistics network, for instance, a chemical rocket burn is a temporally discrete action because for each arc, propellant is consumed instantaneously instead of gradually over time. Also, the launch time windows can be assumed to be discrete, where the launch operation can only happen at a certain time. Although the resource generation or consumption at each node is continuous in time, this event only affects the flows at discrete time windows. Therefore, the space logistics network problem can be modeled as a discrete network optimization problem.

The most widely used approach to discretized dynamic network problems is time-expanded networks [62]. A time-expanded network assumes a discrete-time problems and converts the dynamic network into a static one by duplicating the nodes for each time step in a given time horizon. *Holdover arcs* exist between the same node at time t and $t + 1$, showing the commodities that are stored at that node from time t to $t + 1$. An example of a time-expanded network is shown in Figure 2-6.
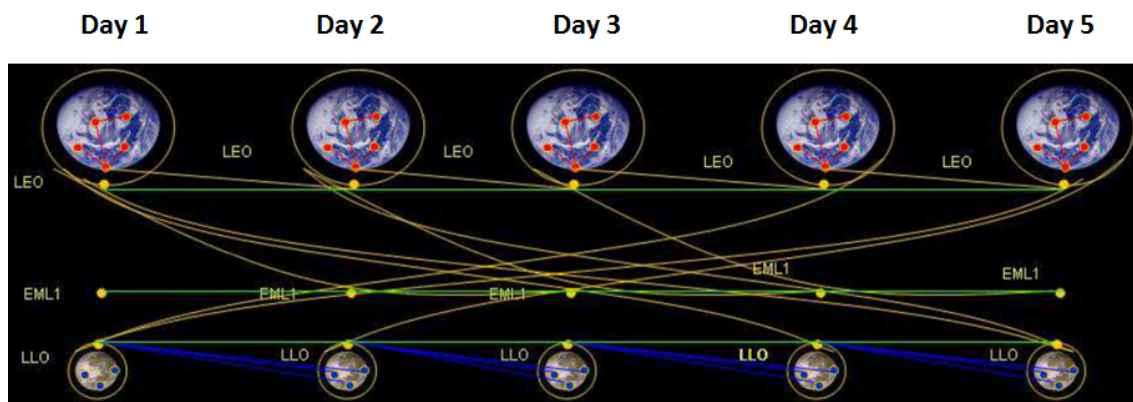
Figure 2-6: Time-expanded network for space logistics [4]. LEO: low-Earth orbit; EML1: Earth-Moon Lagrangian point 1; LLO: low-lunar orbit.

Time-expanded networks have been applied in many areas. Modeling of time-variant traffic flows is one of its typical applications [66]. Some of the space logistics literature has used time-expanded networks for visualization or optimization [38, 42, 49, 67]. Time-expanded networks have also been used together with multi-commodity flows [68, 69] and the generalized flows [70], but they have never been applied to the GMCNF. Application of time-expanded networks for the GMCNF is necessary for efficient computation (via LP) of dynamic flows with commodity conversions such as space logistics flows.

One of the practical limitations of a time-expanded network is the expensive computational effort. Since a time-expanded network duplicates the nodes for each time step, the number of nodes and arcs increases linearly with the number of time steps. As a result, the number of variables and constraints also increases linearly with the number of time steps. In general, the complexity of a time-expanded network is known to be pseudo-polynomial in the input size [67, 68, 72],[2] and therefore the number of time steps is a critical parameter in terms of computation. The complexity also scales with the number of commodity types, and therefore this issue is particularly true in multi-commodity problems [68, 69] and therefore also in the GMCNF.

For that reason, although the most natural way of time discretization is a full time-expanded network as defined in Chapter 3, it is necessary to find other practical methods. For some special cases such as the maximum flow problem, it is possible to find an exact solution efficiently (i.e., temporally repeated flows [62]), but those results are not applicable to general dynamic network flows [73]. Therefore, a practical approach should use fewer time steps for approximation of the full time-expanded network.

In general, finer time step discretization gives better solutions (i.e., with smaller discretization errors) but requires more computational time. Trades between the fineness of time steps and quality of the solutions have been a topic studied for various classes of optimization problems. Particularly, there have been interesting approaches in the literature about discretization of continuous-time optimization problems. For example, Fleischer and Skutella proposed that for some classes of problems, using a well-chosen time discretization (i.e., condensed time-expanded network [69]) can lead to a good approximation of the solution with theoretical error bounds [69, 74]. Their method assumes no time windows for

---

[2]A pseudo-polynomial time algorithm has complexity that is polynomial in the *value* of the input [71]. Note that the *value* of the input is exponential in its *length* (number of bits) For time-expanded networks, the input corresponds to the number of time steps.

transportation or demand/supply, and the resulting optimal solutions never use holdover arcs. However, with time windows for transportation and holdover commodity transformations as considered in the GMCNF, this method is not applicable and holdover arcs can be (and will in most cases) used when the commodity mass waits for the next time windows or when it generates resources (e.g., ISRU process). Another well-studied method for time discretization over time-expanded networks are adaptive time step discretization algorithms [75–79], in which the discretization is improved iteratively based on the gaps between a lower and upper bound. This method, which does not serve the purpose of this research, is useful for discretization of a continuous problem where the full time-expanded network does not provide enough information.

Considering the above literature, this research proposes and compares several time discretization methods for the GMCNF with time windows and applies them to the space logistics network to find a lower bound, an upper bound, or an approximation of the full time-expanded problem, whose exact solution is computationally too expensive to solve directly. Particularly, with time windows, it might be efficient to use different time discretization for each node rather than using the same time steps over the network. The details are described in Chapter 3.

2.4   Systems Staged Deployment Strategies

One of the interesting features of the solution from the proposed formulation is how a network *grows* over time, which suggests concurrently both network construction decisions and network utilization decisions. An important contribution from this formulation is a new staged deployment method for space logistics infrastructure. Therefore, a more detailed literature review is conducted about this specific topic.

For a complex system such as the space logistics system, deploying it in stages can be more efficient than deploying it all at once. The advantages of conventional system staged deployment can be mainly divided into the following two types, although many systems have both of these aspects.

- Conforming to the constraints.
- Adjust the system to internal/external uncertainties.

The simpler type is conforming to the constraints. Limited budget, both financial and

non-financial, can force a system to be deployed in stages. This is a natural decision for a large-scale system such as the ISS project [22], where it is impossible to launch the entire ISS structure at once.

In addition, the staged deployment can deal with uncertainties through the idea of real options analysis. A real option is explained as "a technical element embedded initially into a design that gives the right but not the obligation to decision makers to react to uncertain conditions" [80]. This provides the system with the flexibility to change the variables or not. In the space logistics networks considered in this research, an example of real options can be deploying additional ISRU for unexpected events. This flexible strategy can bring a system closer to the optimal condition than a deterministic decision made at the beginning of a campaign.

One application of real options analysis for dynamic decision making in space systems is staged deployment of a satellite constellation [80]. Here, the demand is assumed as a source of uncertainty. Only a small group of satellites is deployed first, and more satellites are deployed as the demand increases, or as more information about the demand is acquired. If the demand decreases or stays constant, the decision of increasing satellites would not be made. The resulting strategy provides a suboptimal solution in the initial stage to allow flexibility for the later stages, resulting an optimal solution in terms of lifecycle cost. The results from the analysis show the effectiveness of dynamic decision making in system operation in an uncertain environment.

The uncertainties to be considered in real options analysis can be external or internal. External uncertainties include demand fluctuation in the market. The example of staged deployment of communication satellites for an uncertain demand [80] falls under this category. Internal uncertainties include technological uncertainties and system failure possibilities. For example, for a staged deployed satellite constellation, the first stage of the satellite constellation deployment can be used for technology demonstration [81] with limited capability, followed by a second set of satellites to enhance the capability.

Although most stage-deployed systems have both advantages of conforming to constraints and coping with uncertainties, some systems can have other advantages by applying staged deployment properly. In the space logistics problem, the following advantage of using staged deployment has been overlooked in the literature.

- Self-sustained deployment.

In conventional staged deployed systems, all deployment is performed independently for each stage. For example, in the case of staged satellite constellation deployment [80], the second stage of satellites is deployed independently of the first stage launch of the constellation. However, this is not always the optimal solution because the previously deployed stages can also *enable* the following stages to be deployed. In the space logistics example, ISRU plants on the Moon can be deployed in stages. After the first stage of their deployment on the Moon, the ISRU plants start generating propellant. If this propellant can then be used for deployment of subsequent stages, the entire system can be more efficient.

Although the self-sustained deployment strategy brings about benefits, it can be inefficient in some cases with a short time horizon. This is evaluated in detail in this research through lifecycle multi-period optimization as well as trades in the engineering context by considering the role of different technologies.

Chapter 3

Time-Expanded Generalized Multi-Commodity Network Flows (GMCNF)

This chapter describes the mathematical details of the GMCNF formulation and its extension to a time-expanded network formulation. Although the space logistics application is taken as an example throughout the description, the methods and proofs are applicable to any GMCNF problem that contains resource type transformations and infrastructure deployment concurrently.

3.1 Static GMCNF

The static GMCNF is a network optimization formulation based on a graph-theoretic approach that can consider multiple types of commodities and their generation and consumption. Given a network graph, the GMCNF formulation provides an optimal commodity flow solution that meets all demand constraints and achieves the smallest cost. The results can be interpreted as a recommendation for "where to deploy what" as a snapshot of the operational phase. The following shows the mathematical formulation of the GMCNF based on the one proposed by Ishimatsu [5].

Consider a graph composed of a set $\mathcal{N}$ of nodes, a set $\mathcal{A}$ of directed arcs, and k types of commodities. Here, $\mathcal{A}$ includes both *transportation arcs*, which connect a node to a

different node, and *holdover arcs*, which connect a node back to itself. For each arc (i,j) from node i to node j, the multi-commodity flow is split into outflow $\boldsymbol{x}_{ij}^+$ and inflow $\boldsymbol{x}_{ij}^-$, for which the costs $\boldsymbol{c}_{ij}^+$ and $\boldsymbol{c}_{ij}^-$ are assigned. Note that $\boldsymbol{x}_{ij}^+$, $\boldsymbol{x}_{ij}^-$, and $\boldsymbol{c}_{ij}^+$ are k-by-1 vectors whose components show the flows and costs of the corresponding commodities. All flows are nonnegative. Each node i has its demand or supply for each commodity in a vector $\boldsymbol{b}_i$, whose negative component shows a demand and positive component shows a supply. Note that there is no time index in this formulation.

With this set of notations, the GMCNF can be expressed in the following formulation: Minimize

$$\mathcal{J} = \sum_{(i,j)\in\mathcal{A}} \boldsymbol{c}_{ij}^{+\mathrm{T}} \boldsymbol{x}_{ij}^+ \tag{3.1}$$

subject to

$$\sum_{j:(i,j)\in\mathcal{A}} \boldsymbol{x}_{ij}^+ - \sum_{j:(j,i)\in\mathcal{A}} \boldsymbol{x}_{ji}^- \leq \boldsymbol{b}_i \qquad \forall i \in \mathcal{N} \tag{3.2a}$$

$$\boldsymbol{B}_{ij}\boldsymbol{x}_{ij}^+ = \boldsymbol{x}_{ij}^- \qquad \forall\,(i,j) \in \mathcal{A} \tag{3.2b}$$

$$\boldsymbol{C}_{ij}^+\boldsymbol{x}_{ij}^+ \leq \boldsymbol{p}_{ij}^+ \qquad \forall\,(i,j) \in \mathcal{A} \tag{3.2c}$$

$$\boldsymbol{x}_{ij}^\pm \geq \boldsymbol{0}_{k\times 1} \qquad \forall\,(i,j) \in \mathcal{A} \tag{3.2d}$$

Note that the original formulation by Ishimatsu also included the term $\sum_{(i,j)\in\mathcal{A}} \boldsymbol{c}_{ij}^{-\mathrm{T}} \boldsymbol{x}_{ij}^-$ as part of the objective function, but that term can be expressed by the current objective function $\sum_{(i,j)\in\mathcal{A}} \boldsymbol{c}_{ij}^{+\mathrm{T}} \boldsymbol{x}_{ij}^+$ using Eq. (3.2b).

It is known that the GMCNF is a combination of the conventional generalized flow formulation with gain or loss and multi-commodity flow formulation. Eq. (3.2a) shows mass balance constraints. An inequality is used instead of an equality to allow mass loss at each node (e.g., rocket staging).

Eq. (3.2b) with a k-by-k mass transformation matrix $\boldsymbol{B}_{ij}$ shows transformations between commodities as well as gains or losses. This can be used to represent propellant consumption, water/food consumption by crew, and so on. Detailed examples of the mass transformation matrix $\boldsymbol{B}_{ij}$ can be found in the past literature [5] or in Chapter 4. Mass transformations in the GMCNF contain two types: instantaneous ones and continuous ones. Examples of the former include an impulsive burn for a chemical rocket or NTR, whereas

examples of the latter include a continuous burn consumption for a SEP rocket or resource generation at an ISRU plant.[1] A continuous mass transformation can be expressed by the following differential equation: $\frac{d\boldsymbol{x}}{dt} = \boldsymbol{B}^d\boldsymbol{x}$, where $\boldsymbol{B}^d$ is a k-by-k mass transformation rate coefficient matrix. If the mass transformations over arc (i,j) are only of the continuous type, $\boldsymbol{B}_{ij} = \exp\left(\boldsymbol{B}_{ij}^d \Delta t_{ij}\right)$, where Δt_{ij} is the temporal length of that continuous process (typically referred to the arc length). If an arc contains both instantaneous and continuous mass transformations, its mass transformation matrix can be expressed as a serial multiplication of the corresponding matrices. Note that a non-diagonal matrix is generally non-commutative, and so the order of the multiplication should match the actual sequence of the events.

Eq. (3.2c) with an l_C-by-k concurrency matrix $\boldsymbol{C}_{ij}^+$ and an l_C-by-1 vector $\boldsymbol{p}_{ij}^+$ show concurrency constraints. This type of constraint can be used to represent a vehicle or aeroshell mass fraction, a total flow upper bound over all commodities (also known as bundle constraints), and so on. l_C is the number of concurrency constraints. Note that theoretically, as the flow changes its state by a mass transformation matrix over an arc, the concurrency constraints and nonnegativity constraints apply to the flow all the time, which results in an infinite number of constraints. For example, if the flow changes its mass as it moves over an arc, the structure mass should always be large enough to support the payload and the mass is constrained to be nonnegative all the time over that arc. This type of optimization problem is called semi-infinite programming, and typically solved by iterative bi-level programming techniques or approximation of the constraint matrix [82]. Practically, in many systems such as the space logistics case, the monotonicity of the mass change over an arc can be assumed, which leads to a finite number of constraints in the form of Eq. (3.2c). For generality, however, all the remaining theoretical arguments assume that an infinite number of constraints is acceptable.

An alternative of the GMCNF is the following:

Minimize

$$\mathcal{J} = \sum_{(i,j)\in\mathcal{A}} \boldsymbol{c}_{ij}^{+\mathrm{T}} \boldsymbol{x}_{ij}^+ \tag{3.3}$$

subject to

$$\sum_{j:(i,j)\in\mathcal{A}} \boldsymbol{x}_{ij}^+ - \sum_{j:(j,i)\in\mathcal{A}} \boldsymbol{B}_{ji}\boldsymbol{x}_{ji}^+ \leq \boldsymbol{b}_i \qquad \forall i \in \mathcal{N} \tag{3.4a}$$

---

[1]An ISRU plant can have an intermittent duty cycle, which is not considered here.

$$C_{ij}x_{ij}^+ \leq p_{ij} \qquad \forall\,(i,j) \in \mathcal{A} \tag{3.4b}$$

$$x_{ij}^+ \geq \mathbf{0}_{k\times 1} \qquad \forall\,(i,j) \in \mathcal{A} \tag{3.4c}$$

Note that this formulation shown in Eqs. (3.3) - (3.4) is mathematically equivalent to the previous one in Eqs. (3.1) - (3.2) if the following relationships are true:

$$\boldsymbol{C}_{ij} = \begin{bmatrix} \boldsymbol{C}_{ij}^+ \\ -\boldsymbol{B}_{ij} \end{bmatrix} \quad \text{and} \quad \boldsymbol{p}_{ij} = \begin{bmatrix} \boldsymbol{p}_{ij}^+ \\ \mathbf{0}_{k\times 1} \end{bmatrix} \tag{3.5}$$

Although the formulation in Eqs. (3.3) - (3.4) is used for computation, the formulation in Eqs. (3.1) - (3.2) is used for proofs because of its clarity.

Due to the continuous nature of storage, a few assumptions are made for holdover arcs particularly. Holdover arcs are used to model an inflow-dependent demand or supply such as lunar ISRU propellant generation. Each of them only contains a unit-time continuous mass transformation and no instantaneous transformations; therefore $\boldsymbol{B}_{ii} = \exp \boldsymbol{B}_{ii}^d$ for arc (i,i). Also, the same concurrency constraints and nonnegativity constraints for holdover arcs are applied to the flow continuously. This means that the constraints for holdover arc (i,i) can be written in the following way: $\boldsymbol{C}_{ii}^+ \exp\left(\boldsymbol{B}_{ii}^d \Delta t\right)\boldsymbol{x}_{ii}^+ \leq \boldsymbol{p}_{ii}^+, \quad \exp\left(\boldsymbol{B}_{ii}^d \Delta t\right)\boldsymbol{x}_{ii}^+ \geq \mathbf{0}_{k\times 1} \quad \forall \Delta t \in [0,1)$, where Δt is a continuous real number instead of an integer. This means that those constraints should hold at any moment during the unit length time step.

In order to make the GMCNF more generally applicable, Ishimatsu added another concept: a multi-graph for transportation options. This concept considers a graph where multiple arcs are connecting the same pair of end nodes [83]. For example, it can be used when there are multiple discrete alternatives for the propulsion technologies (e.g., NTRs or chemical rockets) or when there are trades between cost and time. By using this formulation, the optimizer can automatically select the best alternative from the multi-graph during the optimization process. As a result, each element of the arc set $\mathcal{A}$ is redefined as (i,j,e), where e is the index for each multi-graph. The flow is redefined as $\boldsymbol{x}_{ije}^{\pm}$ for each arc (i,j,e), and correspondingly all the constraint parameter matrices, cost coefficients, and transit time for each arc also have ije as an index instead of just ij so that each multi-graph can have different cost or transit time if necessary.

Considering the above additional features of holdover arcs and multi-graphs, the formulation Eqs. (3.1) - (3.2) can be rewritten as follows:
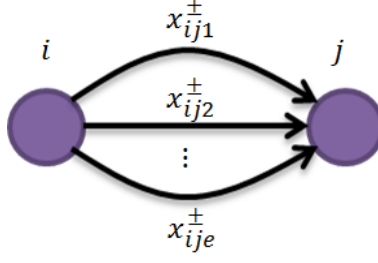
Figure 3-1: Multi-graph Formulation.

Minimize

$$\mathcal{J} = \sum_{(i,j,e)\in\mathcal{A}} {\boldsymbol{c}_{ije}^+}^{\mathrm{T}} \boldsymbol{x}_{ije}^+ \tag{3.6}$$

subject to

$$\sum_{j:(i,j,e)\in\mathcal{A}:i\neq j} \boldsymbol{x}_{ije}^+ + \sum_{(i,i,e)\in\mathcal{A}} \boldsymbol{x}_{iie}^+ - \sum_{j:(j,i,e)\in\mathcal{A}:i\neq j} \boldsymbol{x}_{jie}^- - \sum_{(i,i,e)\in\mathcal{A}} \boldsymbol{x}_{iie}^- \leq \boldsymbol{b}_i \qquad \forall i \in \mathcal{N} \tag{3.7a}$$

$$\boldsymbol{B}_{ije}\boldsymbol{x}_{ije}^+ = \boldsymbol{x}_{ije}^- \qquad \forall (i,j,e) \in \mathcal{A}:i\neq j \tag{3.7b}$$

$$\exp\left(\boldsymbol{B}_{iie}^d\right)\boldsymbol{x}_{iie}^+ = \boldsymbol{x}_{iie}^- \qquad \forall (i,i,e) \in \mathcal{A} \tag{3.7c}$$

$$\boldsymbol{C}_{ije}^+\boldsymbol{x}_{ije}^+ \leq \boldsymbol{p}_{ije}^+ \qquad \forall (i,j,e) \in \mathcal{A}:i\neq j \tag{3.7d}$$

$$\boldsymbol{C}_{iie}^+ \exp\left(\boldsymbol{B}_{iie}^d\Delta t\right)\boldsymbol{x}_{iie}^+ \leq \boldsymbol{p}_{iie}^+ \qquad \forall \Delta t \in [0,1) \quad \forall (i,j,e) \in \mathcal{A} \tag{3.7e}$$

$$\exp\left(\boldsymbol{B}_{iie}^d\Delta t\right)\boldsymbol{x}_{iie}^+ \geq \boldsymbol{0}_{k\times 1} \qquad \forall \Delta t \in [0,1) \quad \forall (i,i,e) \in \mathcal{A} \tag{3.7f}$$

$$\boldsymbol{x}_{ije}^{\pm} \geq \boldsymbol{0}_{k\times 1} \qquad \forall (i,j,e) \in \mathcal{A} \tag{3.7g}$$

Note that the concurrency constraints and nonnegativity constraints over the flows shown in Eqs. (3.7e) - (3.7f) for holdover arcs also apply to transportation arcs as part of Eq. (3.7d), although not explicitly shown. This formulation is nothing more than a simple specialization of the original one in Eqs. (3.1) - (3.2) but will be useful for later extensions, specifically for the expansion to the time dimension.

The static GMCNF is a powerful tool for network optimization problems containing resource transformations. It can deal with conversions between multiple commodities as well as constraints affecting different commodities. The former includes a conversion process from water or food into waste (and back), whereas the latter includes a minimum structure

mass ratio to support the propellants and other commodities that need to be properly contained.

Despite the effectiveness of the static GMCNF, it also has some critical limitations. These are caused by the flow generation loop in the static network and the positive (nonzero) arc transit time. The details were listed in Chapter 2, but some of the most critical ones are restated here.

First, the static GMCNF does not consider the time dimension and so it can allow inconsistent scenarios that contain *time paradoxes*. An example of such scenarios is an ISRU plant being deployed using the propellant that will be generated by that ISRU plant. The static GMCNF simply ensures that the overall cumulative mass budget closes but cannot capture whether "use of propellant generated by ISRU" happens before or after "deployment of the ISRU plant."

Also, the static GMCNF cannot consider the deployment phase. The GMCNF assumes that ISRU plants can be created instantaneously and does not consider how and when they are deployed. In reality, however, ISRU plants can be deployed in stages strategically so that the system is optimal over its entire lifecycle.

In addition, the static GMCNF cannot consider time windows or time-dependent demands and supplies at each node. They include launch windows or resupply from Earth. Ignoring these properties can possibly make that static solution infeasible or far from optimal.

The above limitations are caused by the static nature of the GMCNF. The GMCNF needs to be extended to a dynamic form, as shown in the next section.

3.2   Full Time-Expanded GMCNF

3.2.1   Formulation of Full Time-Expanded GMCNF

In order to deal with some limitations in the GMCNF caused by its static nature, a time-expanded network can be introduced. As described in Chapter 2, a time-expanded network duplicates the nodes for each time step and makes the dynamic flow equivalent to a notional static network. In a similar way as the static GMCNF, arcs in the network correspond to both transportation and storage. The arcs for transportation, or *transportation arcs*, appear as diagonal arcs connecting different nodes at different time steps, and those for storage, or

holdover arcs, appear as horizontal arcs connecting the same node at different time steps. Figure 3-2 shows an example of a full time-expanded network. In this network, for instance, mass at node j at time t can stay at the same node for one time step on a holdover arc and then leave for node i at time $t + 1$ on a transportation arc.
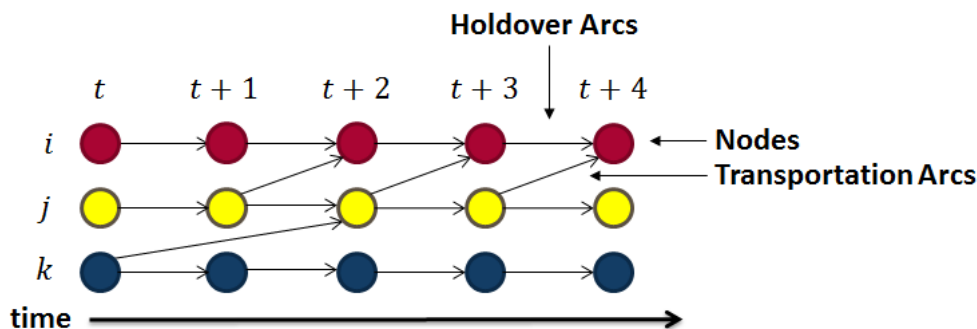
Figure 3-2: Full time-expanded network.

An assumption for the definition of the full time-expanded network is that all the arc transit times, possible departure times, and demand time windows are rational numbers. Thus, it is possible to assume a minimum time step increment as a unit time step, such that all temporal lengths and time windows can be scaled to multiples of this unit time step, and therefore are assumed to be integers. The commodity inflow/outflow is represented by a k-by-1 vector $\boldsymbol{x}^{\pm}_{ijt_d t_a e}$, where t_d denotes the departure time and t_a denotes the arrival time. A positive transit time, Δt_{ije} is given for each transportation arc $(i, j, e) : i \neq j$. (With the transit time defined, it seems redundant to have both departure time and arrival time as the indices, but it will be useful in later discussions.) In the full time-expanded GMCNF, the temporal length Δt_{iie} for each holdover arc (i, i, e) is always a unit time step (i.e., $\Delta t_{iie} = 1 \quad \forall (i, i, e) \in \mathcal{A}$), which is consistent throughout the network and over the entire time horizon.

For each arc (i, j, e), possible departure times $W_{ije} \subseteq [0, T)$ are assigned and the wth element of W_{ije} is denoted by t^w_{ije}. An arc is defined to *have time windows* (or *with time windows*) if it allows commodity flows only at a certain time step. For those arcs with time windows, W_{ije} denotes their departure time windows. For an arc (i, j, e) that does not have time windows, $W_{ije} = \{0, 1 \ldots T - 1\}$. Note that even for the arcs without time windows, their possible departure times are still limited to integer time steps over the full time-expanded network. At this point, all holdover arcs are assumed to have no time windows

47

(i.e., commodity flows are allowed at any time step).

Note that the following is always true given a time horizon T:

$$\min W_{ije} \geq 0 \qquad \forall\, (i,j,e) \in \mathcal{A} \tag{3.8a}$$

$$\max W_{ije} + \Delta t_{ije} < T \qquad \forall\, (i,j,e) \in \mathcal{A} \tag{3.8b}$$

This means that all transport processes have to be completed at the final time horizon T.

A few other assumptions are made here. It is assumed that the arc properties are constant over time. They include Δt_{ije}, $\boldsymbol{B}_{ije}$, $\boldsymbol{C}_{ije}^+$, and $\boldsymbol{p}_{ije}^+$ for each transportation arc (i,j,e), as well as $\boldsymbol{B}_{iie}^d$, $\boldsymbol{C}_{iie}^+$, and $\boldsymbol{p}_{iie}^+$ for each holdover arc (i,i,e). This assumption does not limit the possibility of time-varying arc properties because they can be treated as separate arcs (i.e., multi-graph) with proper time windows although this adds complexity. The supply/demand $\boldsymbol{b}_{it}$ at each node i can vary over time, which corresponds to the time-dependent supply/demand. The cost coefficients $\boldsymbol{c}_{ije}^+$ for each arc (i,j,e) are assumed to be constant to simplify the later proofs, but they can be generalized to different cost weightings over time (e.g., discount rate).

With this set of notations, the full time-expanded GMCNF can be expressed as follows: Minimize

$$\mathcal{J} = \sum_{(i,j,e)\in\mathcal{A}} \sum_{t\in\{0...T-1\}} \boldsymbol{c}_{ije}^{+\,\mathrm{T}} \boldsymbol{x}_{ijt(t+\Delta t_{ije})e}^+ \tag{3.9}$$

subject to

$$\sum_{j:(i,j,e)\in\mathcal{A}} \boldsymbol{x}_{ijt(t+\Delta t_{ije})e}^+ - \sum_{j:(j,i,e)\in\mathcal{A}} \boldsymbol{x}_{ji(t-\Delta t_{jie})te}^- \leq \boldsymbol{b}_{it} \qquad \forall t \in \{0\ldots T-1\} \quad \forall i \in \mathcal{N} \tag{3.10a}$$

$$\boldsymbol{B}_{ije}\boldsymbol{x}_{ijt(t+\Delta t_{ije})e}^+ = \boldsymbol{x}_{ijt(t+\Delta t_{ije})e}^- \qquad \forall t \in W_{ije} \quad \forall\, (i,j,e) \in \mathcal{A} \tag{3.10b}$$

$$\boldsymbol{C}_{ije}^+\boldsymbol{x}_{ijt(t+\Delta t_{ije})e}^+ \leq \boldsymbol{p}_{ije}^+ \qquad \forall t \in W_{ije} \quad \forall\, (i,j,e) \in \mathcal{A} \tag{3.10c}$$

$$\begin{cases} \boldsymbol{x}_{ijt_dt_ae}^{\pm} \geq \boldsymbol{0}_{k\times 1} & \text{if } t_a = t_d + \Delta t_{ije} \text{ and } t_d \in W_{ije} \\ \boldsymbol{x}_{ijt_dt_ae}^{\pm} = \boldsymbol{0}_{k\times 1} & \text{otherwise} \end{cases} \qquad \forall t_d, t_a \in \{0\ldots T-1\} \quad \forall\, (i,j,e) \in \mathcal{A} \tag{3.10d}$$

As can be seen, most of the full time-expanded GMCNF formulation is a natural exten-

sion of the static GMCNF in Eqs. (3.1) - (3.2).

We can define an alternative full time-expanded GMCNF formulation in a similar way as we did for the static GMCNF in Eqs. (3.3) - (3.4), which is used for computation, as follows:

Minimize

$$\mathcal{J} = \sum_{(i,j,e)\in\mathcal{A}} \sum_{t\in\{0...T-1\}} \boldsymbol{c}_{ije}^{+}{}^{\mathrm{T}} \boldsymbol{x}_{ijt(t+\Delta t_{ije})e}^{+} \qquad (3.11)$$

subject to

$$\sum_{j:(i,j,e)\in\mathcal{A}} \boldsymbol{x}_{ijt(t+\Delta t_{ije})e}^{+} - \sum_{j:(j,i,e)\in\mathcal{A}} \boldsymbol{B}_{jie}\boldsymbol{x}_{ji(t-\Delta t_{jie})te}^{+} \leq \boldsymbol{b}_{it} \qquad \forall t \in \{0\ldots T-1\} \quad \forall i \in \mathcal{N}$$

$$(3.12\mathrm{a})$$

$$\boldsymbol{C}_{ije}\boldsymbol{x}_{ijt(t+\Delta t_{ije})e}^{+} \leq \boldsymbol{p}_{ije} \qquad \forall t \in W_{ije} \quad \forall (i,j,e) \in \mathcal{A} \qquad (3.12\mathrm{b})$$

$$\begin{cases} \boldsymbol{x}_{ijt_d t_a e}^{+} \geq \boldsymbol{0}_{k\times 1} & \text{if } t_a = t_d + \Delta t_{ije} \text{ and } t_d \in W_{ije} \\ \boldsymbol{x}_{ijt_d t_a e}^{+} = \boldsymbol{0}_{k\times 1} & \text{otherwise} \end{cases} \qquad \forall t_d, t_a \in \{0\ldots T-1\} \quad \forall (i,j,e) \in \mathcal{A} \quad (3.12\mathrm{c})$$

This formulation shown in Eqs. (3.11) - (3.12) is mathematically equivalent to the previous one in Eqs. (3.9) - (3.10) if the following relationships are true:

$$\boldsymbol{C}_{ije} = \begin{bmatrix} \boldsymbol{C}_{ije}^{+} \\ -\boldsymbol{B}_{ije} \end{bmatrix} \quad \text{and} \quad \boldsymbol{p}_{ije} = \begin{bmatrix} \boldsymbol{p}_{ije}^{+} \\ \boldsymbol{0}_{k\times 1} \end{bmatrix} \qquad (3.13)$$

Note that the full time-expanded GMCNF assumes a constant unit time step for holdover arcs. In the other formulations proposed later, this time steps will vary, which makes B_{iie} for each holdover arc (i, i, e) vary over time depending on the length of its time step. Therefore, it will be useful for later extension to treat holdover arcs separately as follows:

Minimize

$$\mathcal{J} = \sum_{(i,j,e)\in\mathcal{A}} \sum_{t\in\{0...T-1\}} \boldsymbol{c}_{ije}^{+}{}^{\mathrm{T}} \boldsymbol{x}_{ijt(t+\Delta t_{ije})e}^{+} \qquad (3.14)$$

subject to

$$\sum_{j:(i,j,e)\in\mathcal{A}:i\neq j} \boldsymbol{x}_{ijt(t+\Delta t_{ije})e}^{+} + \sum_{(i,i,e)\in\mathcal{A}} \boldsymbol{x}_{iit(t+1)e}^{+} - \sum_{j:(j,i,e)\in\mathcal{A}:i\neq j} \boldsymbol{x}_{ji(t-\Delta t_{jie})te}^{-} - \sum_{(i,i,e)\in\mathcal{A}} \boldsymbol{x}_{ii(t-1)te}^{-}$$

$$\leq \boldsymbol{b}_{it} \qquad \forall t \in \{0\ldots T-1\} \quad \forall i \in \mathcal{N} \quad (3.15\mathrm{a})$$

$$\boldsymbol{B}_{ije}\boldsymbol{x}^+_{ijt(t+\Delta t_{ije})e} = \boldsymbol{x}^-_{ijt(t+\Delta t_{ije})e} \qquad \forall t \in W_{ije} \quad \forall (i,j,e) \in \mathcal{A} : i \neq j \tag{3.15b}$$

$$\exp\left(\boldsymbol{B}^d_{iie}\right)\boldsymbol{x}^+_{iit(t+1)e} = \boldsymbol{x}^-_{iit(t+1)e} \qquad \forall t \in \{0 \dots T-1\} \quad \forall (i,i,e) \in \mathcal{A} \tag{3.15c}$$

$$\boldsymbol{C}^+_{ije}\boldsymbol{x}^+_{ijt(t+\Delta t_{ije})e} \leq \boldsymbol{p}^+_{ije} \qquad \forall t \in W_{ije} \quad \forall (i,j,e) \in \mathcal{A} : i \neq j \tag{3.15d}$$

$$\boldsymbol{C}^+_{iie}\exp\left(\boldsymbol{B}^d_{iie}\Delta t\right)\boldsymbol{x}^+_{iit(t+1)e} \leq \boldsymbol{p}^+_{iie} \qquad \forall \Delta t \in [0,1) \quad \forall t \in \{0 \dots T-1\} \quad \forall (i,i,e) \in \mathcal{A} \tag{3.15e}$$

$$\exp\left(\boldsymbol{B}^d_{iie}\Delta t\right)\boldsymbol{x}^+_{iit(t+1)e} \geq \boldsymbol{0}_{k\times 1} \qquad \forall \Delta t \in [0,1) \quad \forall t \in \{0 \dots T-1\} \quad \forall (i,i,e) \in \mathcal{A} \tag{3.15f}$$

$$\begin{cases} \boldsymbol{x}^{\pm}_{ijt_dt_ae} \geq \boldsymbol{0}_{k\times 1} & \text{if } t_a = t_d + \Delta t_{ije} \text{ and } t_d \in W_{ije} \\ \boldsymbol{x}^{\pm}_{ijt_dt_ae} = \boldsymbol{0}_{k\times 1} & \text{otherwise} \end{cases} \qquad \forall t_d, t_a \in \{0 \dots T-1\} \quad \forall (i,j,e) \in \mathcal{A} \tag{3.15g}$$

Note that the concurrency constraints and nonnegativity constraints over the flows shown in Eqs. (3.15e) - (3.15f) for holdover arcs also apply to transportation arcs as part of Eq. (3.15d), although not explicitly shown.

In the full time-expanded GMCNF, a network containing resource transformation and infrastructure deployment such as a space logistics network containing ISRU can be modeled dynamically. It also introduces *stock* at nodes in addition to the concept of *flow* in the conventional static GMCNF. It can resolve the time paradoxes in the GMCNF by considering the order of each transportation movement. The formulation can also cope with a time-variant demand or supply at the nodes and arcs by multi-graphs and time windows that the static GMCNF cannot.

A caveat of the full time-expanded GMCNF is, however, that it requires a large number of nodes and arcs, and this leads to a large number of constraints and variables and makes the optimization computationally expensive. As shown in Chapter 2, the computational complexity of a time-expanded network is pseudo-polynomial (or exponential) in the input size, and therefore its computational requirement is large for a long time-horizon optimization. If we assume n nodes, at most m multi-graphs per arc, k commodity types, at most l concurrency constraints per arc in the formulation in Eqs. (3.11) - (3.12), and T time steps, the numbers of nodes and arcs over the time-expanded GMCNF are at most nT and n^2mT respectively. As a result, there are at most n^2mkT variables and at most $(nk + n^2ml)T$ constraints, and at most n^2mkT nonnegativity bounds in the full time-expanded GMCNF

in the formulation in Eqs. (3.11) - (3.12). The number of time steps linearly affects the number of constraints and variables, and therefore polynomially affects the LP computation time.

To mitigate that effect, a couple of time discretization methods are proposed for the full time-expanded GMCNF approximation in this research. These methods are not only more computationally efficient than the full time-expanded GMCNF but also capable of providing mathematical lower or upper bounds of its solution.

3.2.2 Node/Arc Aggregation and Lower Bounds of the Full Time-Expanded GMCNF

Although the full time-expanded GNCNF is computationally expensive to solve, its lower bound can be found with a low computational effort with a technique: *node/arc aggregation*. The basic concept is to combine multiple nodes as one group and bundle the arcs that comes into or from any nodes in that group together as shown in Figure 3-3. Note that all group nodes resulting from aggregation contain self-loops that are aggregation of holdover arcs. This also means that the resulting formulation from node/arc aggregation still potentially contains time paradoxes introduced above.
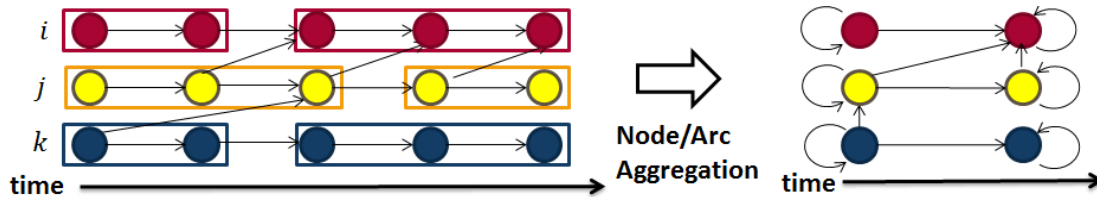
Figure 3-3: Node/arc aggregation in the time-expanded network.

The argument that node/arc aggregation provides a lower bound of the full time-expanded GMCNF is shown along with its mathematical construction. The basic idea comes from constraint aggregation. It is well known that, if multiple constraints are aggregated in an LP minimization problem, the resulting problem has an equivalent or larger tradespace and therefore provides a lower bound of the optimal objective value if both formulations are feasible and bounded [84]. Node/arc aggregation can be interpreted as aggregating the mass balance constraints of multiple nodes followed by removing redundant arcs.

51

Node/arc aggregation results in a new coarser set of time windows for nodes and arcs in two steps:

1. Node aggregation: Aggregation of the time windows into $W_i^a \subseteq \{0 \ldots T - 1\}$ for each node $i \in \mathcal{N}$

2. Arc aggregation: Aggregation of the time windows into $W_{ije}^a \subseteq W_{ije}$ for each arc $(i, j, e) \in \mathcal{A}$

The high-level pseudocode is shown in Algorithm 1.

Algorithm 1: Node/arc aggregation.

Data: A full time-expanded network $(\mathcal{N}, \mathcal{A}, T, W)$

Result: A node/arc aggregated time-expanded network with an updated set of time windows W^a

1 for *each node $i \in \mathcal{N}$* **do**

2 $\quad$ aggregate the time windows into $W_i^a \subseteq \{0 \ldots T - 1\}$;

3 for *each arc $(i, j, e) \in \mathcal{A}$* **do**

4 $\quad$ aggregate the time windows into $W_{ije}^a \subseteq W_{ije}$;

In the following, the wth element of W_{ije}^a is denoted by $t_{ije}^{a,w}$ and the wth element of W_i^a is denoted by $t_i^{a,w}$. Also, each interval of those time windows is defined as follows: $I_{ije}^{a,w} \equiv \left\{ t \in W_{ije} \mid t_{ije}^{a,w} \leq t < t_{ije}^{a,w+1} \right\}$ and $I_i^{a,w} \equiv \left\{ t \in \{0 \ldots T - 1\} \mid t_i^{a,w} \leq t < t_i^{a,w+1} \right\}$.

The first step, node aggregation, aggregates each node i into a coarser set of time windows $W_i^a \subseteq \{0 \ldots T - 1\}$. All nodes on the time-expanded network that correspond to node i during $\left[t_i^{a,w}, t_i^{a,w+1} \right)$ are combined as one aggregated node, and the mass balance constraints only hold for that aggregated node instead of for each time step separately.

The second step, arc aggregation, bundles all arcs that have the same set of aggregated origin and destination as one aggregated arc that departs at the first time step of the aggregated origin and arrives at the first time step of the aggregated destination. This resulting pseudo arc length Δt_{ije}^a of each bundled arc $(i, j, e) \in \mathcal{A}$ can give different time steps from the actual one Δt_{ije} (and sometimes can even be negative). As a result, there can be cases where the pseudo arc length is different for the same arc with the same actual arc length. In order to apply the formulation with constant Δt_{ije}, these arcs are treated as different arcs (i.e., multi-graphs) with different indices e. The results of this second step

include a new set of time windows $W_{ije}^a \subseteq W_{ije}$ for each arc (i, j, e). Also, the flows are summed up for each interval of node i and j, and thus the resulting new flow can be defined as follows: $\boldsymbol{X}_{ijt_i^{a,w}t_j^{a,v}e}^{\pm} \equiv \sum_{t_d \in I_i^{a,w}} \sum_{t_a \in I_j^{a,v}} \boldsymbol{x}_{ijt_dt_ae}^{\pm}$. By definition, the following is true:

$$
\begin{cases}
\boldsymbol{X}_{ijt_dt_ae}^{\pm} \geq \mathbf{0}_{k\times 1} & \text{if } t_a = t_d + \Delta t_{ije}^a \text{ and } t_d \in W_{ije}^a \\
\boldsymbol{X}_{ijt_dt_ae}^{\pm} = \mathbf{0}_{k\times 1} & \text{otherwise}
\end{cases}
\qquad \forall t_d, t_a \in \{0 \ldots T-1\} \quad \forall (i,j,e) \in \mathcal{A} \ (3.16)
$$

Consider a full time-expanded GMCNF problem shown in Eqs. (3.9) - (3.10). The following arguments show that it can be relaxed by aggregating nodes and arcs.

Since the cost coefficient c_{ij} is constant over time, Eq. (3.9) can be written as

$$
\mathcal{J} = \sum_{(i,j,e)\in\mathcal{A}} \sum_{t\in W_{ije}} \boldsymbol{c}_{ije}^{+\ \mathrm{T}} \boldsymbol{x}_{ijt(t+\Delta t_{ije})e}^{+} = \sum_{(i,j,e)\in\mathcal{A}} \sum_{t\in W_{ije}^a} \boldsymbol{c}_{ije}^{+\ \mathrm{T}} \boldsymbol{X}_{ijt(t+\Delta t_{ije}^a)e}^{+} \qquad (3.17)
$$

Eq. (3.10a) can be aggregated over $t \in I_i^{a,w}$ and be relaxed to the following form:

$$
\sum_{j:(i,j.e)\in\mathcal{A}} \sum_{t\in I_i^{a,w}} \boldsymbol{x}_{ijt(t+\Delta t_{ije})e}^{+} - \sum_{j:(j,i,e)\in\mathcal{A}} \sum_{t\in I_i^{a,w}} \boldsymbol{x}_{ji(t-\Delta t_{jie})te}^{-} \leq \sum_{t\in I_i^{a,w}} \boldsymbol{b}_{it} \qquad \forall w \in \{1 \ldots |W_i^a|\} \quad \forall i \in \mathcal{N}
$$

$$
(3.18)
$$

From the definition of the new time windows, the following relationship is true:

$$
\begin{aligned}
\sum_{t\in I_i^{a,w}} \boldsymbol{x}_{ijt(t+\Delta t_{ije})e}^{+} \ &= \ \sum_{t_d\in I_i^{a,w}} \sum_{t_a\in\{0...T-1\}} \boldsymbol{x}_{ijt_dt_ae}^{+} \\
&= \ \sum_{t_d\in I_i^{a,w}} \sum_{v\in\{1...|W_j^a|\}} \sum_{t_a\in I_j^{a,v}} \boldsymbol{x}_{ijt_dt_ae}^{+} \\
&= \ \sum_{v\in\{1...|W_j^a|\}} \boldsymbol{X}_{ijt_i^{a,w}t_j^{a,v}e}^{+} \\
&= \ \sum_{t_a\in W_j^a} \boldsymbol{X}_{ijt_i^{a,w}t_ae}^{+} \qquad \forall w \in \{1 \ldots |W_i^a|\} \quad \forall (i,j,e) \in \mathcal{A} \ (3.19)
\end{aligned}
$$

A similar argument can be made for $\sum_{t\in I_i^{a,w}} \boldsymbol{x}_{ji(t-\Delta t_{jie})te}^-$:

$$
\begin{aligned}
\sum_{t\in I_i^{a,w}} \boldsymbol{x}_{ji(t-\Delta t_{jie})te}^- &= \sum_{t_d\in\{0\ldots T-1\}} \sum_{t_a\in I_i^{a,w}} \boldsymbol{x}_{jit_dt_ae}^- \\
&= \sum_{v\in\{1\ldots|W_i^a|\}} \sum_{t_d\in I_j^{a,v}} \sum_{t_a\in I_i^{a,w}} \boldsymbol{x}_{jit_dt_ae}^- \\
&= \sum_{v\in\{1\ldots|W_i^a|\}} \boldsymbol{X}_{jit_j^{a,w}t_i^{a,v}e}^- \\
&= \sum_{t_d\in W_j^a} \boldsymbol{X}_{jit_dt_i^{a,w}e}^- \qquad \forall w\in\{1\ldots|W_i^a|\} \quad \forall(j,i,e)\in\mathcal{A} \ (3.20)
\end{aligned}
$$

From Eqs. (3.19) - (3.20), Eq. (3.18) can be rewritten as follows:

$$
\sum_{j:(i,j,e)\in\mathcal{A}} \sum_{t_a\in W_j^a} \boldsymbol{X}_{ijtt_ae}^+ - \sum_{j:(j,i,e)\in\mathcal{A}} \sum_{t_d\in W_j^a} \boldsymbol{X}_{jit_dte}^- \leq \sum_{t\in I_i^{a,w}} \boldsymbol{b}_{it} \qquad \forall t\in W_i^a \quad \forall i\in\mathcal{N} \quad (3.21)
$$

$$
\sum_{j:(i,j,e)\in\mathcal{A}} \boldsymbol{X}_{ijt(t+\Delta t_{ije}^a)e}^+ - \sum_{j:(j,i,e)\in\mathcal{A}} \boldsymbol{X}_{ji(t-\Delta t_{jie}^a)te}^- \leq \sum_{t\in I_i^{a,w}} \boldsymbol{b}_{it} \qquad \forall t\in W_i^a \quad \forall i\in\mathcal{N} \quad (3.22)
$$

For the other constraints, the following relaxations can be derived. Eq. (3.10b) for each arc (i,j,e) can be aggregated over $t_d\in I_i^{a,w}$ and $t_a\in I_j^{a,v}$ for each set of $w\in\{1\ldots|W_i^a|\}$ and $v\in\left\{1\ldots|W_j^a|\right\}$:

$$
\boldsymbol{B}_{ije}\sum_{t_d\in I_i^{a,w}}\sum_{t_a\in I_j^{a,v}} \boldsymbol{x}_{ijt_dt_ae}^+ = \sum_{t_d\in I_i^{a,w}}\sum_{t_a\in I_j^{a,v}} \boldsymbol{x}_{ijt_dt_ae}^- \qquad \forall w\in\{1\ldots|W_i^a|\} \quad \forall v\in\{1\ldots|W_j^a|\}
$$
$$
\forall(i,j,e)\in\mathcal{A} \qquad\qquad (3.23)
$$

$$
\boldsymbol{B}_{ije}\boldsymbol{X}_{ijt_dt_ae}^+ = \boldsymbol{X}_{ijt_dt_ae}^- \qquad \forall t_d\in W_i^a \quad \forall t_a\in W_j^a \quad \forall(i,j,e)\in\mathcal{A} \qquad (3.24)
$$

$$
\boldsymbol{B}_{ije}\boldsymbol{X}_{ijt(t+\Delta t_{ije}^a)e}^+ = \boldsymbol{X}_{ijt(t+\Delta t_{ije}^a)e}^- \qquad \forall t\in W_{ije}^a \quad \forall(i,j,e)\in\mathcal{A} \qquad (3.25)
$$

Similarly, Eq. (3.10c) can be aggregated to

$$
\boldsymbol{C}_{ije}^+\sum_{t_d\in I_i^{a,w}}\sum_{t_a\in I_j^{a,v}} \boldsymbol{x}_{ijt_dt_ae}^+ \leq \sum_{t_d\in I_i^{a,w}}\sum_{t_a\in I_j^{a,v}} \boldsymbol{p}_{ije}^+ \qquad \forall w\in\{1\ldots|W_i^a|\} \quad \forall v\in\{1\ldots|W_j^a|\}
$$
$$
\forall(i,j,e)\in\mathcal{A} \qquad\qquad (3.26)
$$

$$
\boldsymbol{C}_{ije}^+\boldsymbol{X}_{ijt_dt_ae}^+ \leq \boldsymbol{P}_{ije}^+ \qquad \forall t_d\in W_i^a \quad \forall t_a\in W_j^a \quad \forall(i,j,e)\in\mathcal{A} \qquad (3.27)
$$

$$C_{ije}^+ X_{ijt(t+\Delta t_{ije}^a)e}^+ \leq P_{ije}^+ \qquad \forall t \in W_{ije}^a \quad \forall (i,j,e) \in \mathcal{A} \tag{3.28}$$

Here, P_{ije}^+ is defined as $\sum_{t_d \in I_i^{a,w}} \sum_{t_a \in I_j^{a,v}} p_{ije}^+ = |I_i^{a,w}||I_j^{a,v}|p_{ije}^+$, but a tighter constraint can be used instead if more information about time windows is available.

The resulting formulation Eq. (3.17) with constraints in Eqs. (3.16), (3.22), (3.25), and (3.28) leads to a node/arc aggregated time-expanded GMNCNF problem as a lower (relaxed) bound of the full time-expanded GMCNF problem if both formulations are feasible and bounded. This formulation and the original full time-expanded GMCNF formulation are defined as the *corresponding* formulations of each other.

From the above derivation, the following important theorem has been proved.

Theorem 1. *A lower bound of the optimal objective of a full time-expanded GMCNF problem can be found by solving its corresponding node/arc aggregated time-expanded GMCNF problem if both problems are feasible and bounded.*

From this theorem, it can be seen that a lower bound of a computationally expensive full time-expanded GMCNF problem can be found by a computationally cheaper node/arc aggregated GMCNF problem if both of them are feasible and bounded.

Note that the static GMCNF is a special type of the node/arc aggregated GMCNF with $W_{ije}^a = \{0\} \quad \forall (i,j,e) \in \mathcal{A}$ and $W_i^a = \{0\} \quad \forall i \in \mathcal{N}$. Therefore, a lower bound of the full time-expanded GMNCNF can be found by its corresponding static GMCNF if both are feasible and bounded.

An interesting observation from this theorem is that it is the relaxation of the constraints that causes the time paradoxes and inconsistencies in the node/arc aggregated GMCNF formulation including the static GMCNF described previously. In order to explain this, we can revisit the derivation of the node/arc aggregated GMCNF from a perspective of decomposing an aggregated GMCNF flow $X_{ijt_dt_ae}^{\pm}$ into a full time-expanded GMCNF flow $x_{ijt_dt_ae}^{\pm}$. Given that B_{ije} and C_{ije}^+ are constant over time, it is always possible to decompose a flow $X_{ijt_dt_ae}^{\pm}$ into a flow $x_{ijt_dt_ae}^{\pm}$ that satisfies Eq. (3.10b) and Eq. (3.10c). However, it may not be possible to find a decomposed flow $x_{ijt_dt_ae}^{\pm}$ that also satisfies the mass balance constraint in Eq. (3.10a) because the aggregated mass balance over time is looser than the mass balance at each time step.

The situation of breaking the mass balance at specific time steps can be qualitatively described as "borrowing some commodity mass at a node and returning it back later," and

this can explain the time paradoxes or inconsistencies described in Chapter 2. For example, when this "borrowing" happens to the ISRU-generated propellant, it leads to a time paradox where an ISRU plant is delivered using the propellant to be generated by itself in the future (See Figure 2-4). When this "borrowing" happens to oxygen or hydrogen, it leads to a time paradox where a chemical rocket can fire from a node with an only-oxygen or only-hydrogen supply although it requires both oxygen and hydrogen at the same time (See Figure 2-5). When this "borrowing" happens to an ISRU plant, it causes the inconsistencies where a large plant mass flow over the ISRU arc loop that does not originate from Earth or any other source nodes.

It is also possible to derive the following corollary from the above argument that the node/arc aggregated GMCNF is more relaxed than its corresponding full time-expanded GMCNF:

Corollary 1. *If a full time-expanded GMCNF problem is feasible, its corresponding node/arc aggregated time-expanded GMCNF problem is feasible. Particularly, if a full time-expanded GMCNF problem is unbounded, its corresponding node/arc aggregated time-expanded GMCNF problem is unbounded.*

This corollary implies that the infeasibility of the full time-expanded GMCNF problem may, although not always, be detected by its corresponding node/arc aggregated GMCNF problem. If a node/arc aggregated GMCNF problem is infeasible, its corresponding full time-expanded GMCNF problem is also infeasible, but the feasibility of a node/arc aggregated GMCNF problem does not guarantee the feasibility of its corresponding full time-expanded GMCNF problem. Also, if a full time-expanded GMCNF problem is feasible and bounded, its lower bound can be found by its corresponding node/arc aggregated time-expanded GMCNF problem, although the resulting "bound" can be unbounded. (Note that if all cost coefficients c_{ije}^+ are nonnegative, which is true in the considered application cases, neither of these formulations is unbounded. In those cases, if a full time-expanded GMCNF problem is feasible, its lower bound can always be found by its corresponding node/arc aggregated time-expanded GMCNF problem.)

An important note is that although it is computationally cheaper to find a lower bound by node/arc aggregation than solving the full time-expanded GMCNF, the resulting lower bound is not always feasible for the full time-expanded GMCNF. In fact, it is infeasible

unless it replicates the exact full time-expanded GMCNF solution. A lower bound can be used as a ballpark estimate for the objective value, but in order to find a feasible set of variables, an upper bound needs to be found. Also, as will be shown later, finding both lower and upper bounds can guarantee the quality of the bounds.

3.2.3 Node/Arc Restriction and Upper Bounds of the Full Time-Expanded GMCNF

As stated above, even if a lower bound of a full time-expanded GNCNF problem can be found with a low computational effort, the resulting solution can be infeasible for that full time-expanded GMCNF problem in most cases. In order to find a feasible solution (that may be suboptimal), an upper bound needs to be found.

The basic concept of finding an upper bound is to eliminate multiple transportation arcs and restrict the number of transportation opportunities. However, only restricting transportation arcs does not reduce the numbers of constraints and variables significantly because a large number of holdover arcs still exist. Therefore, multiple nodes are eliminated (i.e., node time windows are restricted) after the transportation arc restriction step. The basic concept is shown in Figure 3-4.
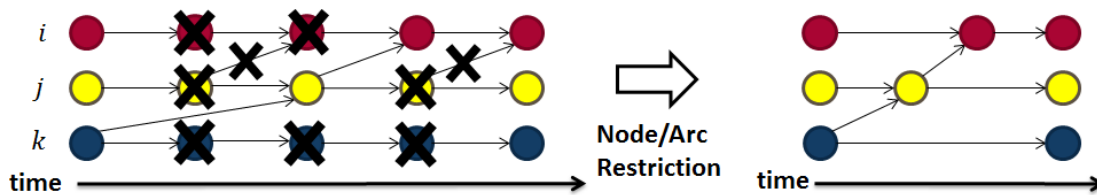
Figure 3-4: Node/arc restriction in the time-expanded network.

In a similar way as the lower bound case, the argument that node/arc restriction provides an upper bound of the full time-expanded GMCNF is shown along with its mathematical construction. The basic idea comes from variable reduction by adding constraints. It is well known that the if constraints are added to an LP minimization problem, the resulting problem has an equivalent or smaller tradespace and therefore provides an upper bound of the objective value if both formulations are feasible and bounded. Node/arc restriction can be interpreted as constraining the variables to be zero over multiple arcs followed by limiting tradespace furthermore by restricting node time windows.[2]

---

[2]Note that constraining variables to be zero in an LP problem corresponds to removing constraints in its

Node/arc restriction results in a new coarser set of time windows for nodes and arcs in two steps:

1. Arc restriction: Restriction of the time windows into $W_{ije}^r \subseteq W_{ije}$ for each transportation arc $(i,j,e) \in \mathcal{A} : i \neq j$

2. Node restriction: Restriction of the time windows into $W_i^r \subseteq \{0 \ldots T-1\}$ for each node $i \in \mathcal{N}$ and $W_{iie}^r \subseteq \{0 \ldots T-1\}$ for each holdover arc $(i,i,e) \in \mathcal{A}$

The high-level pseudocode is shown in Algorithm 2.

Algorithm 2: Node/arc restriction.

Data: A full time-expanded network $(\mathcal{N}, \mathcal{A}, T, W)$

Result: A node/arc restricted time-expanded network with an updated set of time windows W^r

1 for *each transportation arc $(i,j,e) \in \mathcal{A} : i \neq j$* **do**

2 $\quad$ restrict the time windows into $W_{ije}^r \subseteq W_{ije}$;

3 for *each node $i \in \mathcal{N}$* **do**

4 $\quad$ restrict the time windows into $W_i^r \subseteq \{0 \ldots T-1\}$;

5 for *each holdover arc $(i,i,e) \in \mathcal{A}$* **do**

6 $\quad$ restrict the time windows into $W_{iie}^r \subseteq \{0 \ldots T-1\}$;

In the following, the wth element of W_{ije}^r is denoted by $t_{ije}^{r,w}$ and the wth element of W_i^r is denoted by $t_i^{r,w}$.

The first step, arc restriction, is a very intuitive process. It assigns a new coarser time window $W_{ije}^r \subseteq W_{ije}$ for transportation arcs and adds the following constraints in addition to the original ones in Eq. (3.15):

$$\boldsymbol{x}_{ijt_dt_ae}^{\pm} = \boldsymbol{0}_{k \times 1} \qquad \forall t_d \notin W_{ije}^r \quad \forall t_a \in \{0 \ldots T-1\} \quad \forall (i,j,e) \in \mathcal{A} : i \neq j \qquad (3.29)$$

This means that the flows are prohibited over an arc when its newly defined window is closed.

The second step, node restriction, restricts the node time windows and simplifies the problem further. In this process, all nodes over the time-expanded network that have neither

---

dual LP problem.

transportation arcs connected to it nor a demand or supply are eliminated. As a result, a new set of time windows $W_i^r \subseteq \{0 \ldots T-1\}$ is assigned for node i that contain all time steps where there is at least a transportation arc connected to it or where there is a demand or supply. Note that as a result, generally, holdover arcs have different length of time steps over time. Therefore, in order to apply the formulation with constant Δt_{iie}, all holdover arcs with different time steps are considered as multi-graphs with different indices e, and $W_{iie}^r \subseteq \{0 \ldots T-1\}$ is applied to each of these holdover arcs (i,i,e). This step reduces not only the number of constraints but also that of variables because multiple holdover arcs can be combined.

It can be shown that the above two steps actually result in a problem with a smaller tradespace and thus provide an upper bound of the original full time-expanded GMCNF problem if both problems are feasible and bounded. It is obvious that the first step is adding new constraints and therefore the tradespace becomes smaller. The argument for the second step is not as obvious; the following logic provides its reasoning using the assumption that holdover arcs do not have instantaneous mass transformations.

Consider a holdover arc $(i,i,e) \in \mathcal{A}$ with Δt_{iie}. In order to show that the second step is limiting the tradespace, it suffices to show that a holdover arc $(i,i,e) \in \mathcal{A}$ can be relaxed to M equivalent holdover arcs $(i,i,e) \in \mathcal{A}$ with smaller $\Delta t'_{iie}$ $(= \Delta t_{iie}/M)$, as shown in Figure 3-5.
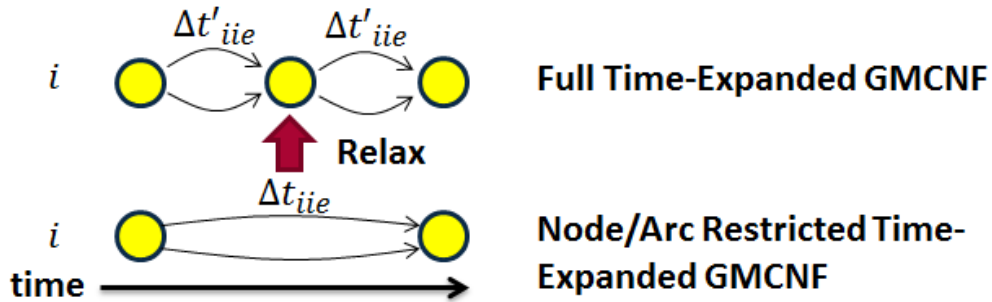
Figure 3-5: Holdover arc relaxation.

From the mass balance and concurrency constraints,

$$
\sum_{j:(i,j,e)\in\mathcal{A}:i\neq j} \boldsymbol{x}^+_{ijt(t+\Delta t_{ije})e} + \sum_{(i,i,e)\in\mathcal{A}} \boldsymbol{x}^+_{iit(t+\Delta t_{iie})e} - \sum_{j:(j,i,e)\in\mathcal{A}:i\neq j} \boldsymbol{x}^-_{ji(t-\Delta t_{jie})te} - \sum_{(i,i,e)\in\mathcal{A}} \boldsymbol{x}^-_{ii(t-\Delta t_{iie})te}
$$
$$
\leq \quad \boldsymbol{b}_{it} \qquad \forall t \in W_i^r \quad \forall i \in \mathcal{N} \tag{3.30a}
$$

$$\exp\left(\boldsymbol{B}_{iie}^{d}\Delta t_{iie}\right)\boldsymbol{x}_{iit(t+\Delta t_{iie})e}^{+} = \boldsymbol{x}_{iit(t+\Delta t_{iie})e}^{-} \qquad \forall t \in W_{iie}^{r} \quad \forall(i,i,e) \in \mathcal{A} \qquad (3.30\text{b})$$

$$\boldsymbol{C}_{iie}^{+}\exp\left(\boldsymbol{B}_{iie}^{d}\Delta t\right)\boldsymbol{x}_{iit(t+\Delta t_{iie})e}^{+} \leq \boldsymbol{p}_{iie}^{+} \qquad \forall \Delta t \in [0,\Delta t_{iie}) \quad \forall t \in W_{iie}^{r} \quad \forall(i,i,e) \in \mathcal{A} \tag{3.30c}$$

$$\exp\left(\boldsymbol{B}_{iie}^{d}\Delta t\right)\boldsymbol{x}_{iit(t+\Delta t_{iie})e}^{+} \geq \boldsymbol{0}_{k\times 1} \qquad \forall \Delta t \in [0,\Delta t_{iie}) \quad \forall t \in W_{iie}^{r} \quad \forall(i,i,e) \in \mathcal{A} \tag{3.30d}$$

Consider the following decomposed flow $\boldsymbol{x}'^{\pm} \geq \boldsymbol{0}$ over the time step from t to $t+M\Delta t'_{iie}$:

$$\boldsymbol{x}'^{+}_{iit\left(t+\Delta t'_{iie}\right)e} = \boldsymbol{x}^{+}_{iit\left(t+M\Delta t'_{iie}\right)e} \tag{3.31a}$$

$$\boldsymbol{x}'^{-}_{ii\left(t+(M-1)\Delta t'_{iie}\right)\left(t+M\Delta t'_{iie}\right)e} = \boldsymbol{x}^{-}_{iit\left(t+M\Delta t'_{iie}\right)e} \tag{3.31b}$$

$$\boldsymbol{x}'^{-}_{ii\left(t+m\Delta t'_{iie}\right)\left(t+(m+1)\Delta t'_{iie}\right)e} = \boldsymbol{x}'^{+}_{ii\left(t+(m+1)\Delta t'_{iie}\right)\left(t+(m+2)\Delta t'_{iie}\right)e} \qquad \forall m \in \{0\ldots M-2\} \tag{3.31c}$$

$$\exp\left(\boldsymbol{B}_{iie}^{d}\Delta t'_{iie}\right)\boldsymbol{x}'^{+}_{ii\left(t+m\Delta t'_{iie}\right)\left(t+(m+1)\Delta t'_{iie}\right)e} = \boldsymbol{x}'^{-}_{ii\left(t+m\Delta t'_{iie}\right)\left(t+(m+1)\Delta t'_{iie}\right)e} \qquad \forall m \in \{0\ldots M-1\} \tag{3.31d}$$

Since $\left[\exp\left(\boldsymbol{B}_{iie}^{d}\Delta t_{iie}/M\right)\right]^{M} = \exp\left(\boldsymbol{B}_{iie}^{d}\Delta t_{iie}\right)$, this set of decomposed arcs satisfies the constraints in Eq. (3.30) for the network with smaller $\Delta t'_{iie}$. Therefore, it is always possible to decompose a holdover arc into multiple feasible holdover arcs with smaller time steps.

Note that the converse is not true: multiple holdover arcs with small time steps might not be able to be combined into a holdover arc with a larger time step. This is because the former has potentially more alternative multi-graphs. Using a larger time step forces a single arc to cover a longer time period, and therefore does not allow, for example, the ISRU technology to change in the middle of a holdover arc.[3]

In summary, it is shown that the decomposition of a holdover arc into multiple ones with smaller time steps is a relaxation process in the optimization formulation. This means that the second step of node/arc restriction that combines multiple holdover arcs into one with a larger time step is a constraining process.

Together with the above argument about the first step, node/arc restriction is shown to provide a smaller tradespace than the full time-expanded GMCNF, and thus provides its upper bound if both formulations are feasible and bounded. The resulting formulation

---

[3]ISRU technology could become better due to upgrade or maintenance and repair, or worse due to degradation or failure

is Eq. (3.14) with constraints in Eqs. (3.15b), (3.15d), (3.15g), (3.29), and (3.30). This formulation and the original full time-expanded GMCNF formulation are defined as the *corresponding* formulations of each other.

From the above derivation, the following important theorem has been proved.

Theorem 2. *An upper bound of the optimal objective of a full time-expanded GMCNF problem can be found by solving its corresponding node/arc restricted time-expanded GMCNF problem if both problems are feasible and bounded.*

From this theorem, it can be seen that an upper bound of a computationally expensive full time-expanded GMCNF problem can be found by a computationally cheaper node/arc restricted GMCNF problem if both are feasible and bounded.

It is also possible to derive the following corollary from the above argument that the node/arc restricted GMCNF is more constrained than its corresponding full time-expanded GMCNF:

Corollary 2. *If a node/arc restricted time-expanded GMCNF problem is feasible, its corresponding full time-expanded GMCNF problem is feasible. Particularly, if a node/arc restricted time-expanded GMCNF problem is unbounded, its corresponding full time-expanded GMCNF problem is unbounded.*

This corollary implies that an upper bound of a full time-expanded GMCNF problem cannot always be found by its corresponding node/arc restricted GMCNF problem. If a node/arc restricted GMCNF problem is infeasible, its corresponding full time-expanded GMCNF problem can be either feasible or infeasible, and no information about the bounds can be gained. On the other hand, if a node/arc restricted GMCNF problem is unbounded, its corresponding full time-expanded GMCNF problem is feasible and unbounded. (Note that if all cost coefficients $\boldsymbol{c}_{ije}^{+}$ are nonnegative, which is true in the considered application cases, neither of these formulations is unbounded. Even in those cases, the upper bound of a full time-expanded GMCNF problem cannot always be found by its corresponding node/arc restricted GMCNF problem because they can be infeasible.)

Note that, by having both node/arc aggregation and restriction, the quality of the bounds found by both methods can be evaluated. The gap of the full time-expanded GMCNF with its lower bound found by node/arc aggregation is bounded by the gap with

61

its upper bound found by node/arc restriction, and vice versa. The relationship between each of these methods are summarized in Figure 3-6.

Upper bound of Full Time-Expanded Network

Node/Arc Restricted Time-Expanded Network

Full Time-Expanded Network

Node/Arc Aggregated Time-Expanded Network

Static

Lower bound of Full Time-Expanded Network
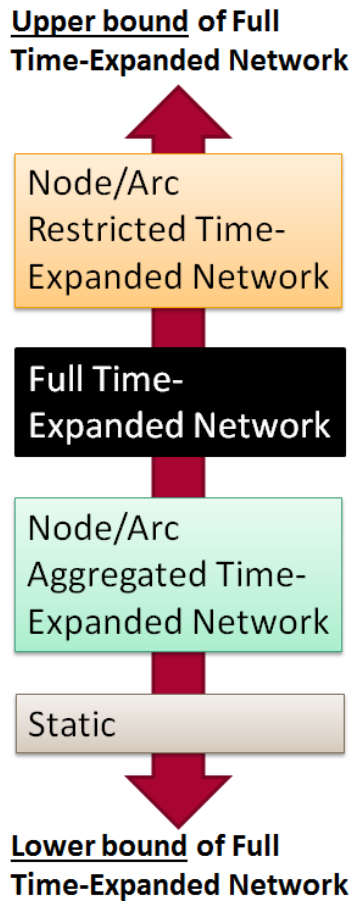
Figure 3-6: Relationship between static, node/arc aggregated time-expanded network, full time-expanded network, and node/arc restricted time-expanded network.

3.3 Uniform Time Step Methods

The concepts of node/arc aggregation and restriction introduced in previous sections provide a direction to find computationally cheaper bounds of the full time-expanded GMCNF. This section describes some typical such methods based on node/arc aggregation and restriction using uniform time steps.

3.3.1 Uniform Time Step Node/Arc Aggregated GMCNF

Node/arc aggregation methods involve combining multiple time steps into one. As shown above, this formulation is always feasible if the full time-expanded network is feasible. The important criteria to evaluate these methods comes down to choosing the time steps for each node so that a good bound can be found with a lower computational effort.

The most typical and general time step selection is a uniform set of time steps for all nodes. In the node/arc aggregation context, this means defining a set of uniform time steps that is common for all nodes and bundling the nodes within the same time interval as well as the arcs connecting the same set of time intervals. Note that if the defined time step is $\{0\}$, then the resulting formulation is identical to the static GMCNF.

3.3.2 Uniform Time Step Node/Arc Restricted GMCNF

Node/arc restriction methods involve restricting time steps. As shown above, this formulation is *not* always feasible even if the full time-expanded one is feasible and bounded. Therefore, an important criteria to evaluate these methods include how to wisely choose the time steps for each node *and* keep the problem feasible so that a good bound can be found with a low computational effort.

As in the case of node/arc aggregation methods, the most typical time step selection is a uniform set of time steps for all nodes. In the node/arc restriction context, this means defining a set of uniform time steps that is common for all nodes and allowing transportation operations only for those time steps.

Unfortunately, unlike the uniform time step node/arc aggregation, the uniform node/arc aggregation is not generally applicable, especially to the cases with time windows present. This is because the formulation does not consider the time windows in time step selection. For example, if none of the time windows of a critical arc are not included in the selected time steps, the problem can become infeasible.

This infeasibility of the node/arc restricted GMCNF can be mitigated by allowing all transportation operations with time windows in addition to the original uniform time steps. This method at least excludes the infeasible cases caused by not selecting the critical time windows as part of the uniform time steps. The uniform node/arc restriction methods appearing later in this research are assumed to allow the arcs with time windows by default.

3.4 Cluster-Based Heuristic Methods

The methods introduced in the previous section assume uniform time steps for the time-expanded network. These methods are not always the most effective especially in a system with time windows as pointed out previously. Heuristics search considering the time windows can improve the performance with a lower computational effort.

3.4.1 Bi-Scale Time-Expanded GMCNF

For problems with transportation or demand/supply time windows, such as the space logistics case, a cluster-based node/arc restriction method, the bi-scale time-expanded GMCNF, can be a good approach for approximation of the full time-expanded GMCNF as well as providing its upper bound. This method is built upon the following assumption:

Assumption 1. *It is possible to cluster the nodes so that the transportation between the same pair of clusters (inter-cluster transportation) has a common time window and temporal length whereas the transportation within each cluster (intra-cluster transportation) does not have time windows (i.e., transportation is allowed anytime within the cluster).*

There are two types of time windows for each cluster: *inward windows* and *outward windows*. An *outward window* opens for a node in a cluster when either of the following events occur:

- Departure of a transportation arc from any node in that luster into a node in another cluster.
- A demand at a node in that cluster.

Similarly, an *inward window* opens for a node in a cluster when either of the following events occur:

- Arrival of a transportation arc at any node in that cluster from a node in another cluster.
- A supply at a node in that cluster.

Note that time windows for demands and supplies are assumed to be instantaneous.

If the above clustering is possible, the nodes in each cluster can be considered separately with different time steps, and the timings around the time windows can be more important than the other timings. In Mars exploration logistics, for example, there exist launch

windows for "cheap" transit between Earth or the Cis-lunar system and Mars if chemical rockets are used. The Cis-lunar transportation occurring long before the next time window opens has much less impact on the Mars exploration campaign than the transportation occurring while the time window is open.

In order to consider this simplification, the bi-scale time-expanded GMCNF, applies a separate scale to the smaller local time-scale dynamic network. More specifically, it divides the entire time sequence into multiple phases with different time scales and effectively creates a hierarchical time-expanded network. In a phase at the cluster scale, larger time steps are used, whereas in a phase at the local node scale, smaller time steps are used. In other words, the resolution of the time steps over the time-expanded network is varied based on the time windows.

The above intuitions and definition lead to Algorithm 3.

Algorithm 3: Bi-scale time-expanded network.

Input: A full time-expanded network

Output: A bi-scale time-expanded network

1 Partition nodes to clusters such that transportation between the same pair of clusters has a common time window and temporal length whereas the transportation within the cluster does not have time windows;

2 Draw a cluster-level time-expanded network that contains the inter-cluster arcs as well as their origins and destinations;

3 **for** *each cluster* **do**

4   add nodes and intra-cluster arcs that correspond to the sub-time steps after each of its *inward time windows* and before each of its *outward windows*;

An example of this algorithm is shown in Figure 3-7.

The first two steps of the algorithm simply allow time windows for inter-cluster transportation, followed by adding sub-time steps for intra-cluster transportation. The difference between the *inward time windows* and *outward time windows* comes from whether the "impact" of the network flow happens before or after the time window. This can be qualitatively explained as follows: at the *inward time windows*, the network "reacts" to the flow arriving from outside of the cluster and therefore the sub-time steps appear after the window, whereas at the *outward time windows*, the network "prepares" itself for the flow departing
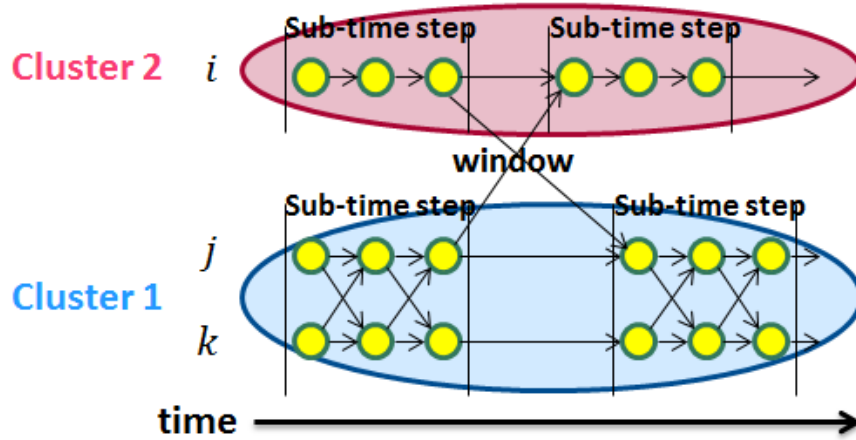
Figure 3-7: Bi-scale time-expanded GMCNF.

the cluster and therefore the sub-time steps appear before the window.

A few important parameter selections need to be made about the sub-time steps. First, in order to make this formulation comparable with the full time-expanded GMCNF, the time step resolution at the sub-time steps should be equal to the one used in the full time-expanded GMCNF. A more critical question is the length of the phase with the sub-time steps within the cluster itself. Note that there is no "correct" answer for this parameter: the larger the better in terms of the solution quality. If this parameter is sufficiently large, the formulation is identical to the full time-expanded GMCNF. The actual length for these intra-cluster phases can be determined by trading the computational effort and the required level of fidelity, but an estimate can be made by considering the functions of the sub-time steps. The meaning of the length of the sub-time step phase corresponds to the speed of spreading the "impact" of each inward or outward time window. This is closely related to the concept of a *diameter* in graph theory [83]. The *diameter* of a graph is defined as the maximum of the shortest path between any pair of nodes in a graph. For the GMCNF, specifically, a slight modification to that definition is applied for the cases where multiple arcs exist over the same pair of nodes. In those cases, the diameter is computed based on the arc that has the longest temporal length over that pair of nodes. With this definition, the length of the sub-time step phase for each cluster can be estimated to be proportional to its cluster diameter. Note that the factor of proportionality is not necessarily one because the "impact" is not always one way. For example, when propellant from lunar ISRU is used to deploy further ISRU plants from Earth, one may first carry the propellant generated

66

by lunar ISRU to an intermediate depot, meet the additional ISRU plants launched from Earth, and then carry the plants back to the Moon with the lunar propellant. In this case, the temporal length of spreading the "impact" of the supply from Earth corresponds to at least a round trip between the Moon and the intermediate depot. Therefore, the sub-time steps within the Earth/Cis-lunar cluster can extend over two cluster diameters. Trading the computational effort and the level of fidelity, this research assumes two as the factor of proportionality. In short, the length of the sub-time step phase is assumed to be twice of the diameter of the cluster that the node belongs to.

Note that this method is based on heuristics and is not guaranteed to be feasible or to provide a better bound than the uniform time step methods. However, as shown in the later computational examples, for the systems where time windows play an important role, this method provides a satisfactory upper bound with a low computational effort in many cases. In addition, the bi-scale time-expanded GMCNF may also be preferred practically to other conventional methods. In the practical operational context, the system may have all transportation movements happening during a short *active* period and leave the remaining period as a *dormant* one. Thus, the results found by the bi-scale time-expanded network can also be a practically preferred solution, where all transportation operations within the clusters happen during the short active sub-time steps.

3.4.2 Partially Static Time-Expanded GMCNF

Although the bi-scale time-expanded GMCNF provides a good approximation of the full time-expanded GMCNF, it is still computationally expensive when a long-term campaign is considered. This section proposes an even more simplified method, the partially static time-expanded GMCNF.

The partially static time-expanded GMCNF is developed from the same motivation as the bi-scale time-expanded GMCNF. It captures the characteristics of the clusters and focuses on the time windows for inter-cluster transportation. The only difference between these two formulations is that the partially static time-expanded GMCNF treats the transportation arcs within the clusters as a static network. Instead of adding sub-time steps at the time windows as in the bi-scale time-expanded GMCNF, the partially static time-expanded GMCNF adds a set of instantaneous transit arcs within the clusters at the time windows assuming all intra-cluster transportation are instantaneous.

The algorithmic steps of the partially static time-expanded GMCNF are shown in Algorithm 4.

Algorithm 4: Bi-scale time-expanded network.

Input: A full time-expanded network

Output: A partially static time-expanded network

1 Partition nodes to clusters such that transportation between the same pair of clusters has a common time window and temporal length whereas the transportation within the cluster does not have time windows;

2 Draw a cluster-level time-expanded network that contains the inter-cluster arcs as well as their origins and destinations;

3 **for** *each cluster* **do**

4   add instantaneous transportation arcs within that cluster at each of its *inward windows* or *outward windows*;

An example is shown in Figure 3-8.
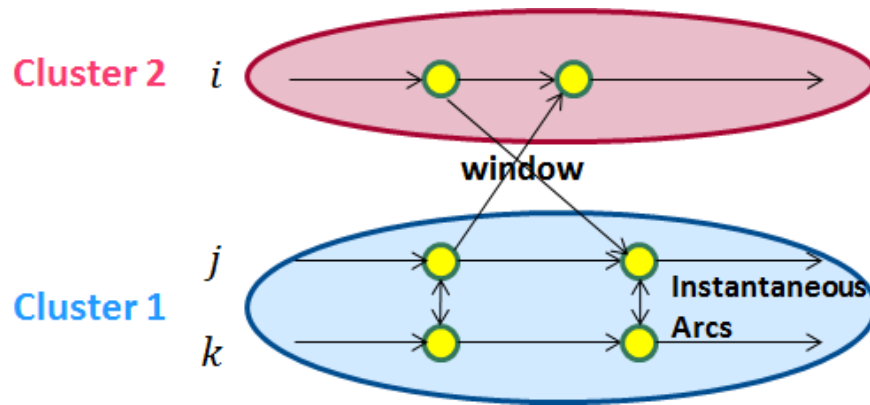
Figure 3-8: Partially static time-expanded GMCNF.

The solution of this partially static time-expanded GMCNF can provide a good approximation of that of the full time-expanded GMCNF with a very low computational effort particularly when the intra-cluster transportation arcs are generally shorter than the inter-cluster transportation arcs, which is true in the space logistics application. However, unlike the other methods listed above, this method cannot provide the mathematical bound of the full time-expanded GMCNF. This is because time paradoxes exist within instantaneous arcs, which drive the optimization to a more relaxed side, whereas it does not allow even

the intra-cluster transportation when the inter-cluster time windows closes, which drive the optimization to a more constrained side. Nevertheless, in order to acquire a quick estimate of the optimal objective value of the full time-expanded GMCNF, this method can provide useful results effectively and efficiently, without being able to claim the results as either lower or upper bounds.

3.5 Computational Example

This section introduces a simple numerical example with three types of commodities and three nodes to show the relationship between the static GMCNF, the full time-expanded GMCNF, the uniform time step node/arc aggregated and restricted GMCNF, the bi-scale time-expanded GMCNF, and the partially static time-expanded GMCNF. Consider the example in Figure 3-9. The property of each node and arc in the system is shown in Tables 3.1 - 3.2.

The network contains three nodes, node 1-3, and the objective of this problem is to minimize the total supply over time coming from node 1 to satisfy the demand at node 3. The optimization is run over a time horizon of $T = 101$ (i.e., $t \in \{0 \dots 100\}$); a demand exists at node 3 at $t = 100$ and a supply exists at node 1 at each of $t = 0$ and $t = 50$ as shown in Table 3.1. The demands are fixed and the sum of the supplies are to be minimized. Node 2 is an intermediate potential resource generation node. In a stylized way, node 1 represents Earth, node 2 lunar ISRU, and node 3 Mars. Following the clustering procedure described previously, node 1 and 2 are categorized into one cluster, and node 3 belongs to its own cluster.

The network also contains four transportation arcs and three holdover arcs at nodes 1, 2, and 3 respectively. Each transportation arc has a mass transformation matrix in the form of $\boldsymbol{B}_{ij}$, whereas each holdover arc has it in the form of $\exp\left(\boldsymbol{B}_{ij}^d t\right)$. No concurrency constraints are considered in this simple example.

The following algorithms are considered for this problem and the results are compared:

- Full Time-Expanded GMCNF
- Uniform Time Step Node/Arc Aggregated Time-Expanded GMCNF with the time steps $\Delta t = 10, 25, 101$ ($\Delta t = 101$ corresponds to the static GMCNF)
- Uniform Time Step Node/Arc Restricted Time-Expanded GMCNF allowing arcs with
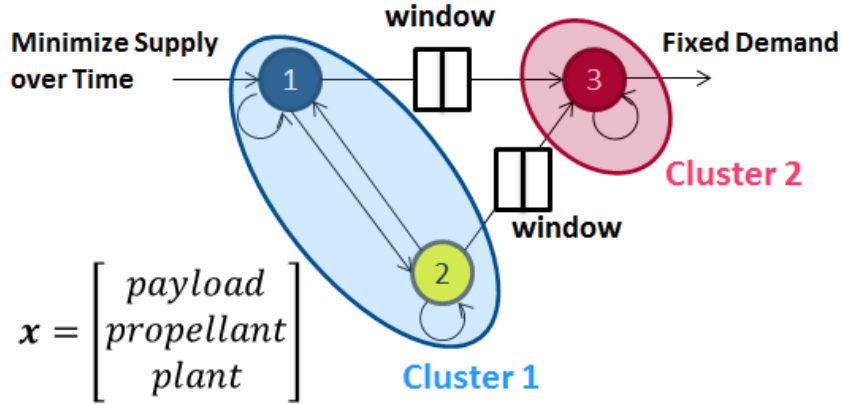
Figure 3-9: Example problem.

Table 3.1: Node properties of the example problem.

| | Demand/Supply [kg] | | | |
	Payload	Propellant	Plant	Demand/Supply Window
1	5000	Inf	Inf	t=0, 50
2	0	0	0	Anytime
3	-10000	0	0	t=100

time windows (See Section 3.3.2) with the time steps $\Delta t = 10, 25, 101$

- Bi-scale Time-Expanded GMCNF
- Partially Static Time-Expanded GMCNF

The results are shown in Table 3.3 and its bar chart is shown in Figure 3-10. As an indicator of computational complexity, the numbers of constraints and variables for each case are also shown in the formulation in Eqs. (3.11) - (3.12).

It can be seen that the proposed computationally cheap methods provide lower and upper bounds as well as good approximations of the computational expensive full time-expanded GMCNF. Although in this simple case, the full time-expanded GMCNF is still a small-size problem and can be run directly easily, for more realistic applications with a large number of constraints and variables it takes a very long time or can even be impossible to run due to "out of memory" errors. For those cases, the proposed methods are effective in that they provide both lower and upper bounds of the full time-expanded GMCNF with a low computational effort, which are often practically useful approximations.

There are some important findings here. First, for the uniform node/arc aggregation or

70

Table 3.2: Arc properties of the example problem.

	Origin	Destination	Mass Transformation	Arc Length	Window
1	1	2	$\boldsymbol{x}_{ij}^- = \begin{bmatrix} 1 & 0 & 0 \\ -0.25 & 0.75 & -0.25 \\ 0 & 0 & 1 \end{bmatrix} \boldsymbol{x}_{ij}^+$	$\Delta t_{ij} = 1$	Anytime
2	2	1	$\boldsymbol{x}_{ij}^- = \begin{bmatrix} 1 & 0 & 0 \\ -0.25 & 0.75 & -0.25 \\ 0 & 0 & 1 \end{bmatrix} \boldsymbol{x}_{ij}^+$	$\Delta t_{ij} = 1$	Anytime
3	1	3	$\boldsymbol{x}_{ij}^- = \begin{bmatrix} 1 & 0 & 0 \\ -0.5 & 0.5 & -0.5 \\ 0 & 0 & 1 \end{bmatrix} \boldsymbol{x}_{ij}^+$	$\Delta t_{ij} = 40$	t=60
4	2	3	$\boldsymbol{x}_{ij}^- = \begin{bmatrix} 1 & 0 & 0 \\ -0.25 & 0.75 & -0.25 \\ 0 & 0 & 1 \end{bmatrix} \boldsymbol{x}_{ij}^+$	$\Delta t_{ij} = 40$	t=60
5	1	1	$\boldsymbol{x}_{ij}^- = \exp\left(\begin{bmatrix} 0 & 0 & 0 \\ 0 & 0 & 0 \\ 0 & 0 & 0 \end{bmatrix} t \right) \boldsymbol{x}_{ij}^+$	–	–
6	2	2	$\boldsymbol{x}_{ij}^- = \exp\left(\begin{bmatrix} 0 & 0 & 0 \\ 0 & 0 & 0.1 \\ 0 & 0 & \log 0.999 \end{bmatrix} t \right) \boldsymbol{x}_{ij}^+$	–	–
7	3	3	$\boldsymbol{x}_{ij}^- = \exp\left(\begin{bmatrix} 0 & 0 & 0 \\ 0 & 0 & 0 \\ 0 & 0 & 0 \end{bmatrix} t \right) \boldsymbol{x}_{ij}^+$	–	–

Table 3.3: Objective value and the numbers of constraints and variables for each method in the computational example.

Method	Objective Value [kg]	# of Constraints	# of Variables
Full Time-Expanded GMCNF	11,713	2451	1527
Uniform $\Delta t = 10$ Aggregated GMCNF	10,078	435	330
Uniform $\Delta t = 25$ Aggregated GMCNF	10,078	201	150
Uniform $\Delta t = 101$ Aggregated GMCNF (i.e., Static GMCNF)	10,078	42	27
Uniform $\Delta t = 10$ Restricted GMCNF	11,810	411	237
Uniform $\Delta t = 25$ Restricted GMCNF	12,045	207	117
Uniform $\Delta t = 101$ Restricted GMCNF	17,055	93	48
Bi-Scale Time-Expanded GMCNF	11,810	177	105
Partially Static Time-Expanded GMCNF	11,781	93	57

restriction, finer time steps provide an equivalent or tighter bound but with more constraints or variables. In addition, the bi-scale time-expanded GMCNF provides a tighter bound of
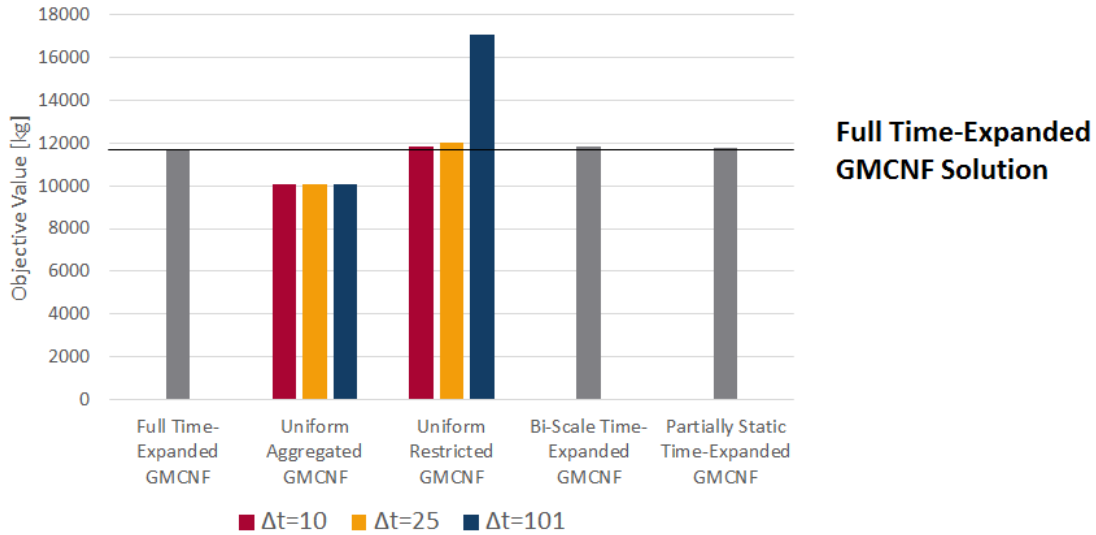
Figure 3-10: Bar chart of the objective value for each method in the computational example.

the full time-expanded GMCNF with a smaller number of constraints and variables than the uniform one. This shows the effectiveness of cluster-based methods at least in this example. Finally, the partially static time-expanded GMCNF provides the best approximation with an extremely small number of constraints and variables. As described before, this method does not provide a rigorous bound for the solution, but it is practically very useful given its performance.

3.6 Chapter Summary

This chapter introduced the mathematics of the dynamic GMCNF and a couple of its variations. Node/arc aggregation provides a lower bound of the full time-expanded GMCNF result, whereas node/arc restriction provides an upper bound of that. In terms of time step selections, in addition to the natural uniform time step methods, two cluster-based heuristics methods are proposed: the bi-scale time-expanded GMCNF and the partially static time-expanded GMCNF. These methods are useful in providing an upper bound or a good approximation of the full time-expanded GMCNF result efficiently especially for the systems where time windows play an important role. Chapter 4 introduces the application of these methods to space logistics design.

Chapter 4

Space Logistics Optimization Problem Formulation

This chapter introduces the details of the graph-theoretic modeling of space logistics, part of which is based on the static GMCNF in [5], as well as other prior modeling work at MIT in the Space Logistics Project. In this graph-theoretic modeling approach, a space logistics network is converted into a graph. Nodes in the graph correspond to potential destinations, storage locations, or transshipment locations either on the surface or in space, and arcs connect the pairs of nodes that spacecraft can transport between. In addition to the nominal *transportation arcs*, which connect a node to a different node, the self-loops, or *holdover arcs*, are also considered, which connect a node to itself. The holdover arcs contain unit-time mass transformations and model an inflow-dependent demand or supply such as possibility of lunar ISRU propellant generation. When a time-expanded network is considered for the space logistics case, the time step size for the full time-expanded network is assumed to be 1 [day] following the assumptions used in the past literature [49].

Considering GMCNF optimization over this equivalent graph provides the optimal commodity flow solution that satisfies all constraints and achieves the smallest objective function. The following sections describe the important modeling details in this research.

4.1   Variables and Objective Function

The variables of the optimization problem correspond to the mass flow of each commodity on each arc. In the Earth-Moon-Mars-NEO logistics case, a graph with nodes and arcs is drawn
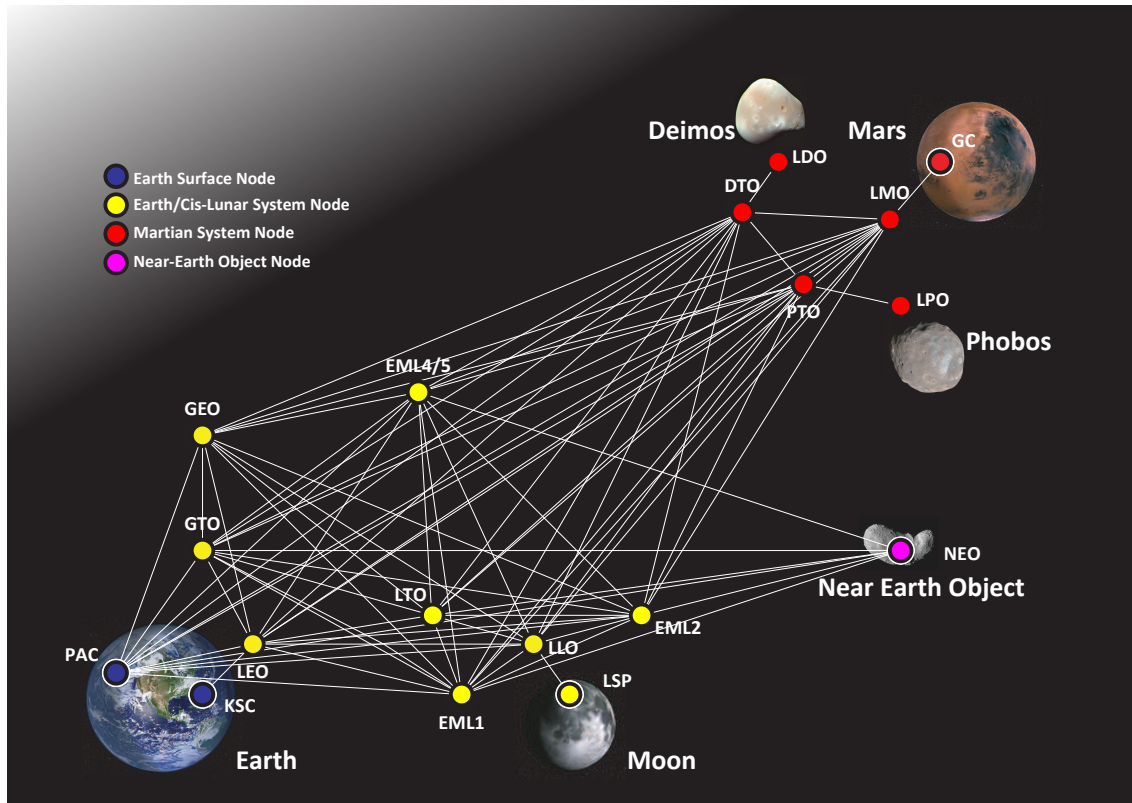
Figure 4-1: Earth-Moon-Mars-NEO logistics network graph based on the figure from [5].

in Figure 4-1 and their clustering is shown in Figure 4-2. The time windows dividing the clusters can be caused by orbital mechanics, launch site availability, or programmatic and budgetary constraints. In the clustered network, the inter-cluster arcs between each cluster pair are limited to one. For example, the arcs between the Earth/Cis-lunar cluster and the Martian cluster are limited to the one between LTO and DTO, and all transportation paths between these clusters go through that arc. This will limit the tradespace to a more realistic transportation options. Note that although there have been numerous advanced propulsion systems proposed that have high specific impulse and would be less sensitive to the time windows [85], this research does not consider them in later application cases. This is because this research intends to compare the results obtained from the dynamic GMCNF methods with the conventional reference architectures, which do not assume these technologies or orbits.

In the graph, the following nodes are considered: Kennedy Space Center (KSC) for launches, a Pacific Ocean splashdown zone (PAC) for return, a 300-km low-Earth orbit (LEO), a 35786-km geostationary Earth orbit (GEO), a geostationary transfer orbit (GTO),
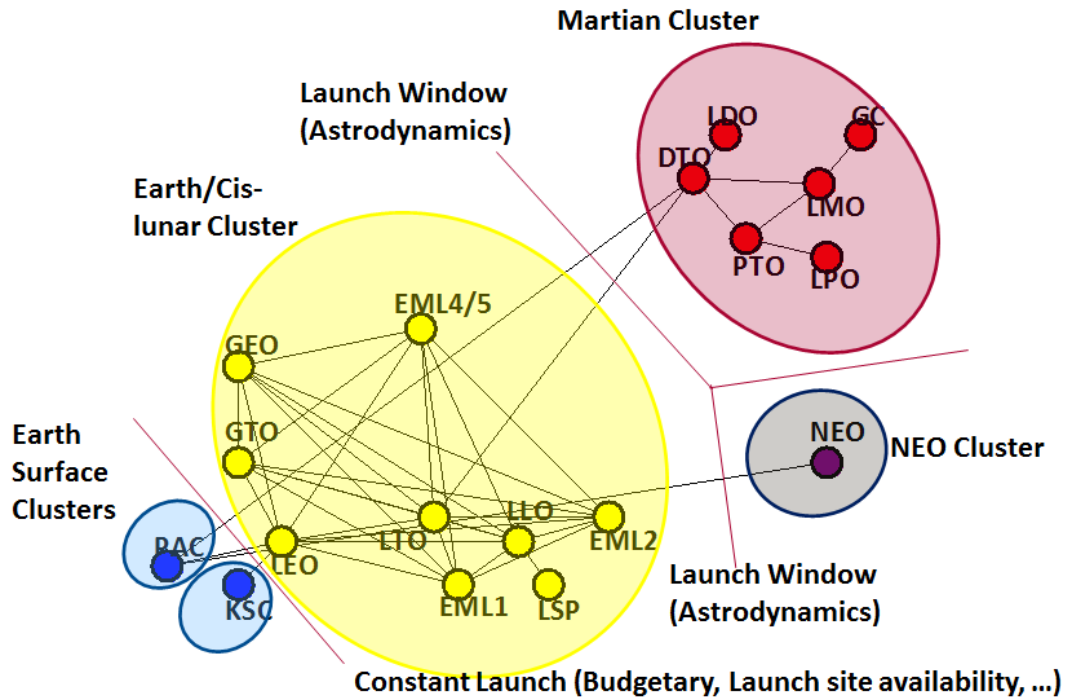
Figure 4-2: Earth-Moon-Mars-NEO logistics network clustering based on time windows (18 nodes, 181 transportation arcs).

the lunar south pole (LSP), a lunar transfer orbit (LTO), a low-lunar orbit (LLO), Earth-Moon Lagrangian points (EML1, EML2, EML 4/5), a low-Phobos orbit (LPO), Phobos transfer orbit (PTO), a low-Deimos orbit (LDO), Deimos transfer orbit (DTO), a low-Mars orbit (LMO), Gale Crater (GC) on the Martian surface, and a representative NEO. Arcs connect each pair of these nodes where transportation is allowed.

For each of the arcs, the following 21 types of commodities are considered:

- Vehicle (Manned)
- Habitat/Payload
- Crew
- Returning Crew/Samples
- Hydrogen
- Oxygen
- Methane
- Water
- Food

- Waste

- LOX/LH2 Inert Mass

- Nuclear Thermal Rockets (NTR) Inert Mass

- LOX/LCH4 Inert Mass

- Hydrogen Tank

- Oxygen Tank

- Methane Tank

- Water Tank

- Aeroshell/Thermal Protection System (TPS)

- Oxygen ISRU Plant

- Water ISRU Plant (with the electrolysis option)

- Methane ISRU Plant

Here, a modelling trick is used to consider Crew and Returning Crew as different commodities in order to make the demand and supply consistent [5]. The crew departs Earth as a commodity "Crew." Once completing the exploration at the destination, it changes its commodity type into "Returning Crew," which is then demanded on Earth. Also, ISRU plants are classified notionally under the following categorization: oxygen generation, water generation, and methane generation.

The objective function is to minimize the total IMLEO coming from KSC over time. This is a typical figure of merit for the "cost" of the space mission or campaign. Other objectives than IMLEO are also possible, but they are not considered in this thesis.

4.2   Demand and Supply

Among these commodities, Habitat/Payload and Crew are demanded on Mars or NEOs depending on the mission, and Returning Crew/Samples are demanded on Earth at a later time. The details are introduced in the corresponding chapter for each case study. Also, infinite supplies are assumed on Earth for all commodities except for Returning Crew/Sample, which originate from the exploration destination.

4.3 Constraints

Important types of constraints include an instantaneous B-matrix, a continuous B-matrix, and a C-matrix.

An instantaneous B-matrix is expressed in the form of $\boldsymbol{x}_{ije}^- = \boldsymbol{B}_{ije}\boldsymbol{x}_{ije}^+$, and is used for impulsive rocket burns and aeroshell staging in the considered application. Both of these constraints consume the resources (e.g., propellants, aeroshell) by an *amount* that is proportional to the entire mass flow. This can be written in the following form:

$$\begin{bmatrix} \text{dry mass} \\ \text{resource} \end{bmatrix}_{ije}^- = \begin{bmatrix} 1 & 0 \\ -\phi & 1-\phi \end{bmatrix}_{ije} \begin{bmatrix} \text{dry mass} \\ \text{resource} \end{bmatrix}_{ije}^+ \tag{4.1}$$

Here, the dry mass stands for all mass that is not resource. In the case of the rocket equation, particularly, ϕ is called the propellant mass fraction and can be computed as follows:

$$\phi_{ije} = 1 - \exp\left(-\frac{\Delta V_{ije}}{I_{\text{sp}}g_0}\right) \tag{4.2}$$

where ΔV_{ije} is the change in the vehicle's velocity along the arc (i,j,e), I_{sp} is the specific impulse of the propulsion system, and g_0 is the standard Earth gravity.

A continuous B-matrix is expressed in the form of $\boldsymbol{x}_{ije}^- = \exp\left(\boldsymbol{B}_{ije}^d \Delta t_{ije}\right)\boldsymbol{x}_{ije}^+$, where Δt_{ije} is the temporal length of the arc (i,j,e). This type of constraint is used for propellant boiloff, crew consumption, waste generation, oxygen leakage, ISRU including its degradation, and continuous rocket thrusting. All of these constraints consume or generate the resources (e.g., propellants, gases, food, waste) by a *rate* that is proportional to the entire or part of the mass flow (e.g., remaining propellants, ISRU plants, crew). In the ISRU example, the resulting equation is in the following form:

$$\begin{bmatrix} \text{ISRU plant} \\ \text{resource} \end{bmatrix}_{ije}^- = \exp\left(\begin{bmatrix} \alpha_d & 0 \\ \beta & \alpha_r \end{bmatrix}_{ije} \Delta t_{ije}\right) \begin{bmatrix} \text{ISRU plant} \\ \text{resource} \end{bmatrix}_{ije}^+ \tag{4.3}$$

where Δt_{ije} is the temporal length of the arc mass transformation. α_d and α_r (≤ 1) show the resource boiloff and degradation of the ISRU plant. β shows the resource generation or loss; $\beta > 0$ if the resource is generated, whereas $\beta < 0$ if it is lost.

If there are multiple processes happening that can be written as B-matrices respectively,

the combined B-matrix can be expressed as a serial multiplication of these corresponding B-matrices:

$$\boldsymbol{B}_{ij} = \boldsymbol{B}_{ij}^{(n)} \cdots \boldsymbol{B}_{ij}^{(2)} \boldsymbol{B}_{ij}^{(1)} \tag{4.4}$$

Note that the order of the multiplication must match the actual sequence of the events since a non-diagonal matrix is generally non-commutative.

A C-matrix, on the other hand, is expressed in the form of $\boldsymbol{C}_{ije}^{+} \boldsymbol{x}_{ije}^{+} \leq \boldsymbol{p}_{ije}^{+}$, and is used for constraints for tank mass, inert mass, crew vehicle mass, aeroshell/TPS mass, and launch capacity. The first four constraints require a certain "carrier" mass to be equal to or larger than an amount that is proportional to the "content."

$$\begin{bmatrix} \eta & -1 \end{bmatrix}_{ije}^{+} \begin{bmatrix} \text{content} \\ \text{carrier} \end{bmatrix}_{ije}^{+} \leq 0 \tag{4.5}$$

where η is the factor of proportionality.

The remaining launch capacity constraints constrain the total mass to be smaller than a certain constant, and therefore can be written in the following way:

$$\begin{bmatrix} 1 & \cdots & 1 \end{bmatrix}_{ije}^{+} \begin{bmatrix} \text{commodity 1} \\ \vdots \\ \text{commodity k} \end{bmatrix}_{ije}^{+} \leq \text{Capacity} \tag{4.6}$$

As described in Chapter 3, in theory, the variables are continuous in time, and therefore an infinite number of constraints are required to describe the flow bounds and constraints. For example, the tank mass needs to support the propellant mass all the time continuously. However, in the space logistics case, the propellant mass would be either monotonically increasing or decreasing over an arc because the arcs are either propellant generation ones (e.g., ISRU) or propellant depletion ones (e.g., boiloff). Although boiloff exists even at the ISRU plant arcs, its rate is so small compared with the ISRU propellant generation rate that we can assume the propellant mass is increasing as a whole at the considered time scale. In this way, the monotonicity of the constraint matrix can be assumed in the space logistics case, which leads to a finite number of constraints.

4.4 Parameters and Assumptions

The following bullet points summarize the major parameters and assumptions used in this research and the subsequent case studies. Other specific parameters and assumptions are listed in each corresponding chapter.

- The time windows for transportation between the Cis-lunar system and the Martian system open every 760 days.

- Launch opportunities from KSC exist every 190 days. The maximum launch capacity for every opportunity is 200 [MT]. This is equivalent to two heavy lift vehicle launches per launch opportunity, or eight heavy lift vehicle launches per Martian system launch window.[1] The reason that a smaller frequency is not considered is due to the compromise between the computational effort and the level of fidelity.

- A one way trip from the Cis-lunar system to the Martian system is assumed to be 200 days.

- LH2/LOX, LH2/LCH4, and NTRs are considered as candidate propulsion technologies. LH2/LCH4 rockets are only used for the Mars descent/ascent stage. NTRs are not allowed for launches from the Earth's surface to LEO for policy and environmental reasons.

- The I_{sp}s of LH2/LOX, LH2/LCH4, and NTRs are assumed to be 450 [s], 369 [s], and 900 [s] respectively [5, 20, 87, 88].

- The tank mass ratios of hydrogen, oxygen, methane, and water, are assumed to be 0.16, 0.02, 0.05, and 0.10 respectively [20, 87, 88]. For depots or long-term transportation (longer than 14 days), a cryocooler is required to store liquid hydrogen, liquid oxygen, or liquid methane. The effective cryocooler inert mass ratio is 0.05 [87].

- The non-tank inert mass ratios of LH2/LOX, LH2/LCH4, and NTRs are assumed to be 0.06, 0.08, 0.14 respectively [5, 20, 87, 88]. These include thruster, propellant feed lines, valves, power processing unit, structural mounts for propulsion system, and any other inert mass except tank.

- The boiloff rates of liquid hydrogen, liquid oxygen, and liquid methane are assumed to be 0.127%, 0.016%, and 0.016% per Earth day respectively, assuming proper tank design [5, 20, 87–89].

---

[1]Space Launch System (SLS) can launch 130 [MT] with its evolved configuration [86].

- For in-space transportation arcs, both propulsive and aerocapture (or direct entry) options are considered whenever applicable. Although crew missions are not allowed to use aerocapture in DRA 5.0 due to the physical size of the crew transfer vehicle [5], that option is considered here as part of the tradespace with proper consideration of the corresponding structure size.

- For aerocapture and entry arcs, an aeroshell/TPS is used. Its mass is assumed to be 40% of the total captured mass. This number follows the assumption in DRA 5.0, which is a significantly larger number than most of the previous analyses [5, 87], and therefore a conservative assumption. It is assumed that an aeroshell/TPS can be reused as long as it stays in orbit, but cannot be reused anymore once it is used for entry at Earth or Mars.

- Every crew member has a mass of 100.00 [kg] including his or her spacesuit.

- Every crew member is assumed to consume 0.88 [kg] of oxygen, 2.90 [kg] of water, and 1.83 [kg] of food, and generates 5.61 [kg] of waste [5, 20] every Earth day.

- Oxygen leakage of 0.00012 [kg] per vehicle unit volume per day is assumed [5].

- ISRU on the Moon is categorized as oxygen generation and water extraction (assuming that water exists) [10]. Electrolysis is possible for the extracted water. For either of these processes, ISRU plant is assumed to generate 5 [kg] of resource per plant mass (in kilogram) per year. This is a very important parameter that was subjected to sensitivity analysis in prior work [5].

- ISRU on Mars is categorized as oxygen generation, methane generation, and water generation (assuming that water exists) [10, 20]. Electrolysis is possible for extracted water. For any of these processes, ISRU plant is assumed to generate 5 [kg] of resource per plant mass (in kilogram) per year for soil- or ice-based oxygen or water generation, and 10 [kg] of resource per plant mass (in kilogram) per year for atmosphere-based oxygen and methane generation [2, 20, 31]. The plant mass defined here does not include the tanks.[2]

- The ISRU degradation is assumed to be effectively 10% plant mass equivalent per year.

- Long-term (longer than 14 days) propellant depots can be placed in a circular orbit

---

[2]For reference, the MOXIE is currently working with a ratio of about 17 [kg] per plant mass (in kilogram) per year [32], but this number does not follow the definition in this research because its plant mass includes the tank mass and excludes the power system mass.

or at a Lagrangian point, but not in a transfer orbits. (Note that these types of constraints were not possible in the static GMCNF formulation.)

- Payloads, vehicles, crew, and ISRU plants cannot be stored in a long-term (longer than 14 days) depot except at LEO for vehicle assembly, but any other commodities (e.g., propulsion systems, consumables, ...) can be stored at any depots for future use.

4.5 Post-Processing

The dynamic GMCNF works well for the space logistics case, but there are also limitations. One of its limitations is its inherent linearization. The results from the LP problem can yield small fractions of mass flow that are not realistically possible. For example, the "optimal" solution can contain a launch that delivers only 1 [kg] of payload to LEO, which is not realistically efficient. In other cases, the "optimal" solution can contain a crew of 0.5 person to flow over an arc, which is infeasible in reality.

This issue can be resolved or mitigated by modeling the system as a mixed-integer linear programming (MILP) problem or by adding post-processing. A MILP can provide an optimal solution with both integer and continuous variables, but it requires a large computational effort. Practically, simple post-processing can provide results that are good enough, and therefore this option is taken here.

In this research, heuristic post-processing is added after every dynamic GMCNF case. When an "optimal" network flow solution is acquired, another optimization is run taking that solution as the initial point. That second optimization includes additional constraints that allow mass to flow over only a subset of the arcs and timings. The excluded sets of arcs and timings are those whose transportation mass flow is smaller than a threshold in the original "optimal" solution. Note that only the corresponding transportation arcs are excluded, while the holdover arcs are not. The threshold is set as 0.50 [MT], which corresponds to a large mini-satellite size. In other words, in the "final" solution after post-processing, no mass is allowed to flow over a transportation arc at a timing when there is a less mass flow than 0.50 [MT] over that arc in the original "optimal" network flow.

In this way, the final solution after the post-processing contains a smaller number of arcs and the flows with unrealistically small mass can be excluded partially. For all cases

considered in this thesis, the IMLEO error caused by the above post-processing is within 1.0%. However, as mentioned previously, the above method does not guarantee the integer constraints. It does not guarantee that all existing flows are above 0.50 [MT], nor does it guarantee that no flows contain only 0.5 person. A complete formulation with MILP is left for future work.

4.6   Chapter Summary

This chapter described the application of the dynamic GMCNF to space logistics network modeling. In addition to the optimization problem formulation, the common assumption for all the later case studies are also introduced. The following chapters show the case studies based on this application.

Chapter 5

Case Study I - Human Exploration of Mars

5.1 Introduction

Human Mars missions have been one of the most important goals in our space exploration history. The final report of the Review of U.S. Human Spaceflight Plans Committee, published in 2009, states that "Mars is the ultimate destination for human exploration of the inner solar system" [7]. Multiple countries, organizations, and even private companies have announced their plans to send humans to Mars [20, 90–94].

One of the most representative mission architectures that have been proposed is Mars Design Reference Architecture 5.0 (DRA 5.0) [20, 95], published in 2009 by NASA.[1] Mars DRA 5.0 provides a systems and operations analysis for the potentially first three missions for human Mars exploration. The architecture is based on the Constellation Program but assumes advanced propulsion systems and ISRU on Mars for a Martian Ascent Vehicle. In the baseline architecture, each crew mission is preceded by a cargo pre-deployment mission. Figure 5-1 shows the baseline architecture of DRA 5.0 as a so-called bat chart, and Figure 5-2 shows the mission sequence timeline as a Gantt chart.

The GMCNF formulation has been applied to the human Mars exploration campaign [5, 97]. Based on this, the objectives of this case study are 1) to demonstrate the usefulness

---

[1]An addendum document was published for DRA 5.0 in 2014 [96], but it has not been integrated into a formal architecture to update DRA 5.0 as of 2015 Spring. Therefore, in this research, the original DRA 5.0 is taken as the baseline architecture.
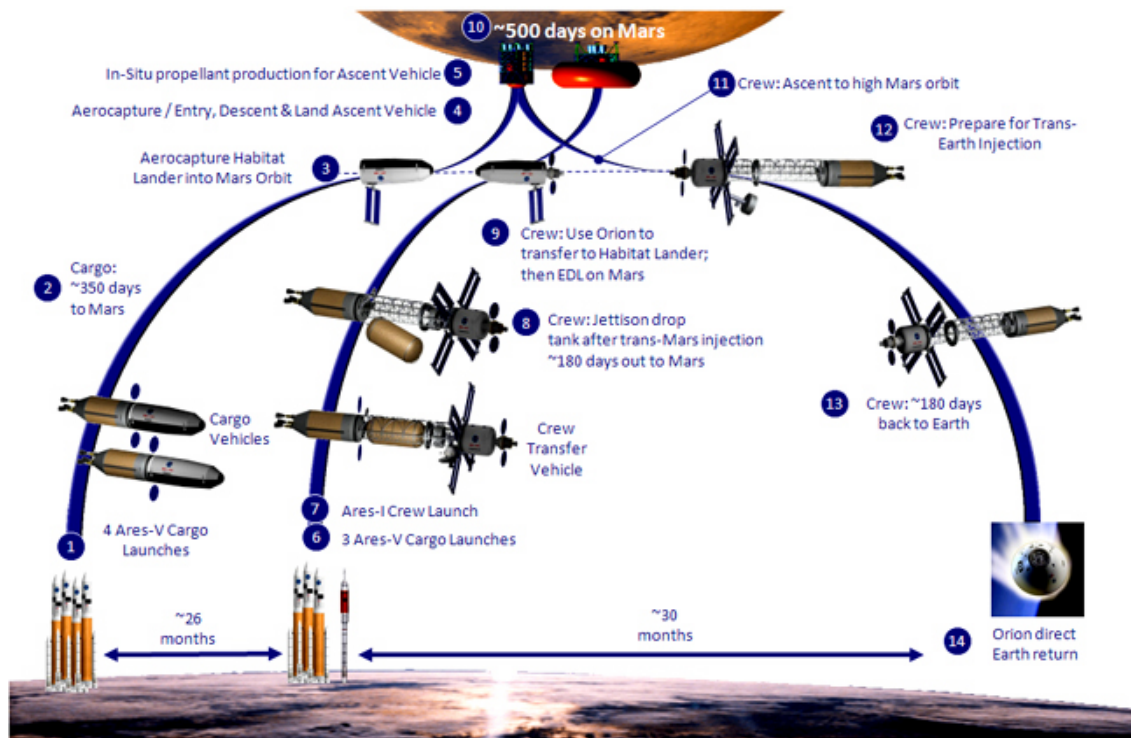
Figure 5-1: Mars DRA 5.0 baseline mission profile.

of the time-expanded GMCNF and 2) to evaluate the potential benefits of using various technologies and architecture decisions in a Mars exploration campaign as well as the trades between them. We assume the same demand/supply and important parameters as DRA 5.0, and evaluate if the dynamic GMCNF can improve the results from DRA 5.0 or the conventional static GMCNF in terms of IMLEO.

In order to assure the accuracy of the model, the dynamic GMCNF model is validated against DRA 5.0 by replicating the scenarios in DRA 5.0. The results are summarized in Table 5.1, and the errors of the resulting IMLEO are within 10%.

Table 5.1: Model Validation against DRA 5.0. "Aero" stands for Aerocapture.

Scenario	DRA 5.0	Dynamic GMCNF Replicating DRA 5.0	Error
NTR	848.7	821.2	3.2%
Chemical + Aero	1,251.8	1,135.9	9.3%

84
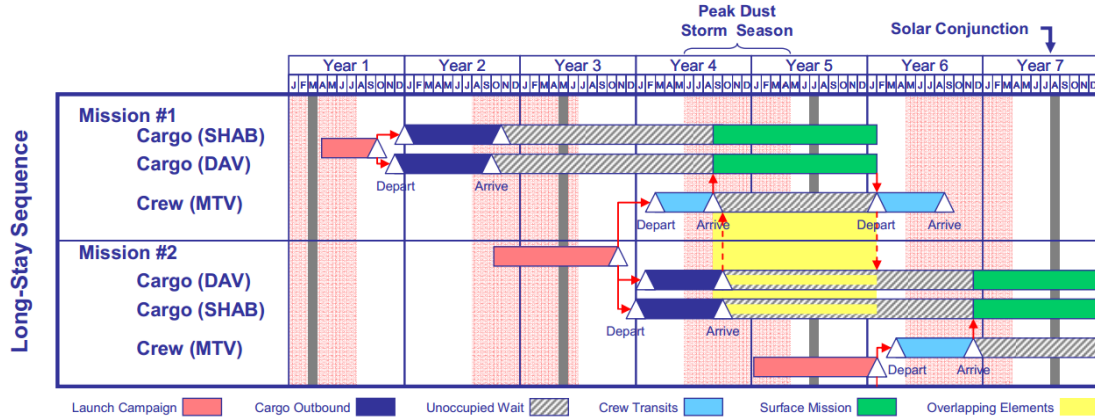
Figure 5-2: Mars DRA 5.0 baseline mission sequence timeline.

5.2 Parameters and Assumption

5.2.1 Demand and Supply

Among the commodities considered in Chapter 4, Habitat/Payload and Crew are demanded on Mars, and Returning Crew/Samples are demanded on Earth. The amount and timing of each demand is specified as an input and is set to be the same as DRA 5.0 [20] as shown in Table 5.2. Habitat mass does not include the consumables, the ISRU plants, or the crew. Also, infinite supplies are assumed to be available on Earth for all commodities except Returning Crew/Samples.

Table 5.2: Demands for each commodity at each location in the Mars exploration case study.

	Habitat [kg]	Crew [ppl]	Crew Return [ppl]	Sample [kg]
Mars	51,700	6	0	0
Earth	0	0	6	250

5.2.2 Other Assumptions

The other parameters and assumptions particularly used in this case study are summarized as follows:

- The crew parks 10 days in space (the Earth/Cis-lunar cluster) before the launch window to the Martian cluster opens.

- The first mission (to LEO) starts 760 days plus the parking period (10 days) before the first Mars launch window opens.

- The Martian surface stay is assumed to be 530 days including the descent/ascent transportation.

- Crew transportation requires a Mars transit habitat (27.54 [MT]) for in-space transportation arcs, a descent/ascent vehicle or crew exploration vehicle (10 [MT]) for descent/ascent/entry transportation arcs, and a surface habitat (51.7 [MT]) for surface stay holdover arcs [20].

For the Mars missions, a similar timeline as the first two missions in DRA 5.0 is considered. The timeline has a cargo pre-deployment mission to Mars followed by a crew mission at the subsequent Mars launch window. The detailed timeline of the time windows is shown in Table 5.3. This information is taken as an input to the optimization.

Table 5.3: Time window assumptions in the Mars exploration case study.

Time [day]	Event
0	Earth's Surface → LEO
190	Earth's Surface → LEO
380	Earth's Surface → LEO
570	Earth's Surface → LEO
760	Earth's Surface → LEO
770	Earth/Cis-lunar Cluster → Martian Cluster
950	Earth's Surface → LEO
1140	Earth's Surface → LEO
1330	Earth's Surface → LEO
1500	Martian Cluster → Earth/Cis-lunar Cluster
1520	Earth's Surface → LEO
1530	Earth/Cis-lunar Cluster → Martian Cluster
1710	Earth's Surface → LEO
1900	Earth's Surface → LEO
2090	Earth's Surface → LEO
2260	Martian Cluster → Earth/Cis-lunar Cluster
2280	Earth's Surface → LEO

5.3   Results and Implications

This section summarizes the results of the Mars case study and their implications.

5.3.1 Results

The comparison between each formulation is shown first in Table 5.4. For reference, the scenario in DRA 5.0 Addendum 2 with the combination of SEP and chemical rockets is also included, although this scenario has not been integrated into the Mars design reference architecture [96]. The numbers of constraints and variables in the formulation in Eqs. (3.11) - (3.12) are used as an indicator of the computational effort in addition to the actual CPLEX optimization time using a desktop computer (Windows 7; Intel(ER) Core(TM) i5-2540M CPU @ 3.40 GHz; RAM 4.00 GB). Note that the numbers of constraints and variables in Table 5.4 contain the entire space logistics map, including the nodes that do not have demands or supplies (e.g., NEOs).

Table 5.4: Comparison of the IMLEO results from each method in the Mars exploration case study.

Method	IMLEO [MT]	Improvement	# of Constraints	# of Variables	Optimization Time [sec]
Reference Architecture (DRA 5.0 NTR Case [20])	848.7	baseline	-	-	-
Reference Architecture (DRA 5.0 Addendum 2 SEP/Chemical Case [96])	~780	-	-	-	-
Static GMCNF	153.8	-81.9%	7,020	4,620	1
Full Time-Expanded GMCNF	Out of Memory	-	~17,000,000	~11,000,000	-
Bi-scale Time-Expanded GMCNF	443.7	-47.7%	807,876	536,319	53,037
Partially Static Time-Expanded GMCNF	431.4	-49.2%	101,868	67,956	217
Uniform Node/Arc Restricted GMCNF	Infeasible	-	936,288	554,589	-

It can be seen that the static GMCNF, which has been presented in the past literature, requires the smallest computational effort and shows a 81.9% improvement in terms of IMLEO. However, this result is unrealistically optimistic as analyzed later.

The full time-expanded GMCNF cannot be run due to its extremely large problem size; therefore the approximation methods discussed in Chapter 3 are applied. The bi-scale time-expanded GMCNF gives a realistic and practically useful solution, which improves the IMLEO by 47.7% relative to the DRA 5.0 baseline. This improvement is much smaller than

the static case, which shows how unrealistic the static GMCNF can be. The computational effort for the bi-scale time-expanded GMFNF is manageable but is still very large. The partially time-expanded GMCNF provides a very good estimate of the realistic solution with a much smaller computational effort.

For reference, the uniform time step GMCNF case that has a similar computational effort to the bi-scale time-expanded GMCNF is shown. This case has 80 uniform time steps, and all the transportation flows that do not happen at those time steps are eliminated. In order to avoid trivial infeasibility, the inter-cluster arcs are exceptionally enabled even if they are not occurring at the selected time steps. However, the results show that even with this exception, the uniform time-step case is still infeasible, although the bi-scale time-expanded GMCNF provides a feasible and realistic solution. This is because the bi-scale time-expanded GMCNF selects its time steps based not only on the inter-cluster arcs and but also on the flows before and after them. This shows the importance of considering the *active* state before and after the time windows.

Note that even if we compare the above results against the case with SEP and chemical rockets, the conclusions are still similar, because that scenario does not improve the IMLEO dramatically from the baseline. However, we can expect that a combination of SEP and chemical rockets can be effective if we use the former for the cargo pre-deployment mission and the latter for the crew mission. Quantification of this effects is left for future work.

Next, a qualitative analysis of the results is shown. Here, the results of the bi-scale time-expanded GMCNF (and the post-processing) are used because it provides the most realistic results.

Figure 5-3 shows the flows of all types of commodities. This shows a complex architecture in the Earth/Cis-lunar cluster and the Martian cluster, where LLO, EML2, and LEO are used for structure storage or propellant depots. Lunar ISRU is used for transportation. When the launch window opens after 760 days, the cargo is launched to Mars for exploration, and another 760 days after that, the crew is launched to Mars.

Figure 5-4 shows the crew flow, and Figure 5-5 shows the ISRU plant deployment flow. In addition, Table 5.5 shows the IMLEO breakdown for each launch.

The result shows that both the crew and ISRU plant transportation operations mainly rely on chemical rockets except the first plant launch, which mainly uses NTRs. In fact in Figure 5-3, we can observe a dynamic shift from NTRs use to increased use of chemical
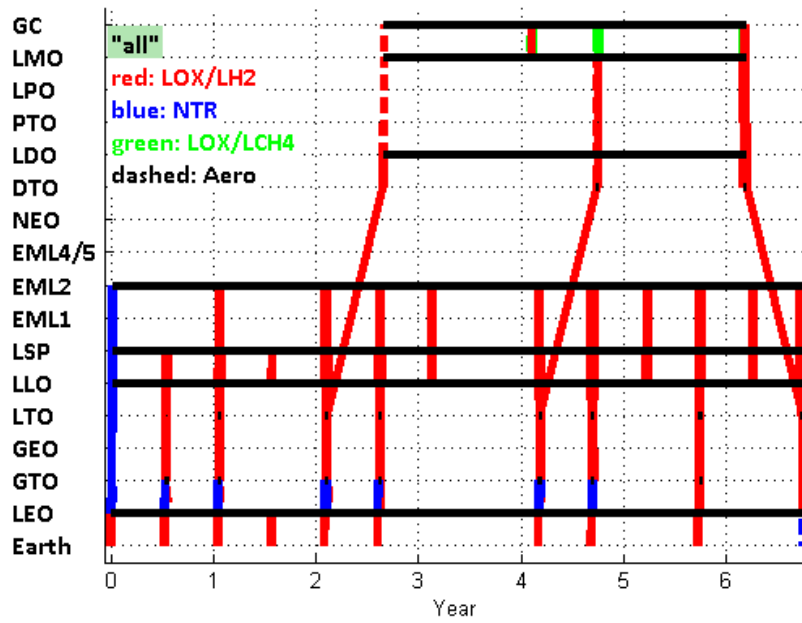
Figure 5-3: Bat chart: all commodity flows for the Mars exploration case study. "Aero" stands for aerocapture/entry.
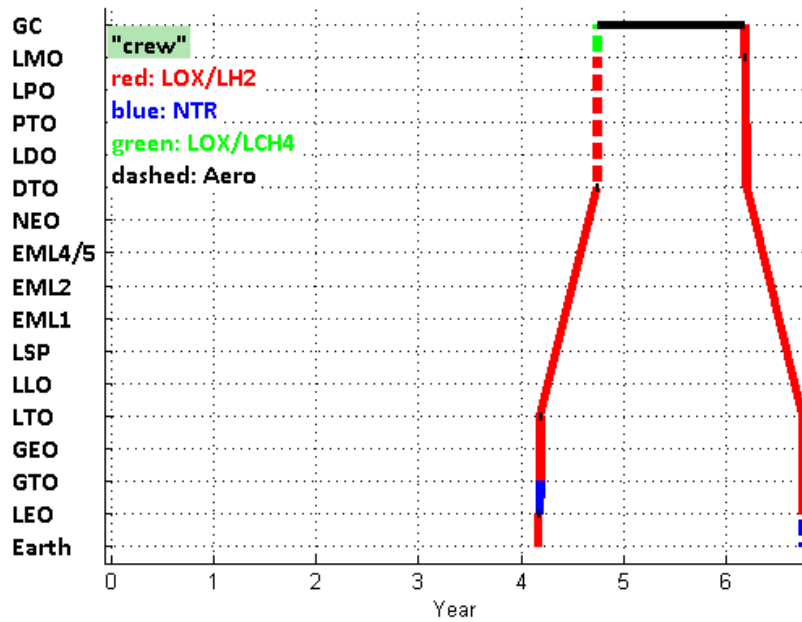
Figure 5-4: Bat chart: crew flow for the Mars exploration case study. "Aero" stands for aerocapture/entry.
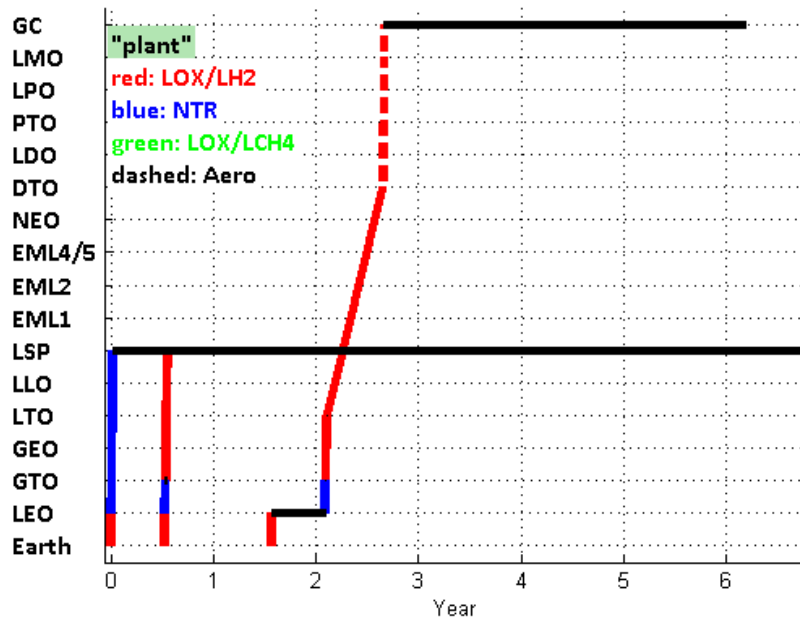
Figure 5-5: Bat chart: ISRU plant flow for the Mars exploration case study. "Aero" stands for aerocapture/entry.

rockets as time evolves. This can be explained as follows: Chemical rockets require both oxygen and hydrogen as the propellants and have a low inert mass ratio but a low I_{sp}, whereas NTRs only require hydrogen and have a high I_{sp} but a high inert mass ratio. Thus, chemical rockets can be particularly useful if their relatively low I_{sp} can be compensated by increasingly using ISRU-generated resources. In other words, as the ISRU plants generate more oxygen, chemical rockets become preferable to NTRs despite their low I_{sp}. Table 5.5 also shows that no oxygen or methane needs to be launched from Earth (except for LOX in the Earth to LEO launch). Oxygen and methane can be generated entirely by ISRU, and NTRs are used before that occurs and chemical rockets are used after it. (Table 5.5 also shows launches of a large amount of water ISRU plant, which shows the importance of water as well as oxygen and hydrogen processed from it as a potential ISRU-generated resource.)

A similar trend can also be observed for aerocapture. Aerocapture does not require propellant but requires a large aeroshell/TPS mass. When the ISRU plants have not generated a sufficient amount of resources yet, the aerocapture option is preferred for Mars arrival. However, as the lunar ISRU system matures, there are enough propellant so that part of the

Table 5.5: IMLEO breakdown for each commodity at each launch from Earth in the Mars exploration case study.

Launch Date [day]	0	190	380	570	760	950	1020	1710	2090
Vehicle [MT]	0	0	0	0	27.54	0	10.00	0	0
Habitat/Payload [MT]	0	0	39.11	0	0	0	12.59	0	0
Crew [MT]	0	0	0	0	0	0	0.60	0	0
Hydrogen [MT]	14.98	8.93	4.19	0	62.55	1.55	48.79	0	0
Oxygen [MT]	0	0	0	0	0	0	0	0	0
Methane [MT]	0	0	0	0	0	0	0	0	0
Water [MT]	0	0	0	0	0	0	0	0	0
Food [MT]	0	8.93	0	0	0	0	2.32	0	0.03
LOX/LH2 Inert [MT]	1.01	0	5.98	0	0.01	6.31	0.01	0.50	0
NTR Inert [MT]	3.16	1.06	0	1.16	0	0	0	0	0
LOX/LCH4 Inert [MT]	0	0	0	2.68	0	0	0	0	0
Hydrogen Tank [MT]	2.85	1.70	0.80	0	11.91	0.29	9.29	0	0
Oxygen Tank [MT]	1.12	0	6.31	0	0	0.86	0	0	0
Methane Tank [MT]	0	0	0	0	1.31	0	0	0	0
Water Tank [MT]	0	0	0.97	0	0	0	0	0	0
Aeroshell/TPS [MT]	1.97	0	0	58.31	0	35.96	0	0	4.05
Oxygen ISRU Plant [MT]	0	0	0	2.34	0	0	0	0	0
Water ISRU Plant [MT]	11.04	15.46	0	11.09	0	0	0	0	0
Methane ISRU Plant [MT]	0	0	0	2.02	0	0	0	0	0
Total [MT]	36.13	36.08	57.36	77.61	103.33	44.98	83.60	0.50	4.08

mass can be transported using chemical rockets and the ISRU-generated propellant instead of the aerocapture system. This results from the trade between the aeroshell/TPS mass and the ISRU capability. If there are additional constraints on the available IMLEO profile, the optimal technology selection can vary accordingly.

The above effects cannot be observed in the static model because it does not consider the amount of propellant the ISRU plants have generated before the crew departure. It overoptimistically assumes that plenty of ISRU-generated oxygen is available for chemical rockets, but it turns out that this is actually not feasible due to the time paradoxes mentioned in Chapter 2. Therefore, the overoptimistic static GMCNF can lead to qualitatively inaccurate conclusion without considering the dynamic technology choice, which is one of the reasons why the dynamic GMCNF is necessary.

Also, the optimal solution shows that, after the first ISRU plant deployment to LSP, the propellant generated by it is used for reusable vehicles including tankers between the ISRU

surface plants and the on-orbit depots. These vehicles can be used for propellant supply for the depots, tank structure supply for the ISRU plants, and even deployment of further ISRU plants. In the optimal solution, two types reusable vehicles are considered, one in the Earth/Cis-lunar cluster and the other in the Martian cluster. The former connects the Moon, the depots at LLO and EML2, and the Earth orbits, using LOX/LH2 as the propellants. This reflects the abundant ISRU-generated resources on the Moon and the expensive launch from Earth. The latter connects the Martian surface and LMO, using LOX/LCH4 as the propellants. This reflects the relatively easier access to oxygen and methane from the Martian atmosphere than hydrogen from the water ice/soil. This use of the ISRU-based vehicles implies that previous mission can *enable* subsequent missions by transforming and prepositioning propellant to the right location at the right time, which is not observed in the static results.

Here, we can see a new type of systems deployment architecture: *self-sustained deployment*. This means the system is deployed in stages, and after deployment of the first stage, the subsequent stages are deployed with the *help* of the previous stages. In this case, the ISRU plants are deployed in stages using the propellant from the previously deployed ISRU. This trend is expected to be more obvious and beneficial with a longer campaign.

Another interesting observation about aeroshell/TPS is that, in the optimal solution, the crew does not return to Earth directly from the Mars. When the crew enters the Earth/Cis-lunar cluster, a new set of aeroshell/TPS hardware is launched and docked with the return vehicle, which is then used for Earth reentry. This adds complexity to the system, but can save the IMLEO because the vehicle does not need to carry the Earth reentry aeroshell/TPS all the way to Mars and back.

All of the above results show important hidden trades among propulsion, aerocapture technologies, and ISRU. Technologies for NTR and SEP, aerocapture, and ISRU have been developed relatively separately so far, and not many studies have considered the trades among them. However, it is shown here that it is important to consider these technologies together because their usages are highly coupled.

It requires additional discussion whether this proposed mission architecture is operationally feasible or not, but it is shown numerically that this architecture is mass efficient with the assumptions considered here. It is possible to create a more detailed model of the propulsion and other systems and plug it into the optimization to gain results with a higher

level of fidelity. Future work will also explore the Pareto front between IMLEO, complexity, and risk.

5.3.2 Sensitivity Analysis

This subsection discusses a sensitivity analysis for the results from the dynamic GMCNF presented in the previous section. As an approximation method for the dynamic GMCNF, the partially static time-expanded GMCNF is used since it provides a very good estimate of the optimal IMLEO with a small computational effort. The purpose of the sensitivity analysis is to evaluate how technology development and maturity can impact the results, particularly the IMLEO.

As shown previously, the dynamic GMCNF improves the IMLEO by about 50% compared with DRA 5.0. This is a large improvement and is due to the combination of propulsion technologies as well as the ISRU availability. The following discusses the breakdown of that improvement.

The DRA 5.0 baseline assumes availability of NTRs from Earth and LOX from the Martian atmosphere harvested via ISRU. The mission sequence of the DRA 5.0 baseline uses NTRs for all the in-space transportation operations and Martian ISRU is only used for ascent from the Martian surface. ISRU has a rather limited local role in DRA 5.0. In contrast, the solution provided by the dynamic GMCNF assumes availability of both chemical rockets and NTRs as well as aerocapture, lunar ISRU for oxygen and water, and Martian ISRU for oxygen, water, and methane. The relative contribution of each technology to that improvement is shown in Figure 5-6.

Figure 5-6 shows that the effect of the combination of propulsion technologies only improves the IMLEO by about 9%. Instead of using only NTRs or only chemical rockets for all the transportation operations, using both of them as well as aerocapture strategically can benefit IMLEO. This is especially true when we view the campaign dynamically. For example, when the ISRU plants have not generated enough oxygen yet, NTRs are preferred, but as more oxygen is generated, chemical rockets are preferred because they use oxygen as the oxidizer and have a lower inert mass fraction.

This propulsion system flexibility can improve the IMLEO performance especially if it is combined with ISRU. Availability of Martian ISRU for water and oxygen further improves the IMLEO by about 29%. Additionally, lunar ISRU can improve the performance by about
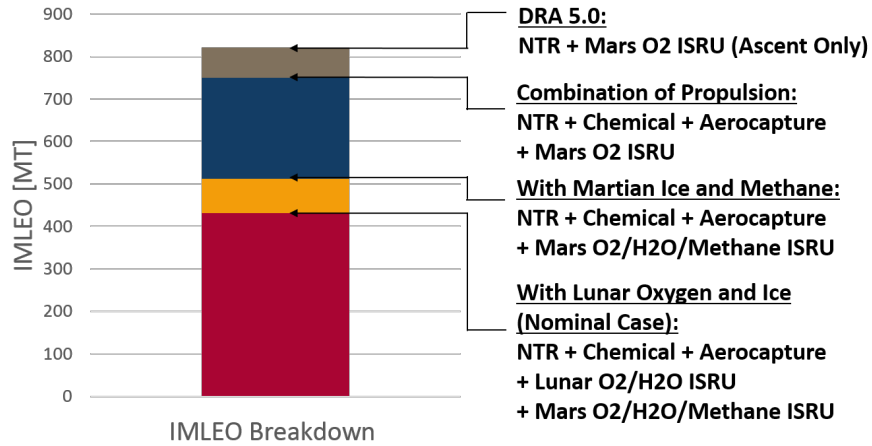
Figure 5-6: Breakdown of the IMLEO improvement relative to DRA 5.0 by propulsion, aerocapture, and ISRU technologies in the Mars exploration case study.

10% more. These results show the importance of ISRU availability, which further justifies various existing missions to the Moon or Mars searching for water ice.

For the combination of propulsion technologies, another type of sensitivity analysis is performed. Here, the problem setting is changed to only NTRs or only chemical rockets with aerocapture as DRA 5.0 assumed. The difference between this results and DRA 5.0 is availability of ISRU. DRA 5.0 only assumes oxygen generation on Mars as the baseline, but this study assumes other processes as described previously both on the Moon and Mars. The results are shown in Table 5.6.

Table 5.6: Comparison of the IMLEO results from the scenarios with only NTRs and only chemical rockets + aerocapture in the Mars exploration case study. "Aero" stands for aerocapture.

Scenario	IMLEO [MT]
DRA 5.0 NTR	848.7
DRA 5.0 Chemical + Aero	1,251.8
Dynamic GMCNF NTR + ISRU	736.0
Dynamic GMCNF Chemical + Aero + ISRU	528.7

From these results, it can be seen that availability of ISRU provides significant improvement for the chemical rocket option, but not so much for the NTR option. This is because with ISRU available both on the Moon and Mars, chemical rockets require less IMLEO than NTRs, which is the opposite of the results in DRA 5.0. This shows the interaction between

ISRU and propulsion technologies, which leads to initially counterintuitive results.

In addition, a sensitivity analysis against uncertainties in technology development and maturity can also be performed. One of the largest technological uncertainties in the proposed architecture is the ISRU capability, especially on the Moon, defined as the amount of resource generated by unit mass of plant per year [5]. ISRU technologies still have a low Technology Readiness Level (TRL), and no hardware has been launched to space for testing as of early 2015.[2] Therefore, instead of simply fixing the ISRU capability at one value, we need to vary that parameter to see how it affects the IMLEO performance. The results from varying levels of the lunar ISRU capability are shown in Figure 5-7.
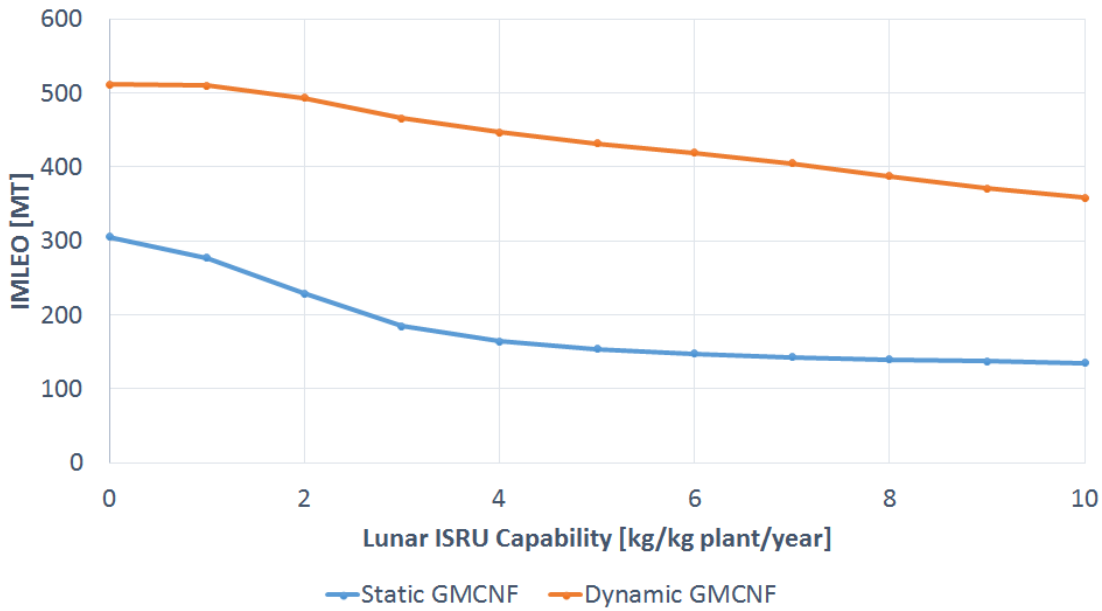
Figure 5-7: Sensitivity of the IMLEO results against the lunar ISRU capability in the Mars exploration case study.

As can be seen in Figure 5-7, in the dynamic GMCNF, as the lunar ISRU capability increases, the required IMLEO decreases. When the ISRU capability is 5 [kg/kg plant/year], our baseline assumption, the IMLEO is reduced by about 15.7% (from 511.5 [MT] to 431.4 [MT]) from the no-ISRU case. This shows that it is very critical to improve the capability of lunar ISRU technologies.

Another interesting finding is that the IMLEO from the static GMCNF is more sensitive to the lunar ISRU capability than that from the dynamic GMCNF when the ISRU capability

---

[2]The first ISRU experiemnt in space will be MOXIE on the Mars 2020 rover mission [32].

is less than 5 [kg/kg plant/year]. This effect is caused by the drawback of the static GMCNF not considering the time dimension. In the optimal solution from the static GMCNF without consideration of a time horizon, the cargo and crew missions happen after a sufficient amount of propellant is generated by ISRU, no matter how long it takes, and use chemical rockets as the main propulsion system with ISRU-generated resources. Therefore, the mission heavily relies on ISRU, and even if the ISRU capability is low, the IMLEO is still very sensitive to the ISRU capability. In reality, however, this is not accurate because we have a limited time horizon and if the ISRU capability is low, we cannot wait for a long time until enough propellant is generated; instead we also need to think about relying more on NTRs with Earth-originating resources particularly in the initial stages of the campaign. This results in the fact that the architecture relies less on lunar ISRU and so its IMLEO is less sensitive to the lunar ISRU capability than that from the static GMCNF when the ISRU system is not very capable. The necessity to capture the effects of the time dimension is the very reason to use the dynamic GMCNF.

Note that the gap between the static GMCNF and the dynamic GMCNF results is expected to shrink as the number of missions increases. This is because as the time horizon increases, ISRU pays off over time and the system gradually enters a steady state.

Besides ISRU, aerocapture is also an area that requires significant technology development. As shown in Chapter 4, this research assumes that the aerocapture and entry arcs require an aeroshell/TPS that is 40% of the total captured mass. This number is estimated based on DRA 5.0, but it is significantly larger than in the past literature, which typically uses 15% as the ratio of aeroshell/TPS to the total captured mass [5,87]. Given this modeling uncertainty, instead of simply fixing the aeroshell/TPS requirement as a fixed value, we need to vary that parameter to see how it will affect the system's performance. The result is shown in Figure 5-8.

The results show that the improvement we can get by improving the aeroshell/TPS mass fraction is significant. If we could improve the ratio of the aeroshell/TPS to the total captured mass from 40% to 15%, then the IMLEO can be improved by 39.3% (from 431.4 [MT] to 262.0 [MT]). This can be explained by the large gear ratio (i.e., ΔV) required to deliver the aeroshell/TPS all the way to Mars. This shows that the resulting architecture heavily relies on the aerocapture technology, and that it is important to improve the performance of aerocapture and entry as well as modeling the technology accurately.
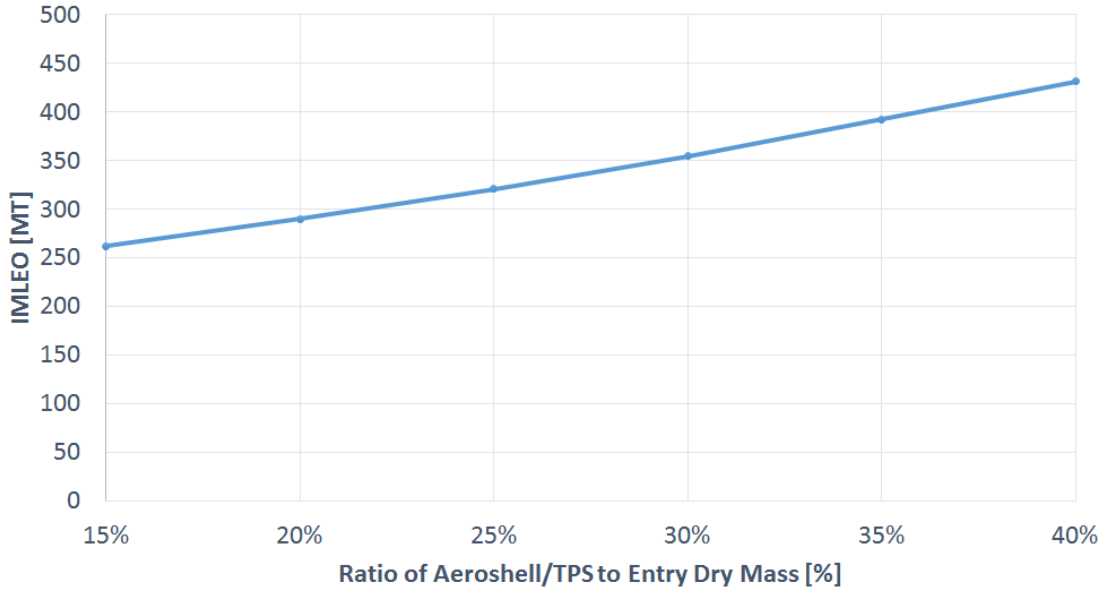
Figure 5-8: Sensitivity of the IMLEO results against the aeroshell/TPS fraction in the Mars exploration case study.

Finally, another important technology that needs to be considered is boiloff control for the propellant depots. This research assumes a boiloff rate of 0.127% per Earth day for liquid hydrogen, 0.016% per Earth day for liquid oxygen, and 0.016% per Earth day for liquid methane as shown in Chapter 4, but it is important to assess the effect of boiloff in the propellant depots or propulsion system design throughout the entire mission. Table 5.7 shows the effects of boiloff. Since the propellant boiloff is highly related to the time dimension, the static results are also shown for reference.

Table 5.7: Comparison of the IMLEO results from the scenarios with boiloff and without boiloff in the Mars exploration case study.

Scenario	IMLEO [MT]
Static GMCNF with boiloff	153.8
Static GMCNF without boiloff	152.6
Dynamic GMCNF with boiloff	431.4
Dynamic GMCNF without boiloff	397.0

The results show that the improvement by removing boiloff is 8.0% in terms of IMLEO when the dynamic GMCNF is considered. The static GMCNF shows an inaccurate result, 0.7% improvement, because it does not consider the time dimension accurately. Controlling

boiloff requires additional mass and complexity such as thermal management and attitude control systems, and it is important to evaluate whether zero boiloff technology pays off or not. More detailed studies on the effect of improved boiloff control technology are left for future work.

5.4   Case Study Summary

In this case study, the human Mars exploration scenario is analyzed. DRA 5.0 is assumed as the baseline, and the dynamic GMCNF is evaluated how the space infrastructure can support the missions and improve the IMLEO performance from the baseline.

The results show that a strategically deployed Cis-lunar and Martian infrastructure can improve the IMLEO significantly, resulting in an about 50% IMLEO reduction. The ISRU system is deployed in stages in a *self-sustained* manner, where the first unit is deployed using NTRs and the remaining stages are deployed using chemical rockets and the resources generated by the previously deployed ISRU plants. After the ISRU plants have generated a sufficient amount of propellant, chemical rockets are used for the major transportation operations between Earth and Mars. Reusable chemical rockets are used for the transportation operations between the ISRU plants and the depots in both the Earth/Cis-lunar cluster and the Martian cluster. Overall, the resulting Mars exploration architecture relies heavily on both lunar ISRU and Martian ISRU.

The results imply an important technology trades between ISRU, NTRs, chemical rockets, and aerocapture technology development as well as boiloff control at propellant depots. As ISRU technologies mature, chemical rockets might be preferred to NTRs due to the easy accessibility of oxygen from the Moon or Mars. However, during the deployment of ISRU plants, NTRs and aerocapture are still important technologies to be used. In the longer term, NTRs could then be deployed to pioneer human exploration beyond mars towards the outer solar system.

Chapter 6

Case Study II - Human Exploration of a Near Earth Objects (NEO)

6.1 Introduction

Near-Earth objects (NEOs) are the asteroids and comets whose orbits approach or intersect the Earth's orbit in the solar system [6]. One of the advantages of exploring NEOs is preparation for future exploration on the Moon and Mars. In a NEO mission, we can test and validate the hardware and operations for future exploration missions beyond LEO [98]. Another important advantage of exploring NEOs is the scientific return. NEOs contain a significant amount of information about our early solar system history, as demonstrated by the past robotic missions such as Hayabusa [99]. Crew missions to NEOs can enhance the quality of scientific data collected from NEOs.

The concepts of human exploration to NEOs is not new; the first published NEO mission, proposed by Smith [100] in 1966, was a 527-day trip to 433 Eros with upgraded Apollo/Saturn 5 hardware. More recently, NASA has performed a feasibility analysis for human missions to 1999 AO10, 2000 SG344, and 2006 DQ14 using the hardware from the Constellation Program (i.e., Ares vehicles and Orion spacecraft) [6, 98]. Even after the Constellation Program was canceled in 2011, NASA's Human Architecture Team has been exploring detailed designs for missions to 2008 EV5 [101, 102] using the SLS and Multi-

Purpose Crew Vehicle (MPCV).

In this case study, the 14-day-stay 1999 AO10 mission [6] is considered as the baseline. The trajectory plot of this 2025-2026 mission is shown in Figure 6-1. The objectives of this case study analysis are 1) to further demonstrate the usefulness of the time-expanded GM-CNF and 2) to evaluate the potential benefits of using various technologies and architecture decisions in the NEO exploration case as well as the trades between them. We compare our results with NASA's planned mission for 1999 AO 10, and evaluate how the dynamic GMCNF can improve the results using the Cis-lunar infrastructure.
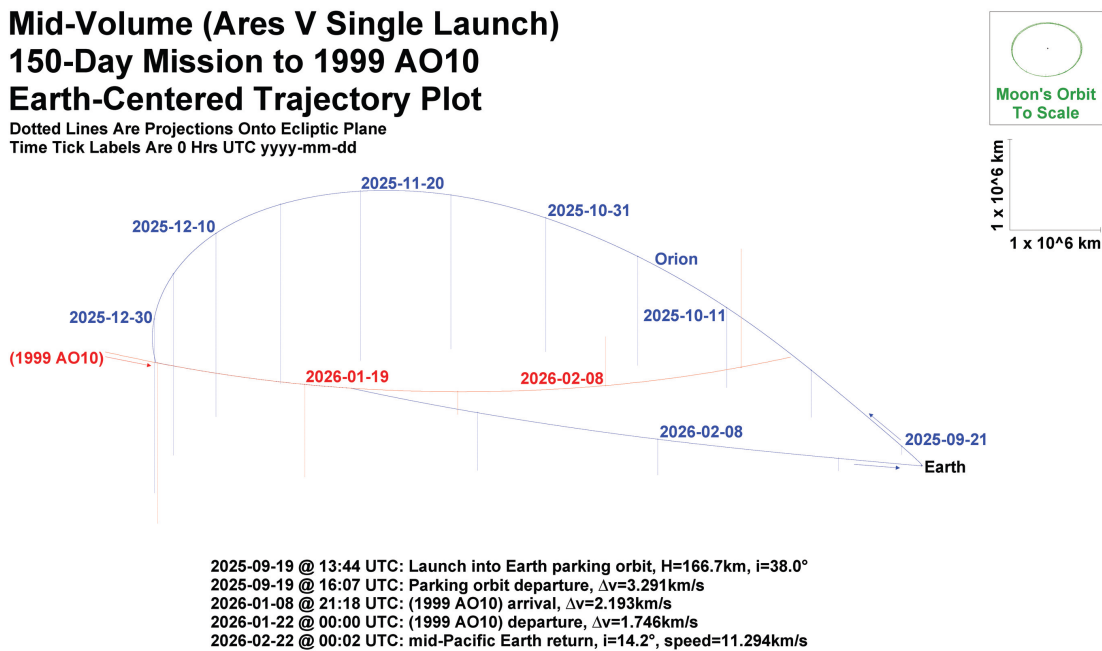
Figure 6-1: An Earth-centered trajectory plot showing a possible 150-day mission profile to NEO 1999 AO10 [6]. The Moons orbit is shown for scale in the upper right.

6.2 Parameters and Assumption

6.2.1 Demand and Supply

Among the commodities considered in Chapter 4, Payload and Crew are demanded on the NEO 1999 AO10, and Returning Crew is demanded on Earth. The amount and timing of each demand, shown in Table 6.1, are notional. Note that for the NEO mission, since the exploration is so short that it does not require a specific surface habitat, science equipment

payload is demanded during the surface operation. In the optimization, the timings of the demands are also specified as an input. As before, infinite supplies are assumed to be available on Earth for all commodities except Returning Crew.

Table 6.1: Demands of each commodity at each location in the NEO exploration case study.

	Habitat/Payload [kg]	Crew [ppl]	Crew Return [ppl]
NEO	1,000	2	0
Earth	0	0	2

6.2.2 Other Assumptions

For this case study, the trajectory shown in Figure 6-1 is used. The other parameters and assumptions particularly used in this case study are summarized as follows:

- The crew parks 10 days in space (the Earth/Cis-lunar cluster) before the launch window to the NEO 1999 AO10 opens.
- The first mission (to LEO) starts 700 days plus the parking period (10 days) before the first 1999 AO10 launch window opens.
- Crew transportation requires a transit habitat (12.5 [MT]) for in-space or entry arcs.

The detailed timeline of the time windows is shown in Table 6.2. The first four launch windows to LEO are used for infrastructure pre-deployment.

Table 6.2: Time window assumptions in the NEO exploration case study.

Time [day]	Event
0	Earth's Surface → LEO
190	Earth's Surface → LEO
380	Earth's Surface → LEO
570	Earth's Surface → LEO
700	Earth's Surface → LEO (Crew Launch)
710	Earth/Cis-lunar Cluster → NEO
760	Earth's Surface → LEO
835	NEO → Earth/Cis-lunar Cluster

6.3 Results and Implications

This section provides the results of the NEO case study and their implications.

101

6.3.1 Results

In the similar way as the Mars case study, the comparison between each formulation is shown first in Table 6.3. One Ares V launch is used as the baseline. The numbers of constraints and variables in the formulation in Eqs. (3.11) - (3.12) are used as an indicator of the computational effort in addition to the actual CPLEX optimization time using a desktop computer (Windows 7; Intel(ER) Core(TM) i5-2540M CPU @ 3.40 GHz; RAM 4.00 GB). Note that the numbers of constraints and variables in Table 6.3 contain the entire space logistics map, including the nodes that do not have demands or supplies (e.g., Mars).

Table 6.3: Comparison of the IMLEO results from each method in the NEO exploration case study.

Method	IMLEO [MT]	Improvement	# of Constraints	# of Variables	Optimization Time [sec]
Reference Architecture (No ISRU; Chemical Rockets [6])	141.2	baseline	-	-	-
Static GMCNF	24.1	-82.9%	7,020	4,620	< 1
Bi-scale Time-Expanded GMCNF	73.2	-48.1%	315,786	209,937	6,070
Partially Static GMCNF	73.3	-48.1%	42,300	28,287	25

As with the Mars case study, the static GMCNF shows a significant improvement (82.9%), but this is overoptimistic. The bi-scale time-expanded GMCNF, which provides an upper bound of the full time-expanded GMCNF still improves the IMLEO by 48.1%. Note that this bi-scale time-expanded GMCNF does not only provide the bound, but is also practically useful because it considers the active and dormant phase as discussed previously. Finally, the partially static time-expanded GMCNF is shown to give a good estimate of the realistic IMLEO with a small computational effort.

Next, a qualitative analysis of the results is shown. Here, the results of the bi-scale time-expanded GMCNF (and the post-processing) are used because it provides the most realistic results.

Figure 6-2 shows the flows of all types of commodities. This shows a complex architecture in the Earth/Cis-lunar cluster, where LLO and LEO are used for structure storage or propellant depots. Lunar ISRU is used for transportation. When the launch window opens after 700 days, the crew and cargo are launched to the NEO for exploration. Note that

although from the results it seems that a NTR has to reenter Earth's atmosphere, which is not favorable for policy and environmental reasons, in reality the final deceleration is performed using direct entry, and so the NTR engine itself can be staged before the entry to Earth's atmosphere.
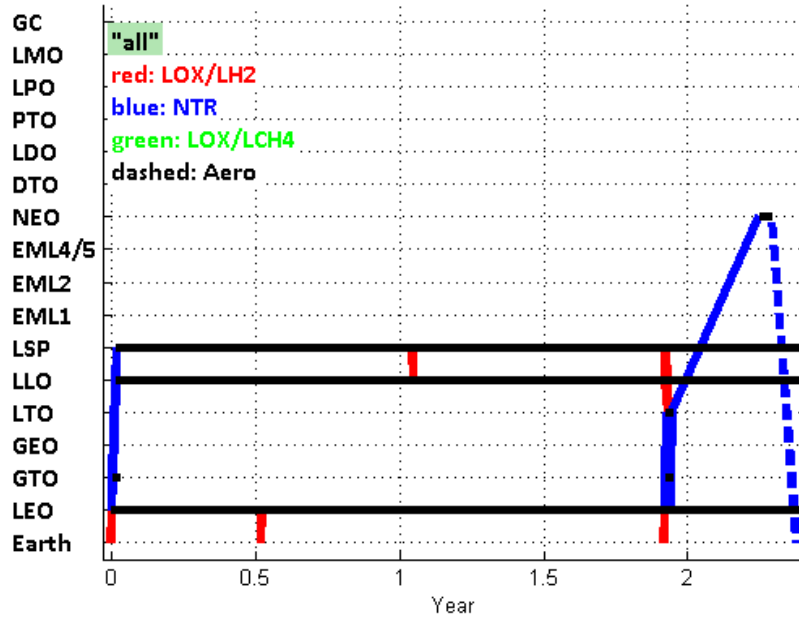
Figure 6-2: Bat chart: all commodity flows for the NEO exploration case study. "Aero" stands for aerocapture/entry.

As in the Mars exploration case, the focus is put on the crew transportation and ISRU plant deployment. Figure 6-3 shows the crew flow, and Figure 6-4 shows the ISRU plant deployment flow. In addition, Table 6.4 shows the IMLEO breakdown for each launch.

The result shows that both the crew and plant transportation operations mainly rely on NTRs. This can be explained as follows: As shown in Chapter 5, chemical rockets can be useful if their low I_{sp} can be compensated by using the oxygen generated by lunar ISRU. However, given the timeline and the required propellant for the considered NEO case, unlike in the Mars case, it turns out that it is more beneficial to use NTRs for the major transportation operations between Earth and NEO than to use chemical rockets. (The hydrogen for the NTR transportation operations is partly from the lunar ISRU.)

However, chemical rockets are still used for the transportation operations between the lunar surface (i.e., LSP) and the depots in LLO. Reusable tanker vehicles transport both
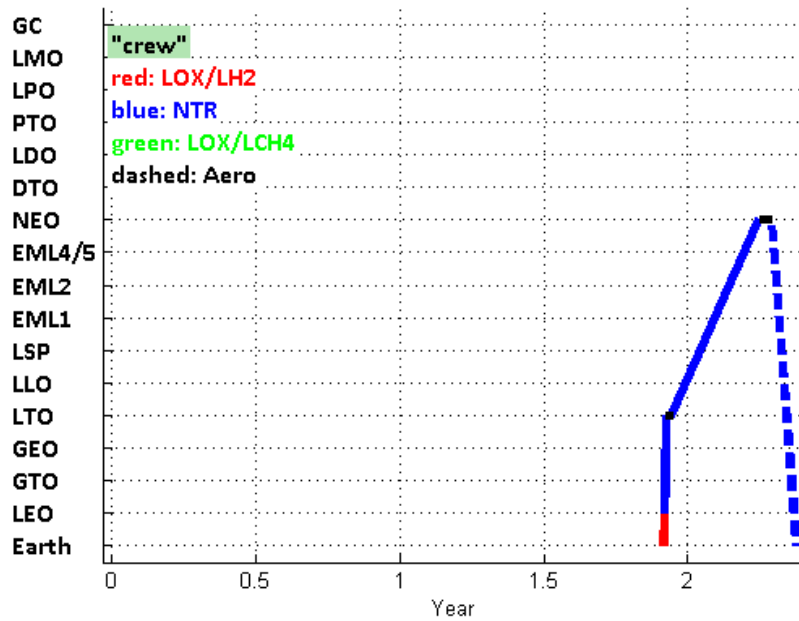
Figure 6-3: Bat chart: crew flow for the NEO exploration case study. "Aero" stands for aerocapture/entry.
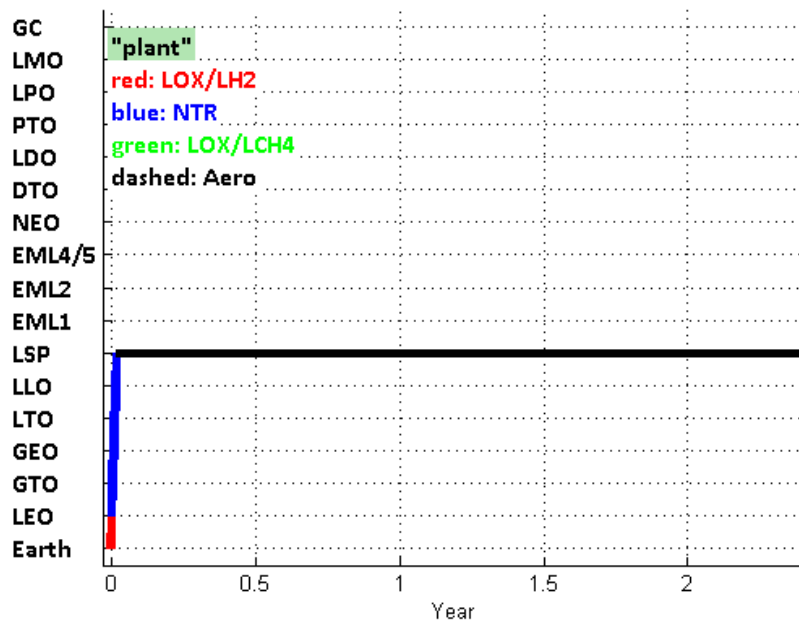
Figure 6-4: Bat chart: ISRU plant flow for the NEO exploration case study. "Aero" stands for aerocapture/entry.

Table 6.4: IMLEO breakdown for each commodity at each launch from Earth in the NEO exploration case study.

Launch Date [day]	0	190	700
Vehicle [MT]	0	0	12.51
Habitat/Payload [MT]	0	1.00	0
Crew [MT]	0	0	0.20
Hydrogen [MT]	1.01	0	36.82
Oxygen [MT]	0	0	0.01
Methane [MT]	0	0	0
Water [MT]	0	0	0.02
Food [MT]	0	0.61	0
LOX/LH2 Inert [MT]	0.17	0	0
NTR Inert [MT]	5.33	0	0
LOX/LCH4 Inert [MT]	0	0	0
Hydrogen Tank [MT]	0.19	0	7.01
Oxygen Tank [MT]	0.07	0	0
Methane Tank [MT]	0	0	0
Water Tank [MT]	0.11	0	0.01
Aeroshell/TPS [MT]	0	7.67	0
Oxygen ISRU Plant [MT]	0	0	0
Water ISRU Plant [MT]	0.51	0	0
Methane ISRU Plant [MT]	0	0	0
Total [MT]	7.39	9.28	56.59

propellants for the depots and the tank structure for the ISRU plants, and use the outputs of the lunar ISRU plants as their propellants. Because these transportation operations happen near the ISRU plants on the Moon, it is more efficient to use oxygen from the Moon to take advantage of the low inert mass ratio of chemical rockets. This trend is similar to the ISRU self-sustained deployment we observed in the Mars case, but in this case the plants need not to be deployed in stages because their mass is small.

In a similar way as the Mars case, this case provides another convincing results showing the importance of considering NTR and ISRU technologies together because their usages are highly coupled. In some cases such as the Mars exploration case, ISRU is very effective, whereas in other cases such as the NEO exploration case, ISRU is not effective and instead NTR technology is important. Note that in order to implement the resulting architecture, there needs to be a trade against the system complexity and operational feasibility and risk. The model can be made more detailed to consider these trades, which is left for future

work.

6.3.2 Sensitivity Analysis

This subsection discusses a sensitivity analysis for the results from the dynamic GMCNF. As an approximation method for the dynamic GMCNF, the partially static time-expanded GMCNF is used since it gives a very good estimate of the optimal IMLEO with a small computational effort.

First, the sensitivity of the results against the propulsion technology capability is shown. In a similar way as the Mars case study, the problem setting is changed to only NTRs or only chemical rockets. The results are shown in Table 6.5.

Table 6.5: Comparison of the IMLEO results from the scenarios with only NTRs and only chemical rockets in the NEO exploration case study.

Scenario	IMLEO [MT]
Dynamic GMCNF NTR + ISRU	74.3
Dynamic GMCNF Chemical + ISRU	100.7

The NTR option provides lower IMLEO than the chemical rocket option even with ISRU available. In fact, the NTR + ISRU case is almost the same as the dynamic GMCNF case in Table 6.3. This means that the ISRU system is not as helpful in this case study as in the Mars case study.

A natural question would be: is ISRU helpful as it becomes more capable? Therefore, the sensitivity analysis against the lunar ISRU capability is also analyzed. The results are shown in Figure 6-5.

According to the dynamic GMCNF, the ISRU system becomes useful when the ISRU capability is larger than 6 [kg/kg plant/year]. The increase of the ISRU capability from 0 [kg/kg plant/year] to 5 [kg/kg plant/year] only saves the IMLEO by 1.3% (from 74.3 [MT] to 73.3 [MT]), whereas the increase of the ISRU capability from 5 [kg/kg plant/year] to 10 [kg/kg plant/year] decreases the IMLEO by 12.1% (from 73.3 [MT] to 64.4 [MT]). This shows the importance of improving the capability of ISRU technologies.

The above trend cannot be seen in the static GMCNF because it gives overoptimistic results. In the static GMCNF, the IMLEO reduction per unit ISRU capability increase is the largest when the ISRU capability is small, which is the same trend we observed in the
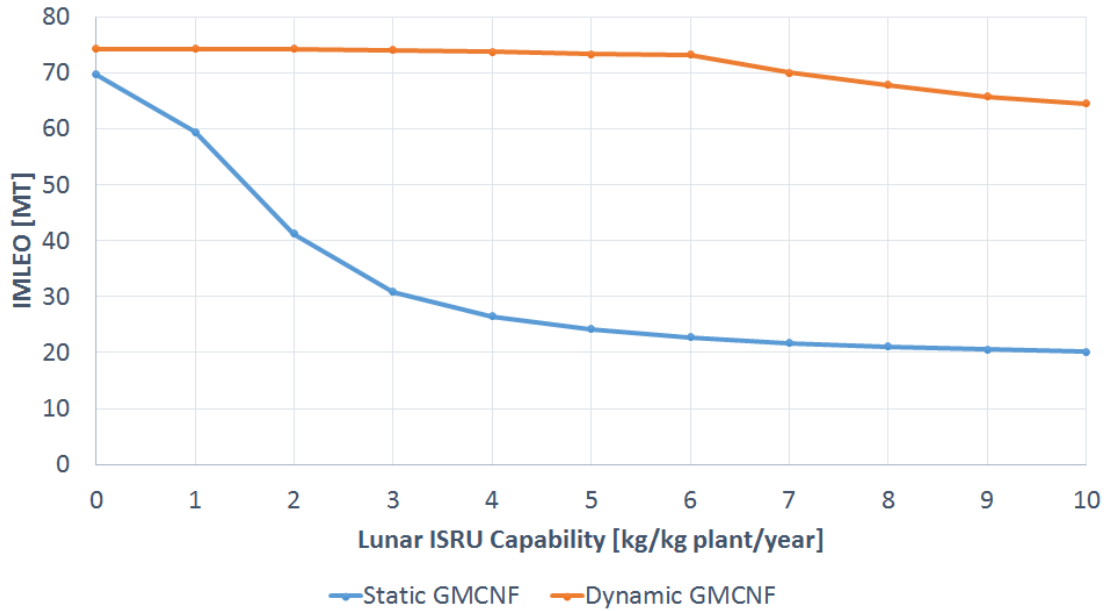
Figure 6-5: Sensitivity of the IMLEO results against the lunar ISRU capability in the NEO exploration case study.

Mars exploration case study. This is caused by the drawback of the static GMCNF in not considering the time dimension, which is why the dynamic GMCNF is necessary.

Next, uncertainties in some other technologies are considered.

Figure 6-6 shows the sensitivity against the aeroshell/TPS mass fraction. Improving the ratio of the aeroshell/TPS to the total captured mass from 40% to 15% results in the 27.6% IMLEO improvement (from 73.3 [MT] to 53.1 [MT]). This can be explained by the large gear ratio (i.e., ΔV) required to deliver the aeroshell/TPS all the way to NEO and back. The results show that the system relies on the entry during the return trip, but the dependence on the aeroshell/TPS mass fraction is smaller than in the Mars exploration case study.

Table 6.6 shows the sensitivity against the boiloff rate. As can be seen, the improvement by removing boiloff is 4.2% in terms of IMLEO. The static GMCNF shows an inaccurate result, 1.0% improvement, which again shows the necessity of the dynamic formulation. The effect of boiloff is smaller than the Mars exploration case because the campaign horizon is shorter.
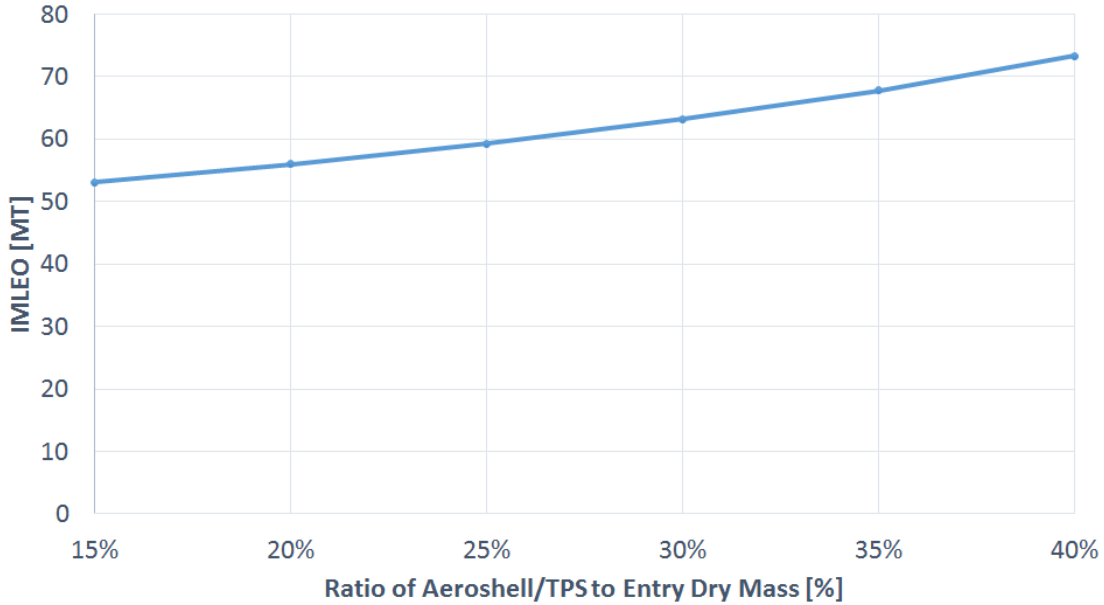
Figure 6-6: Sensitivity of the IMLEO results against the aeroshell/TPS fraction in the NEO exploration case study.

Table 6.6: Comparison of the IMLEO results from the scenarios with boiloff and without boiloff in the NEO exploration case study.

Scenario	IMLEO [MT]
Static GMCNF with boiloff	24.1
Static GMCNF without boiloff	23.9
Dynamic GMCNF with boiloff	73.3
Dynamic GMCNF without boiloff	70.3

6.4 Case Study Summary

In this case study, a specific human NEO exploration scenario is analyzed. A trip to 1999 AO10 is considered and the results are compared with the baseline developed in the past literature. The analysis evaluated how the Cis-lunar infrastructure can support the missions.

The results show that the Cis-lunar space infrastructure can improve the IMLEO significantly, resulting in an about 50% IMLEO reduction. NTRs are used for the major transportation operations between Earth and the NEO, and reusable chemical rockets are used for the transportation operations between the ISRU plants on the Moon and the depots. Overall, lunar ISRU is not as useful as it is in the Mars case study. The sensitivity analysis shows that ISRU can pay off if its capability is large enough.

Chapter 7

Case Study III - Flexible Path: Human Exploration of Mars and a NEO

7.1 Introduction

The previous chapters considered the missions to specific destinations such as Mars and NEOs separately. For future space exploration, however, this might not be the most efficient mission architecture.

In this context, the Review of U.S. Human Spaceflight Plans Committee proposed the Flexible Path concept in their report [7] in 2011, which has become the basis of the current NASA human space exploration strategy. In the Flexible Path concept, we will visit the sites that we have never visited before. These include new lunar orbits, Earth-Moon Langrangian points, NEOs, the orbits around Mars, and the moons of Mars, as shown in Figures 7-1 - 7-2. In 2010, President Obama announced a new national space policy, which mentions that we will send humans to an asteroid by 2025, and that we will send humans to orbit Mars and return them safely to Earth by the mid-2030s, followed by a landing on Mars [103].

The space infrastructure will play an important role for this kind of long-term goal of space exploration. In order to achieve an efficient space exploration strategy, we need to consider various missions to different destinations together as an example, and find a set of common space infrastructure elements in support of these missions. Particularly, we are
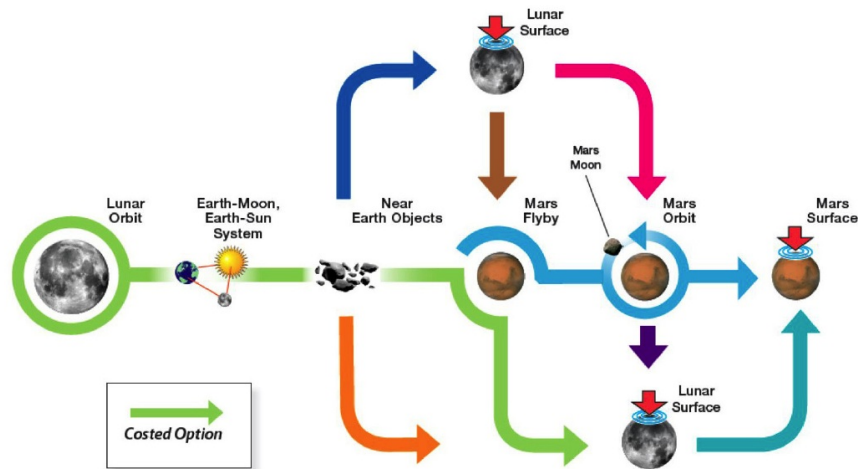
Figure 7-1: Options for exploration within the Flexible Path strategy [7].
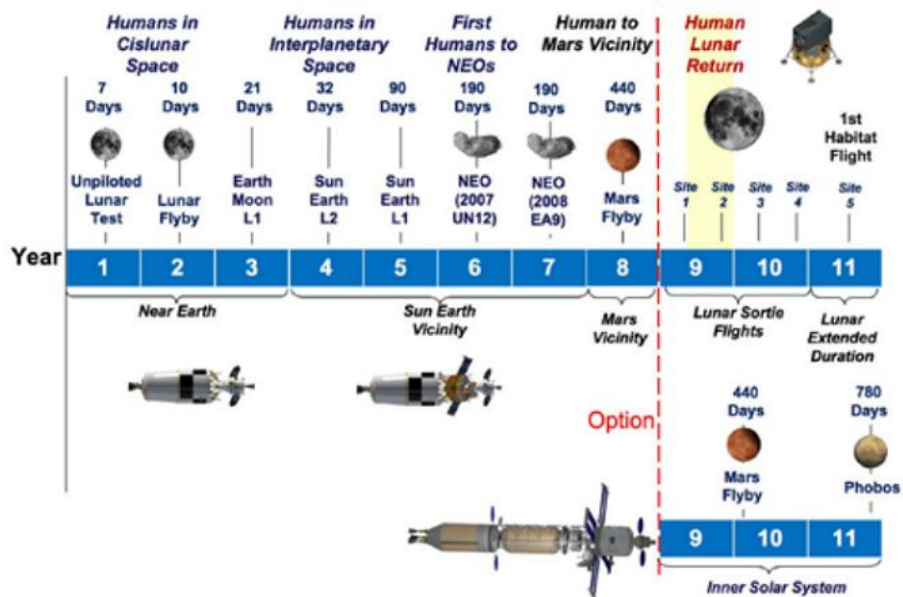
Figure 7-2: Timeline of the Flexible Path strategy [7].

interested in what ISRU systems and other Cis-lunar infrastructure elements can be used to support multiple missions.

To explore that question, this case study considers multiple destinations (NEO 1999 AO10 and Mars), and examines the magnitude of the benefits from designing these missions together compared with considering them separately. Although this case study is not a full representation of the originally proposed Flexible Path architecture, it is consistent with

the concept that we visit the sites that we have never visited before to prepare for human Mars exploration, and therefore is called the Flexible Path case study.

7.2 Parameters and Assumption

All demands and supplies as well as other assumptions are inherited from the Mars and NEO exploration cases with the difference in the timeline.

The detailed timeline of the time windows is shown in Table 7.1. In this timeline, the first Mars mission happens approximately five years after the NEO launch, and the crew mission to Mars happens about two years after that. Note that by defining the time windows in this way, the human Mars and NEO missions are not allowed to happen concurrently, but one after the other. Although no specific dates are specified in this research, time windows in mid-2020s to early-2030s are assumed.

7.3 Results and Implications

This section provides the results of the Flexible Path case study and their implications. The partially static time-expanded GMCNF is used as an approximation of the dynamic GMCNF method.

7.3.1 Results

This case study analyzes the difference between the Mars only case, the NEO only case, and the combination of them (i.e., Flexible Path). The comparison between the static and dynamic GMCNF for each case is shown first in Table 7.2. The improvement of the Mars + NEO case is represented by the following ratio:

$$Improvement = \frac{IMLEO_{Mars+NEO}}{IMLEO_{MarsOnly} + IMLEO_{NEOOnly}} - 1 \qquad (7.1)$$

where $IMLEO_{MarsOnly}$, $IMLEO_{NEOOnly}$, and $IMLEO_{Mars+NEO}$ denotes the IMLEO for the Mars only case (Chapter 5), the NEO only case (Chapter 6), and the Flexible Path case respectively.

In Table 7.2, there is an additional case considered for the Mars exploration for the following reason. As shown previously, the timeline considered in this case study visits

Table 7.1: Time window assumptions in the Mars only, NEO only, and Mars + NEO exploration case study.

Time [day]	Event
0	Earth's Surface → LEO
190	Earth's Surface → LEO
380	Earth's Surface → LEO
570	Earth's Surface → LEO
700	Earth's Surface → LEO (Crew Launch)
710	Earth/Cis-lunar Cluster → NEO
760	Earth's Surface → LEO
835	NEO → Earth/Cis-lunar Cluster
950	Earth's Surface → LEO
1140	Earth's Surface → LEO
1330	Earth's Surface → LEO
1520	Earth's Surface → LEO
1710	Earth's Surface → LEO
1900	Earth's Surface → LEO
2090	Earth's Surface → LEO
2280	Earth's Surface → LEO
2470	Earth's Surface → LEO
2660	Earth's Surface → LEO
2670	Earth/Cis-lunar Cluster → Martian Cluster
2850	Earth's Surface → LEO
3040	Earth's Surface → LEO
3230	Earth's Surface → LEO
3400	Martian Cluster → Earth/Cis-lunar Cluster
3420	Earth's Surface → LEO
3430	Earth/Cis-lunar Cluster → Martian Cluster
3610	Earth's Surface → LEO
3800	Earth's Surface → LEO
3990	Earth's Surface → LEO
4160	Martian Cluster → Earth/Cis-lunar Cluster
4180	Earth's Surface → LEO

NEO first and then Mars, which changes the departure for Mars exploration compared with the Mars case study considered previously in Chapter 5. (In Chapter 5, the first mission to Mars is deployed 760 days after the campaign start, whereas in this case study, the first mission to Mars is deployed 2,670 days after the campaign start.) This change would allow more time for infrastructure deployment and ISRU generation, and therefore benefit the resource economy of the entire campaign. Thus, a direct comparison of the Flexible Path results with those from Chapter 5 is practically important, but is not fair. In this analysis,

a separate case, Mars only with its timeline adjusted to a longer pre-deployment period, is considered, which has the same campaign time horizon as the one considered in the Flexible Path case.

Table 7.2: Comparison of the IMLEO results from each method in the Mars only, NEO only, and Mars + NEO exploration case study.

Method	Mars Only IMLEO [MT]	Mars Only IMLEO [MT] (Adjusted)	NEO Only IMLEO [MT]	Mars+NEO IMLEO [MT]	Mars+NEO Improvement	Mars+NEO Improvement (Adjusted)
Static GMCNF	153.8	153.8	24.1	177.9	-0.0%	-0.0%
Bi-scale Time-Expanded GMCNF	443.7	374.5	73.2	420.0	-18.8%	-6.2%
Partially Static Time-Expanded GMCNF	431.4	363.6	73.3	410.2	-18.7%	-6.1%

As can be seen in Table 7.2, the improvement by designing the Mars and NEO missions concurrently can reduce the total IMLEO in the dynamic GMCNF. Without timeline adjustment, this improvement is about 19%; even with the adjustment, it is still about 6%. This improvement comes from reuse of the propellant depots and other space infrastructure elements as well as efficient use of lunar ISRU plants, which can now support both missions (but not at the same time). For example, if there is only one crew mission, the pre-deployed ISRU plants would be useless after the mission is completed even if they are still capable of generating propellant. If there is a subsequent mission, even if it is for a different destination, the ISRU plants that have already been deployed can be very useful. This is the power of the dynamic campaign-level analysis; a mission-level analysis cannot lead to this result.

Another interesting finding is that the above IMLEO reduction by considering multiple missions concurrently does not appear in the static GMCNF. This is because the static GM-CNF does not consider the interdependency between each mission. In the LP formulation in the static GMCNF, the results of summing two missions is equivalent to simply summing

two objective functions. In reality, however, each mission is interacting with one another; a previous mission can *support* the subsequent missions, and the Cis-lunar infrastructure can be useful for multiple destinations. Furthermore, the timeline adjustment does not affect the static GMCNF. This is because the static GMCNF does not consider the time dimension, which is the very reason why the dynamic GMCNF is critical.

Next, a qualitative analysis of the results for the Flexible Path case is shown. Here, the dynamic commodity flow is shown based on the bi-scale time-expanded GMCNF (and the post-processing) because it provides the most realistic results.

Figure 7-3 shows the flow of all types of commodities. This shows a complex architecture in the Earth/Cis-lunar and the Martian clusters. EML2, LLO, LDO, and LMO are used for structure storage or propellant depots, and EML1 and GEO are also used temporarily. Both lunar and Martian ISRU are used. Note that transfer orbits such as GTO, LTO, DTO, and PTO are not allowed to store structure mass or propellant depots. Crew and cargo are transported to Mars or the NEO when their time windows open.
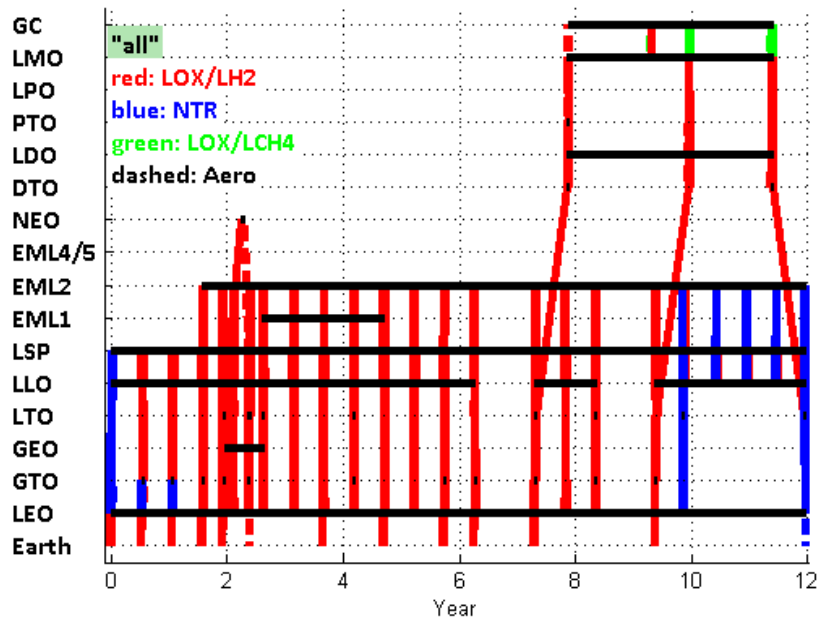
Figure 7-3: Bat chart: all commodity flow for the Mars + NEO exploration case study. "Aero" stands for aerocapture/entry.

As in the Mars and NEO exploration case, we are interested in the crew transportation and ISRU plant deployment. Figure 7-4 shows the crew flow, and Figure 7-5 shows the

ISRU plant deployment flow. In addition, Table 7.3 shows the IMLEO breakdown for each launch.
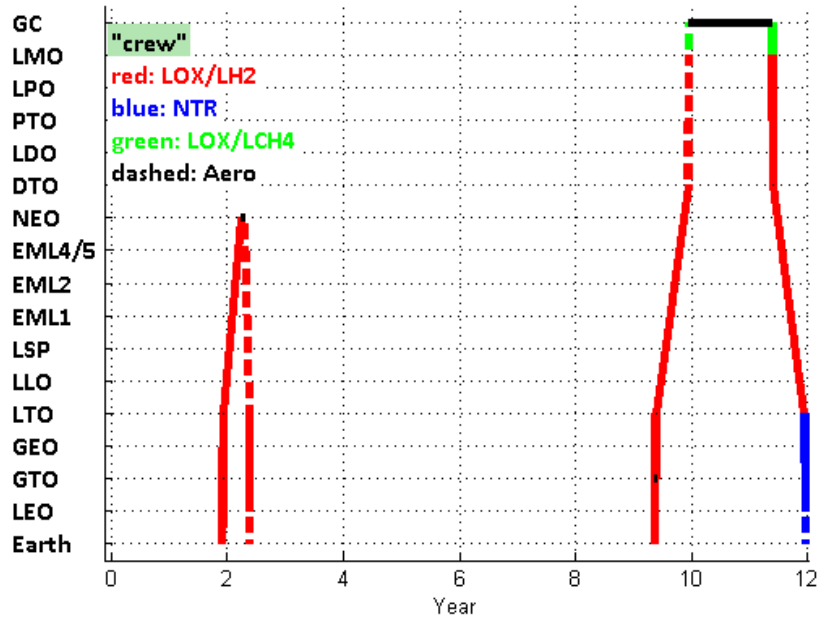
Figure 7-4: Bat chart: crew flow for the Mars + NEO exploration case study. "Aero" stands for aerocapture/entry.

As can be seen from the figures, the transportation operations largely depend on chemical rockets using the ISRU-generated resources, although the initial deployment of the ISRU plants uses NTRs. Here, again, a dynamic shift from NTRs to chemical rockets is observed. In addition, as can be seen in Table 7.3, no oxygen, water, or methane are launched from Earth (except for LOX in the Earth to LEO launch); all of these resources are supplied by ISRU. This shows that the campaign highly depends on the resources generated by ISRU.

In addition to the similar conclusions as in the Mars only (Chapter 5) and NEO only (Chapter 6) cases, there are some more interesting findings by comparing the above results with the Mars only and NEO only cases.

First, NTRs are also used for the transportation operations after the last crew launch to Mars (i.e., Year 9-11), which is not observed in the Mars only case. The purpose of these transportation operations is to support the crew return trip from the Mars. Instead of directly heading back to Earth, the crew stops by the propellant depots to be refueled for the last burns to enter the Earth's atmosphere. The required propellant for those last burns
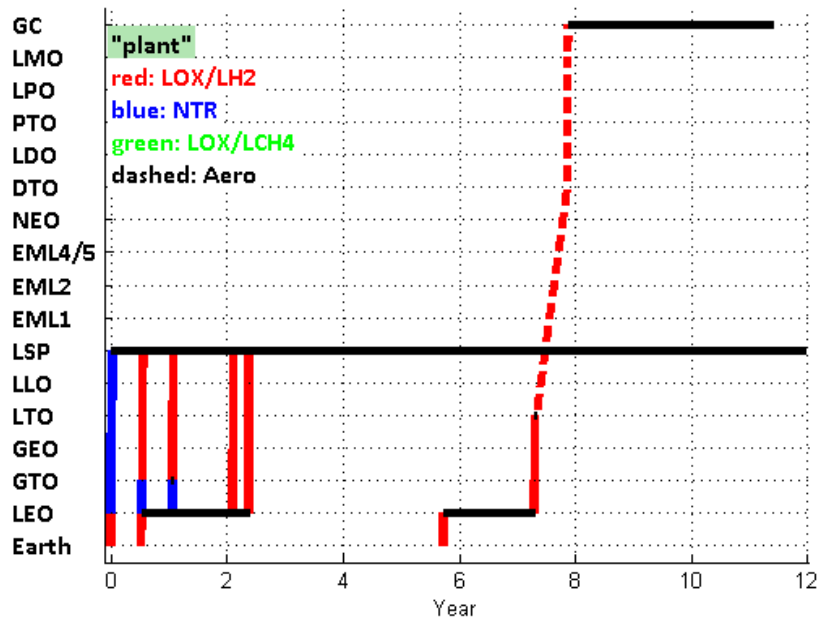
Figure 7-5: Bat chart: ISRU plant flow for the Mars + NEO exploration case study. "Aero" stands for aerocapture/entry.

is not large, and the initially launched ISRU plants have already degraded at that moment. Therefore, it turns out to be inefficient to rely on chemical rockets and the ISRU-generated resources in the same way as the earlier major transportation operations. Instead, it is more efficient to use NTRs with a high I_{sp} with the Earth-originated resources. That is why NTRs are used after the last crew launch to Mars. This trend is not observed in the Mars only case because the time horizon considered in the Mars only case is not long enough for the ISRU system to dramatically degrade, and therefore it is still preferable to use chemical rockets with the ISRU-generated resources.

In addition, in the NEO only mission, the major transportation operations to the NEO in the optimal solution rely little on the ISRU-generated resources but heavily on NTRs. However, the Mars + NEO results indicate that if there is a subsequent Mars mission after the NEO mission, it is more efficient to launch more ISRU plants and use their resources to launch chemical rockets for the NEO mission than using NTRs. This shows that there is not only a numerical IMLEO difference, but also a qualitative architecture difference between the optimal solutions for designing missions together and designing them separately.

Comparing Table 6.4 and 7.3, it can be seen that, in the Mars + NEO case, a larger

116

Table 7.3: IMLEO breakdown for each commodity at each launch from Earth in the Mars + NEO exploration case study.

Launch Date [day]	0	190	380	570	700	1,330	1,710	2,090	2,280	2,660	3,420
Vehicle [MT]	9.18	0	0	0	3.33	0	0	0	27.54	0	10.00
Habitat /Payload [MT]	0	0	0	1.00	0	0	0	51.70	0	0	0
Crew [MT]	0	0	0	0	0.20	0	0	0	0	0	0.60
Hydrogen [MT]	20.88	12.91	14.51	0.40	3.33	0	0	0.07	0.12	7.90	4.61
Oxygen [MT]	0	0	0	0	0	0	0	0	0	0	0
Methane [MT]	0	0	0	0	0	0	0	0	0	0	0
Water [MT]	0	0	0	0	0	0	0	0	0	0	0
Food [MT]	0	11.83	0	0	0	0	0	0.06	0	0	0
LOX/LH2 Inert [MT]	4.04	0	0	0	6.47	0	0	0	0	2.99	1.08
NTR Inert [MT]	3.29	0	0	0	0	0	0	0	0	0	0
LOX/LCH4 Inert [MT]	0	0	0	0	0	0	2.58	0	0	0	0
Hydrogen Tank [MT]	3.98	2.46	2.76	0.08	0.63	0	0	0.01	0.02	1.50	0.88
Oxygen Tank [MT]	0.69	2.52	0	4.83	0	0	0	1.01	0	0	0
Methane Tank [MT]	0	1.36	0	0	0	0	0	0	0	0	0
Water Tank [MT]	0	0.11	0	0	0.11	0.68	0.07	0	0	0	0
Aeroshell /TPS [MT]	0.98	100.48	0	0	0	0	0	0	0	0	0
Oxygen ISRU Plant [MT]	0	0	0	0	0	0	0	0.81	0	0	0
Water ISRU Plant [MT]	15.75	65.28	0	0	0	0	0	10.80	0	0	0
Methane ISRU Plant [MT]	0	0	0	0	0	0	0	1.57	0	0	0
Total [MT]	58.79	196.94	17.27	6.30	14.08	0.68	2.66	66.05	27.68	12.39	17.17

mass (293.4 [MT]) is deployed before the NEO crew launch than that in the NEO only case (73.2 [MT]). That large mass is used not only for the NEO missions but also for the Mars mission after it, which makes the entire campaign efficient. This is the very reason why we need a common infrastructure for multiple missions to different destinations, and this

analysis cannot be provided by the static GMCNF analysis or individual mission studies.

7.3.2 Sensitivity Analysis

This subsection discusses a sensitivity analysis for the results from the dynamic GMCNF.

First, the sensitivity of the results against the propulsion technology selection is shown in the same way as in the previous case studies. Here, the problem setting is changed to only NTRs or only chemical rockets with aerocapture, and the results are compared. The results are shown in Table 7.4.

Table 7.4: Comparison of the IMLEO results from the scenarios with only NTRs and only chemical rockets + aerocapture in the Mars only, NEO only, and Mars + NEO exploration case study. "Aero" stands for aerocapture.

Scenario	Mars Only IMLEO [MT]	Mars Only IMLEO [MT] (Adjusted)	NEO Only IMLEO [MT]	Mars+NEO IMLEO [MT]	Mars+NEO Improvement	Mars+NEO Improvement (Adjusted)
Dynamic GMCNF NTR + ISRU	736.0	724.5	74.3	789.8	-2.5%	-1.1%
Dynamic GMCNF Chemical + Aero + ISRU	528.7	379.9	100.7	442.2	-29.7%	-8.0%

The results show that although the improvement by considering the Mars and NEO missions concurrently is large for the chemical + aerocapture scenario, it is not as large for the NTR scenario. Chemical rockets rely on ISRU more heavily than NTRs because the ISRU oxygen generation can make chemical rockets more attractive than NTRs. Therefore, the results in Table 7.4 imply that the more the system relies on ISRU, the larger the benefits accruing to the combination case of the Mars and NEO missions. This is an important interaction between the propulsion and ISRU technology development, which is consistent with the findings of the Mars only and NEO only cases.

A similar trend can also be observed in the sensitivity analysis against the lunar ISRU capability. The results of the IMLEO sensitivity analysis are shown in Figure 7-6, and the sensitivity of the improvement by considering the Mars and NEO missions concurrently is

shown in Figures 7-7 - 7-8 with and without the timeline adjusted respectively.
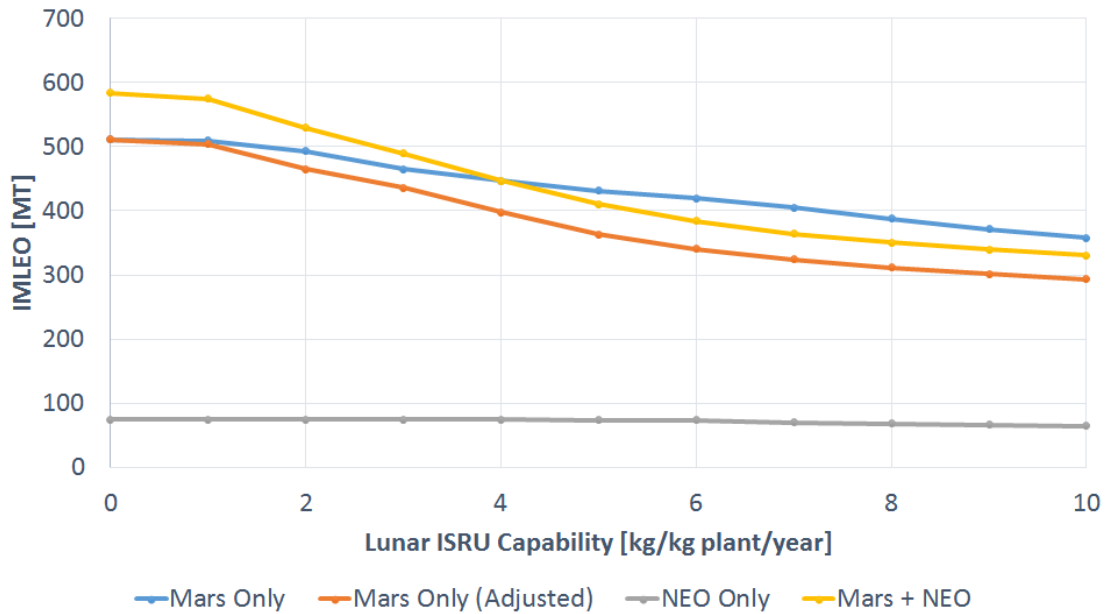
Figure 7-6: Sensitivity of the IMLEO against the lunar ISRU capability in the Mars only, NEO only, and Mars + NEO exploration case study.
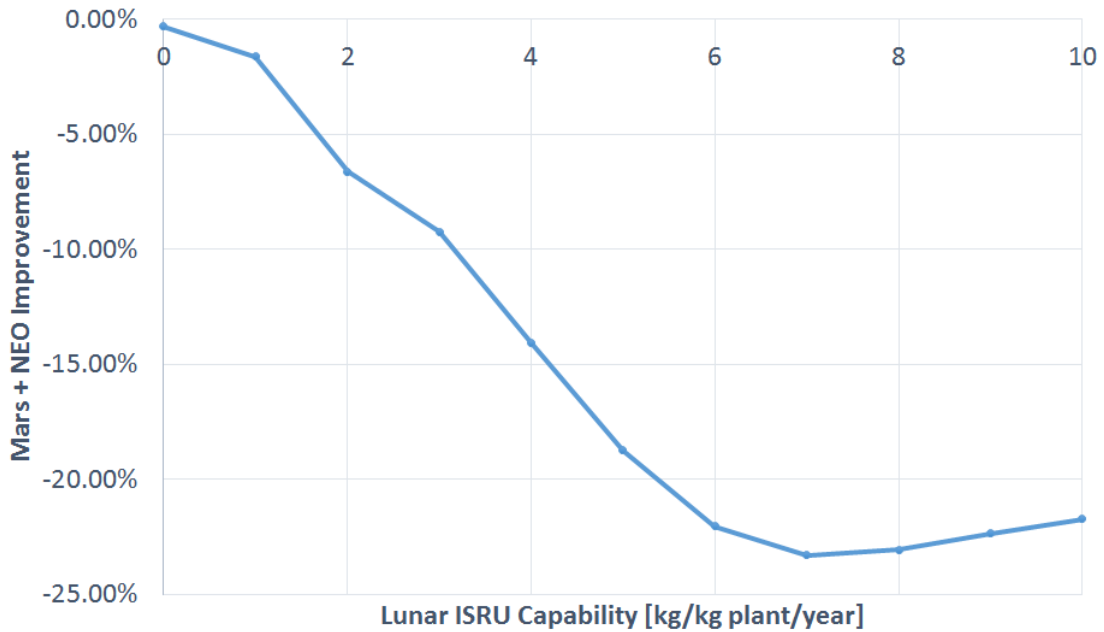
Figure 7-7: Sensitivity of the IMLEO improvement by considering Mars + NEO exploration case against the lunar ISRU capability.

Figure 7-6 shows that, as we have seen in the previous chapters, a better ISRU capability
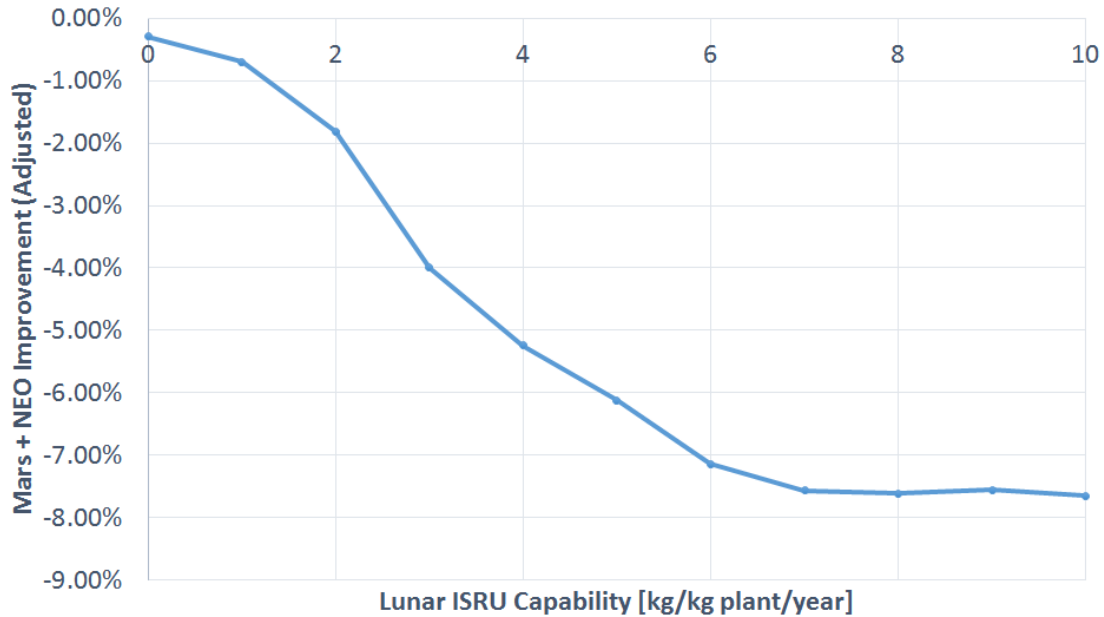
Figure 7-8: Sensitivity of the IMLEO improvement by considering Mars + NEO exploration case (with the timeline adjusted) against the lunar ISRU capability.

improves the IMLEO performance for all missions, but there are some interesting findings in their sensitivity to the IMLEO capability.

First, Figures 7-6 - 7-8 show that, when the ISRU capability is small, the improvement by considering the Mars and NEO missions at the same time (i.e., Mars + NEO improvement) grows as the lunar ISRU capability increases. This implies that the more capable the ISRU system is, the more efficient it is to use a common space infrastructure for multiple missions even if they are for different destinations.

The "S-curve" in Figure 7-8 can be qualitatively explained as follows: When the ISRU capability is small, the ISRU plant demand grows as the ISRU system becomes more capable, but when the ISRU system is capable enough, the ISRU plant demand shrinks because a small plant mass can generate enough propellant. The Mars + NEO improvement is sensitive to the ISRU capability when the campaign relies more on (i.e., launches more) the common infrastructure elements such as the ISRU plants, and therefore the sensitivity is largest when the ISRU capability is moderate (1-7 [kg/kg plant/year]).

Furthermore, if the timeline is not adjusted, which leads to a practically important comparison, the benefits of pre-deployment also affect the shape of the curve, in addition to the above factors. This makes the Mars + NEO improvement decrease (in terms of absolute

120

value) when the ISRU system is very capable (7-10 [kg/kg plant/year]), as shown in Figure 7-7. because a highly capable ISRU system gains little out of its pre-deployment.

Another numerically interesting finding in Figure 7-6 is that, without the timeline adjustment, the Mars mission can require more IMLEO than the Mars + NEO mission when the ISRU capability is larger than 5 [kg/kg plant/year]. This means that starting the missions early and preparing for the subsequent Mars missions while pursuing the NEO can make the NEO mission almost a "free ride." This is another demonstration of the reason why we need to consider multiple missions concurrently.

Overall, it can be seen that it would be very beneficial to design the Mars and NEO missions together, if the lunar ISRU technology can achieve and exceed the range 1-7 [kg/kg plant/year]. Ishimatsu has shown previously that a lunar ISRU target for resource generation at about 3.5 [kg/kg plant/year] is important and it falls within this range.

Next, uncertainties in some other technologies are considered.

Figure 7-9 shows the sensitivity of the improvement by considering the Mars and NEO missions concurrently (with the timeline adjusted) against the aeroshell/TPS mass fraction. The result shows that the more the aeroshell/TPS is required, the less the improvement by considering the Mars and NEO missions together would be. This is because aerocapture is heavily used in the Mars mission but not much in the NEO mission, and therefore more aeroshell/TPS mass corresponds to a smaller amount of common infrastructure. Nevertheless, the IMLEO improvement is not very sensitive to the aeroshell/TPS mass fraction.

Table 7.5 shows the sensitivity of the improvement by considering the Mars and NEO missions concurrently (with the timeline adjusted) against the boiloff rate. The results show that excluding boiloff can provide more benefits of considering the Mars and NEO missions together. This is because a common space infrastructure requires propellant storage in orbit for a long time, which can result in a large boiloff loss. If the propellant boiloff can be controlled properly, the benefits of considering multiple missions can be larger.

7.4 Case Study Summary

In this case study, the Flexible Path case with both the Mars and NEO exploration missions is analyzed. The case combines the Mars only and the NEO only cases and evaluates how
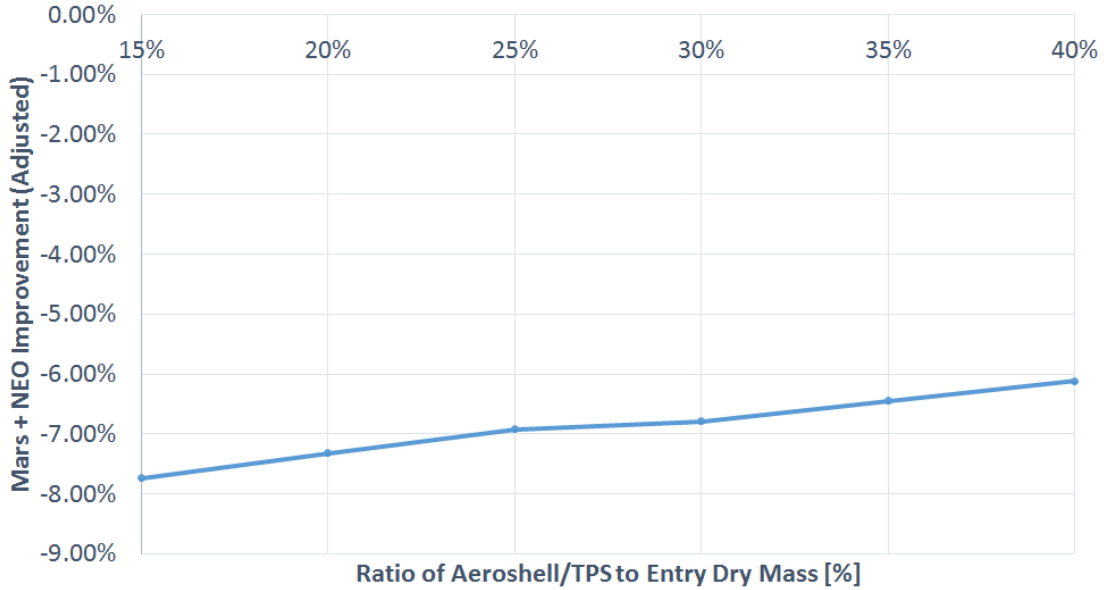
Figure 7-9: Sensitivity of the IMLEO improvement by considering Mars + NEO exploration case (with the timeline adjusted) against the aeroshell/TPS fraction.

Table 7.5: Comparison of the IMLEO results from the scenarios with boiloff and without boiloff in the NEO exploration case study.

Scenario	IMLEO [MT]
Mars + NEO Improvement (Adjusted) with boiloff	-6.1%
Mars + NEO Improvement (Adjusted) without boiloff	-7.9%

a common space infrastructure can support both missions when one mission follows the other.

The results show that designing the Mars + NEO missions with a common space infrastructure can reduce the IMLEO by 19%, which is a significant improvement. The ISRU system, propellant depots, and reusable vehicles that can be commonly used for different missions turn out to provide a large benefit to the campaign resource economy. NTRs are useful for the initial ISRU launch or after the last crew launches, whereas chemical rockets are useful for the major cargo and crew transportation operations. The sensitivity analysis shows that the improvement from designing multiple missions together (with the timeline adjustment) is particularly large when chemical rockets are used or when the ISRU capability is large.

Chapter 8

Conclusions

8.1 Thesis Summary

In this thesis, a dynamic logistics network formulation for lifecycle optimization of human-robotic mission sequences is proposed and applied to 1) human exploration of Mars, 2) human exploration of a NEO, and 3) the Flexible Path. The proposed methods can find the optimal combination of technologies and operations to be used at each stage of the campaign. The necessity of the dynamic model comes from the long deployment/assembly phase of space systems, where only considering the steady state does not lead to realistic results.

The proposed methods combine the GMCNF with a time-expanded network to model the dynamic movement of commodities and infrastructure elements over time. Given that the full time-expanded GMCNF is prohibitively computationally expensive, this thesis develops its approximation methods. The developed methods are based on the ideas of node/arc aggregation and restriction, which respectively provide lower and upper bounds for the solution of the full time-expanded GMCNF. This research also proposes the cluster-based time-expanded GMCNF methods: the bi-scale time-expanded GMCNF and the partially static time-expanded GMCNF, which are practically useful for time window critical systems. The basic ideas for these methods are as follows: Instead of using uniform time steps, the bi-scale time-expanded GMCNF allocates fine time steps around the inter-cluster time windows, whereas the partially static time-expanded GMCNF assumes the intra-cluster transportation as instantaneous arcs that exist at the inter-cluster time windows. The former formulation provides a realistic solution reflecting the active and dormant phases of a

campaign, whereas the latter formulation provides a good estimate of the realistic solution computationally efficiently.

Furthermore, unlike the earlier static space logistics optimization models, the proposed model considers the dynamic interaction with technology options. The numerical analysis results not only show the effectiveness of the methods, but also captures the trades and provide recommendations for human space exploration. The provided recommendations include trades between ISRU, propellant depot, propulsion, and aerocapture technologies.

Finally, the proposed methods can be used to evaluate the interdependency between the missions, which was not possible to do by the earlier space logistics methods. One important finding is that there is a clear trend that designing multiple missions can lead to a large performance improvement compared with designing them separately as shown in the Flexible Path case. This trend occurs because we can deploy a common space infrastructure including ISRU systems, propellant depots, and reusable vehicles. This leads to an important conclusion that development of a common space infrastructure is extremely important not only for an initial mission but also for future missions, whose destination may or may not be the same as the initial one. This conclusion will be very important for future human and robotic space exploration, where we may transition from a mission focus to a campaign-level resource economy focus.

8.2   Future Work

Space logistics is still an emerging field; there are various directions for future work in order to make the proposed dynamic GMCNF framework more useful and more generally applicable.

One direction is to use Mixed Integer Programming and/or Nonlinear Programming to improve the model's level of fidelity. The additional components would include more realistic models of propulsive and non-propulsive vehicles, integer constraints for crew or vehicle stages, and a more detailed model for demand and cost estimates. The ideal model would be an integrated system-level optimization model, considering a space habitat, its logistics and ISRU network, and its supporting vehicles concurrently. A problem in implementing such a model is its expensive computational effort. Techniques or algorithms need to be developed to deal with these complex systems efficiently.

124

Another related direction can be theoretical development of dynamic optimization, especially given the recent research trends for large-scale optimization problems. Solving these types of problems typically utilizes interior point methods or problem decomposition and often involves parallel computing. One possibility would be to leverage supercomputers such as the one at the National Center for Supercomputing Applications at University of Illinois Urbana-Champaign. For example, it is possible that, with some refinement, we can use nested decomposition techniques with parallel computing for this research [104, 105]. In that case, for example, the transportation in the Earth/Cis-lunar cluster and that in the Martian cluster can be computed in separate processors with little interaction. Applying these methods to the bi-scale time-expanded network or even directly to the full time-expanded network is one interesting future work direction.

The third direction is about uncertainties. One of the largest advantages about the proposed common infrastructure option in this research is its flexibility. Once we have the Cis-lunar and Martian infrastructure deployed, we can use it for exploration missions to NEOs, Earth-Moon Lagrangian points, Phobos, Deimos, and even Mars. Even if the mission destination changes in the middle of a campaign due to a programmatic or technical reason, or if there is a shift in launch windows and delays, the deployed infrastructure is still useful. In order to quantify the value of this flexibility, we need to use stochastic methods (e.g., Monte Carlo Simulation, Stochastic Optimization, ...) to consider the uncertain future in combination with a real options analysis. This direction can lead to an interesting study and it will reveal another strength of the space infrastructure proposed in this study.

Furthermore, although this research considers IMLEO as the only objective, it is possible to extend the formulation for multi-objective optimization problems. Some of the other objective functions include recurring/non-recurring cost for the space infrastructure, system complexity, and risk. For example, the Pareto solutions considering the cost and risk can be very interesting to explore.

One of the ultimate goals of dynamic space campaign analysis is to create a technology roadmap for future space exploration. Our research considered when and where each technology would be necessary for an optimal space logistics plan, but it did not consider development of these technologies. Integrating campaign-level GMCNF with technology roadmapping can be one of the interesting directions to pursue.

Another related interesting research direction is about the economics of space infrastruc-

ture and associated resources. This research has proposed that the space infrastructure can be very useful for space exploration, but it is unlikely that a single national space agency can build all of it as we did in the Apollo Program. Future space exploration will probably require collaboration between the national space agencies, governments, and private companies. The financial aspect of the proposed space infrastructure needs to be analyzed. There have been past studies for pricing of ISRU-generated propellant [27] or cargo revenue management for space logistics [106], but there is room for studies to combine the logistics optimization and its underlying economics.

Finally, this research applied the proposed methods to human space exploration, but the mathematics behind them are not only for that application. The model is general enough to be used to examine the conceptual design of various space or terrestrial logistics missions that involve dynamic resource management. An interesting application can be to model expanding business and franchises who must fuel later expansions with revenues generated during earlier phases of growth. It would be an interesting future work to explore other applications of this research and refine the methods to make them more generally applicable.

Appendix A

ΔV and Time of Flight Tables

This appendix lists the ΔV and arc lengths (i.e. times of flight) for the case studies.

Figure A-1 and Figure A-2 list the ΔV and the time of flight for each arc respectively [5, 6, 107]. The values assume high thrust propulsion systems and availability of Oberth maneuvers when applicable [108]. The pink cells represent the options with aerocapture/entry.

Figure A-1: ΔV [km/s] used in the analysis.

ΔV [km/s] FROM \ TO	KSC	PAC	LEO	GTO	GEO	LTO	EML1	EML2	EML4/5	LLO	LSP	1999 AO10	DTO	LDO	PTO	LPO	LMO	GC
KSC			9.50															
PAC																		
LEO		9.50 / 0.01		2.50	4.33	3.18	3.77	3.43	3.97	4.04								
GTO			2.50 / 0.23		1.83	0.68	1.27	0.93	1.47	1.54								
GEO			4.33 / 2.06	1.83		2.51	1.38	1.47	1.71	2.05								
LTO			3.18 / 0.45	0.68	2.51		0.58	0.35	0.69	0.86		2.40	1.69 / 0.69					
EML1			3.77 / 0.77	1.27	1.38	0.58		0.14	0.33	0.64								
EML2			3.43 / 0.33	0.93	1.47	0.35	0.14		0.34	0.64								
EML4/5			3.97 / 0.84	1.47	1.71	0.69	0.33	0.34		0.98								
LLO			4.04 / 1.31	1.54	2.05	0.86	0.64	0.65	0.98		1.87							
LSP										1.87								
1999 AO10		1.75				1.75												
DTO		14.33 / 1.01				1.69 / 1.01								0.66	0.40 / 0.01		1.10 / 0.01	
LDO													0.66					
PTO													0.40			0.55	0.70 / 0.01	
LPO															0.55			
LMO													1.10		0.70			4.10 / 0.61
GC																	4.10	

Aerocapture/Entry

Time of Flight [days]	KSC	PAC	LEO	GTO	GEO	LTO	EML1	EML2	EML4/5	LLO	LSP	1999 AO10	DTO	LDO	PTO	LPO	LMO	GC
KSC			1															
PAC																		
LEO		1		1	1	1	3	4	4	4								
GTO			1		1	1	3	4	4	4								
GEO			1	1		1	3	4	4	4								
LTO			1	1	1		2	3	3	3		111	200					
EML1			3	3	3	2		1	4	1								
EML2			4	4	4	3	1		4	1								
EML4/5			4	4	4	3	4	4		4								
LLO			4	4	4	3	1	1	4		1							
LSP										1								
1999 AO10		32				30												
DTO		202				200								1	1		2	
LDO													1					
PTO													1			1	1	
LPO															1			
LMO													2		1			1
GC																	1	

Figure A-2: Time of flight [days] used in the analysis.

Appendix B

Input Spreadsheets for Analysis

This appendix lists the input information for the dynamic GMCNF used in the case studies. The input information is compiled as spreadsheets for node clusters (Figure B-1), nodes (Figures B-2 - B-3), transportation arcs (Figures B-4 - B-6), and holdover arcs (Figure B-7). Some common parameters (e.g., propellant mixture ratios, boil-off rates, time windows) are not shown here; they are shown in each corresponding chapter.

The figures are for the most part self-explanatory, but a few comments need to be made. First, the crews from the Mars and NEO missions are assumed to return to different locations, denoted as PAC and PAC2 respectively. In Figure B-7, a "wait" holdover arc is assigned to PAC and PAC2 to allow an early return if possible. Also, in Figure B-7, a "tempStay" holdover arc is used to express a short stay (14 days or shorter), which is assumed to have different properties from a long-term "depot" holdover arc (longer than 14 days) as described in Chapter 4.

name	ID	diameter	supply/demand window interval [days]
Earth Surface (KSC)	1	0	190
Earth Surface (KSC2)	2	0	1.00E+12
Earth System	3	5	190
Martian System	4	3	760
1999 AO10	5	0	1.00E+12
Earth System (PAC)	6	0	760
Earth System (PAC2)	7	0	1.00E+12

Figure B-1: Input spreadsheet for node clusters. 10^{12} is used for infinity.

name	ID	cluster	supply/demand Rate [kg/time step]									
			vehicle	habitat+ payload	crew	crewRe/ Sample	hydrogen	oxygen	methane	water	food	waste
KSC	1	1	1.00E+12	1.00E+12	1.00E+12	0.00	1.00E+12	1.00E+12	1.00E+12	1.00E+12	1.00E+12	1.00E+12
KSC2	2	2	1.00E+12	1.00E+12	1.00E+12	0.00	1.00E+12	1.00E+12	1.00E+12	1.00E+12	1.00E+12	1.00E+12
PAC	3	6	0.00	0.00	0.00	-850.00	0.00	0.00	0.00	0.00	0.00	0.00
PAC2	4	7	0.00	0.00	0.00	-200.00	0.00	0.00	0.00	0.00	0.00	0.00
LEO	5	3	0.00	0.00	0.00	0.00	0.00	0.00	0.00	0.00	0.00	0.00
GTO	6	3	0.00	0.00	0.00	0.00	0.00	0.00	0.00	0.00	0.00	0.00
GEO	7	3	0.00	0.00	0.00	0.00	0.00	0.00	0.00	0.00	0.00	0.00
LTO	8	3	0.00	0.00	0.00	0.00	0.00	0.00	0.00	0.00	0.00	0.00
LSP	9	3	0.00	0.00	0.00	0.00	0.00	0.00	0.00	0.00	0.00	0.00
LLO	10	3	0.00	0.00	0.00	0.00	0.00	0.00	0.00	0.00	0.00	0.00
EML1	11	3	0.00	0.00	0.00	0.00	0.00	0.00	0.00	0.00	0.00	0.00
EML2	12	3	0.00	0.00	0.00	0.00	0.00	0.00	0.00	0.00	0.00	0.00
EML4/5	13	3	0.00	0.00	0.00	0.00	0.00	0.00	0.00	0.00	0.00	0.00
DTO	14	4	0.00	0.00	0.00	0.00	0.00	0.00	0.00	0.00	0.00	0.00
LDO	15	4	0.00	0.00	0.00	0.00	0.00	0.00	0.00	0.00	0.00	0.00
PTO	16	4	0.00	0.00	0.00	0.00	0.00	0.00	0.00	0.00	0.00	0.00
LPO	17	4	0.00	0.00	0.00	0.00	0.00	0.00	0.00	0.00	0.00	0.00
LMO	18	4	0.00	0.00	0.00	0.00	0.00	0.00	0.00	0.00	0.00	0.00
GC	19	4	0.00	-51700.00	-600.00	850.00	0.00	0.00	0.00	0.00	0.00	0.00
NEO	20	5	0.00	-1000.00	-200.00	200.00	0.00	0.00	0.00	0.00	0.00	0.00

Figure B-2: Input spreadsheet for nodes. 10^{12} is used for infinity.

name	ID	cluster	supply/demand Rate [kg/time step]										
			inertLOX	inertNTR	inertLCH4	tankLH2	tankLOX	tankLCH4	tankH2O	aeroshell /TPS	plant_o2	plant_h2o	plant_me thane
KSC	1	1	1.00E+12	1.00E+12	1.00E+12	1.00E+12	1.00E+12	1.00E+12	1.00E+12	1.00E+12	1.00E+12	1.00E+12	1.00E+12
KSC2	2	2	1.00E+12	1.00E+12	1.00E+12	1.00E+12	1.00E+12	1.00E+12	1.00E+12	1.00E+12	1.00E+12	1.00E+12	1.00E+12
PAC	3	6	0.00	0.00	0.00	0.00	0.00	0.00	0.00	0.00	0.00	0.00	0.00
PAC2	4	7	0.00	0.00	0.00	0.00	0.00	0.00	0.00	0.00	0.00	0.00	0.00
LEO	5	3	0.00	0.00	0.00	0.00	0.00	0.00	0.00	0.00	0.00	0.00	0.00
GTO	6	3	0.00	0.00	0.00	0.00	0.00	0.00	0.00	0.00	0.00	0.00	0.00
GEO	7	3	0.00	0.00	0.00	0.00	0.00	0.00	0.00	0.00	0.00	0.00	0.00
LTO	8	3	0.00	0.00	0.00	0.00	0.00	0.00	0.00	0.00	0.00	0.00	0.00
LSP	9	3	0.00	0.00	0.00	0.00	0.00	0.00	0.00	0.00	0.00	0.00	0.00
LLO	10	3	0.00	0.00	0.00	0.00	0.00	0.00	0.00	0.00	0.00	0.00	0.00
EML1	11	3	0.00	0.00	0.00	0.00	0.00	0.00	0.00	0.00	0.00	0.00	0.00
EML2	12	3	0.00	0.00	0.00	0.00	0.00	0.00	0.00	0.00	0.00	0.00	0.00
EML4/5	13	3	0.00	0.00	0.00	0.00	0.00	0.00	0.00	0.00	0.00	0.00	0.00
DTO	14	4	0.00	0.00	0.00	0.00	0.00	0.00	0.00	0.00	0.00	0.00	0.00
LDO	15	4	0.00	0.00	0.00	0.00	0.00	0.00	0.00	0.00	0.00	0.00	0.00
PTO	16	4	0.00	0.00	0.00	0.00	0.00	0.00	0.00	0.00	0.00	0.00	0.00
LPO	17	4	0.00	0.00	0.00	0.00	0.00	0.00	0.00	0.00	0.00	0.00	0.00
LMO	18	4	0.00	0.00	0.00	0.00	0.00	0.00	0.00	0.00	0.00	0.00	0.00
GC	19	4	0.00	0.00	0.00	0.00	0.00	0.00	0.00	0.00	0.00	0.00	0.00
NEO	20	5	0.00	0.00	0.00	0.00	0.00	0.00	0.00	0.00	0.00	0.00	0.00

Figure B-3: Input spreadsheet for nodes (cont'd). 10^{12} is used for infinity.

name	origin	destination	propellant	ID	origin ID	destination ID	origin cluster	destination cluster	TOF [days]	ΔV [km/s]	Isp [s]	IMF	aeroshell/TPS
KSC - LEO	KSC	LEO	LOX/LH2	1001	1	5	1	3	1	0.00	450	0.1	0%
KSC - LEO	KSC2	LEO	LOX/LH2	1002	2	5	2	3	1	0.00	450	0.1	0%
LMO - GC	LMO	GC	LOX/LCH4	1003	18	19	4	4	1	0.61	369	0.1	40%
GC - LMO	GC	LMO	LOX/LCH4	1004	19	18	4	4	1	4.10	369	0.1	0%
LEO - GTO	LEO	GTO	LOX/LH2	1005	5	6	3	3	1	2.50	450	0.1	0%
LEO - GEO	LEO	GEO	LOX/LH2	1006	5	7	3	3	1	4.33	450	0.1	0%
LEO - LTO	LEO	LTO	LOX/LH2	1007	5	8	3	3	1	3.18	450	0.1	0%
LEO - LLO	LEO	LLO	LOX/LH2	1008	5	10	3	3	4	4.04	450	0.1	0%
LEO - EML1	LEO	EML1	LOX/LH2	1009	5	11	3	3	3	3.77	450	0.1	0%
LEO - EML2	LEO	EML2	LOX/LH2	1010	5	12	3	3	4	3.43	450	0.1	0%
LEO - EML4/5	LEO	EML4/5	LOX/LH2	1011	5	13	3	3	4	3.97	450	0.1	0%
GTO - LEO	GTO	LEO	LOX/LH2	1012	6	5	3	3	1	2.50	450	0.1	0%
GTO - GEO	GTO	GEO	LOX/LH2	1013	6	7	3	3	1	1.83	450	0.1	0%
GTO - LTO	GTO	LTO	LOX/LH2	1014	6	8	3	3	1	0.68	450	0.1	0%
GTO - LLO	GTO	LLO	LOX/LH2	1015	6	10	3	3	4	1.54	450	0.1	0%
GTO - EML1	GTO	EML1	LOX/LH2	1016	6	11	3	3	3	1.27	450	0.1	0%
GTO - EML2	GTO	EML2	LOX/LH2	1017	6	12	3	3	4	0.93	450	0.1	0%
GTO - EML4/5	GTO	EML4/5	LOX/LH2	1018	6	13	3	3	4	1.47	450	0.1	0%
GEO - LEO	GEO	LEO	LOX/LH2	1019	7	5	3	3	1	4.33	450	0.1	0%
GEO - GTO	GEO	GTO	LOX/LH2	1020	7	6	3	3	1	1.83	450	0.1	0%
GEO - LTO	GEO	LTO	LOX/LH2	1021	7	8	3	3	1	2.51	450	0.1	0%
GEO - LLO	GEO	LLO	LOX/LH2	1022	7	10	3	3	4	2.05	450	0.1	0%
GEO - EML1	GEO	EML1	LOX/LH2	1023	7	11	3	3	3	1.38	450	0.1	0%
GEO - EML2	GEO	EML2	LOX/LH2	1024	7	12	3	3	4	1.47	450	0.1	0%
GEO - EML4/5	GEO	EML4/5	LOX/LH2	1025	7	13	3	3	4	1.71	450	0.1	0%
LTO - LEO	LTO	LEO	LOX/LH2	1026	8	5	3	3	1	3.18	450	0.1	0%
LTO - GTO	LTO	GTO	LOX/LH2	1027	8	6	3	3	1	0.68	450	0.1	0%
LTO - GEO	LTO	GEO	LOX/LH2	1028	8	7	3	3	1	2.51	450	0.1	0%
LTO - LLO	LTO	LLO	LOX/LH2	1029	8	10	3	3	3	0.86	450	0.1	0%
LTO - EML1	LTO	EML1	LOX/LH2	1030	8	11	3	3	2	0.58	450	0.1	0%
LTO - EML2	LTO	EML2	LOX/LH2	1031	8	12	3	3	3	0.35	450	0.1	0%
LTO - EML4/5	LTO	EML4/5	LOX/LH2	1032	8	13	3	3	3	0.69	450	0.1	0%
LTO - DTO	LTO	DTO	LOX/LH2	1033	8	14	3	4	200	1.69	450	0.15	0%
LTO - NEO	LTO	NEO	LOX/LH2	1034	8	20	3	5	111	2.40	450	0.15	0%
LSP - LLO	LSP	LLO	LOX/LH2	1035	9	10	3	3	1	1.87	450	0.1	0%
LLO - LEO	LLO	LEO	LOX/LH2	1036	10	5	3	3	4	4.04	450	0.1	0%
LLO - GTO	LLO	GTO	LOX/LH2	1037	10	6	3	3	4	1.54	450	0.1	0%
LLO - GEO	LLO	GEO	LOX/LH2	1038	10	7	3	3	4	2.05	450	0.1	0%
LLO - LTO	LLO	LTO	LOX/LH2	1039	10	8	3	3	3	0.86	450	0.1	0%
LLO - LSP	LLO	LSP	LOX/LH2	1040	10	9	3	3	1	1.87	450	0.1	0%
LLO - EML1	LLO	EML1	LOX/LH2	1041	10	11	3	3	1	0.64	450	0.1	0%
LLO - EML2	LLO	EML2	LOX/LH2	1042	10	12	3	3	1	0.65	450	0.1	0%
LLO - EML4/5	LLO	EML4/5	LOX/LH2	1043	10	13	3	3	4	0.98	450	0.1	0%
EML1 - LEO	EML1	LEO	LOX/LH2	1044	11	5	3	3	3	3.77	450	0.1	0%
EML1 - GTO	EML1	GTO	LOX/LH2	1045	11	6	3	3	3	1.27	450	0.1	0%
EML1 - GEO	EML1	GEO	LOX/LH2	1046	11	7	3	3	3	1.38	450	0.1	0%
EML1 - LTO	EML1	LTO	LOX/LH2	1047	11	8	3	3	2	0.58	450	0.1	0%
EML1 - LLO	EML1	LLO	LOX/LH2	1048	11	10	3	3	1	0.64	450	0.1	0%
EML1 - EML2	EML1	EML2	LOX/LH2	1049	11	12	3	3	1	0.14	450	0.1	0%
EML1 - EML4/5	EML1	EML4/5	LOX/LH2	1050	11	13	3	3	4	0.33	450	0.1	0%
EML2 - LEO	EML2	LEO	LOX/LH2	1051	12	5	3	3	4	3.43	450	0.1	0%
EML2 - GTO	EML2	GTO	LOX/LH2	1052	12	6	3	3	4	0.93	450	0.1	0%
EML2 - GEO	EML2	GEO	LOX/LH2	1053	12	7	3	3	4	1.47	450	0.1	0%
EML2 - LTO	EML2	LTO	LOX/LH2	1054	12	8	3	3	3	0.35	450	0.1	0%
EML2 - LLO	EML2	LLO	LOX/LH2	1055	12	10	3	3	1	0.64	450	0.1	0%
EML2 - EML1	EML2	EML1	LOX/LH2	1056	12	11	3	3	1	0.14	450	0.1	0%
EML2 - EML4/5	EML2	EML4/5	LOX/LH2	1057	12	13	3	3	4	0.34	450	0.1	0%
EML4/5 - LEO	EML4/5	LEO	LOX/LH2	1058	13	5	3	3	4	3.97	450	0.1	0%
EML4/5 - GTO	EML4/5	GTO	LOX/LH2	1059	13	6	3	3	4	1.47	450	0.1	0%
EML4/5 - GEO	EML4/5	GEO	LOX/LH2	1060	13	7	3	3	4	1.71	450	0.1	0%
EML4/5 - LTO	EML4/5	LTO	LOX/LH2	1061	13	8	3	3	3	0.69	450	0.1	0%
EML4/5 - LLO	EML4/5	LLO	LOX/LH2	1062	13	10	3	3	4	0.98	450	0.1	0%

Figure B-4: Input spreadsheet for transportation arcs. "TOF" stands for the time of flight and "IMF" stands for the inert mass ratio.

name	origin	destination	propellant	ID	origin ID	destination ID	origin cluster	destination cluster	TOF [days]	ΔV [km/s]	Isp [s]	IMF	aeroshell/TPS
EML4/5 - EML1	EML4/5	EML1	LOX/LH2	1063	13	11	3	3	4	0.33	450	0.1	0%
EML4/5 - EML2	EML4/5	EML2	LOX/LH2	1064	13	12	3	3	4	0.34	450	0.1	0%
DTO - LTO	DTO	LTO	LOX/LH2	1065	14	8	4	3	200	1.69	450	0.15	0%
DTO - LDO	DTO	LDO	LOX/LH2	1066	14	15	4	4	1	0.66	450	0.1	0%
DTO - PTO	DTO	PTO	LOX/LH2	1067	14	16	4	4	1	0.40	450	0.1	0%
DTO - LMO	DTO	LMO	LOX/LH2	1068	14	18	4	4	2	1.10	450	0.1	0%
LDO - DTO	LDO	DTO	LOX/LH2	1069	15	14	4	4	1	0.66	450	0.1	0%
PTO - DTO	PTO	DTO	LOX/LH2	1070	16	14	4	4	1	0.40	450	0.1	0%
PTO - LPO	PTO	LPO	LOX/LH2	1071	16	17	4	4	1	0.55	450	0.1	0%
PTO - LMO	PTO	LMO	LOX/LH2	1072	16	18	4	4	1	0.70	450	0.1	0%
LPO - PTO	LPO	PTO	LOX/LH2	1073	17	16	4	4	1	0.55	450	0.1	0%
LMO - DTO	LMO	DTO	LOX/LH2	1074	18	14	4	4	2	1.10	450	0.1	0%
LMO - PTO	LMO	PTO	LOX/LH2	1075	18	16	4	4	1	0.70	450	0.1	0%
GC - LMO	GC	LMO	LOX/LH2	1076	19	18	4	4	1	4.10	450	0.1	0%
LEO - PAC	LEO	PAC	LOX/LH2	1077	5	3	3	6	1	0.01	450	0.1	40%
GTO - LEO	GTO	LEO	LOX/LH2	1078	6	5	3	3	1	0.23	450	0.1	40%
GEO - LEO	GEO	LEO	LOX/LH2	1079	7	5	3	3	1	2.06	450	0.1	40%
LLO - LEO	LLO	LEO	LOX/LH2	1080	10	5	3	3	4	1.31	450	0.1	40%
EML1 - LEO	EML1	LEO	LOX/LH2	1081	11	5	3	3	3	0.77	450	0.1	40%
EML2 - LEO	EML2	LEO	LOX/LH2	1082	12	5	3	3	4	0.33	450	0.1	40%
EML4/5 - LEO	EML4/5	LEO	LOX/LH2	1083	13	5	3	3	4	0.84	450	0.1	40%
LTO - LEO	LTO	LEO	LOX/LH2	1084	8	5	3	3	1	0.45	450	0.1	40%
DTO - PAC	DTO	PAC	LOX/LH2	1085	14	3	4	6	202	1.01	450	0.15	40%
DTO - LTO	DTO	LTO	LOX/LH2	1086	14	8	4	3	200	1.01	450	0.15	40%
LMO - GC	LMO	GC	LOX/LH2	1087	18	19	4	4	1	0.61	450	0.1	40%
NEO - PAC	NEO	PAC2	LOX/LH2	1088	20	4	5	7	32	1.75	450	0.15	40%
NEO - LTO	NEO	LTO	LOX/LH2	1089	20	8	5	3	30	1.75	450	0.15	40%
LEO - PAC	LEO	PAC2	LOX/LH2	1090	5	4	3	7	1	0.01	450	0.1	40%
LTO - DTO	LTO	DTO	LOX/LH2	1091	8	14	3	4	200	0.69	450	0.15	40%
DTO - PTO	DTO	PTO	LOX/LH2	1092	14	16	4	4	1	0.01	450	0.1	40%
DTO - LMO	DTO	LMO	LOX/LH2	1093	14	18	4	4	2	0.01	450	0.1	40%
PTO - LMO	PTO	LMO	LOX/LH2	1094	16	18	4	4	1	0.01	450	0.1	40%
LEO - GTO	LEO	GTO	NTR	1095	5	6	3	3	1	2.50	900	0.3	0%
LEO - GEO	LEO	GEO	NTR	1096	5	7	3	3	1	4.33	900	0.3	0%
LEO - LTO	LEO	LTO	NTR	1097	5	8	3	3	1	3.18	900	0.3	0%
LEO - LLO	LEO	LLO	NTR	1098	5	10	3	3	4	4.04	900	0.3	0%
LEO - EML1	LEO	EML1	NTR	1099	5	11	3	3	3	3.77	900	0.3	0%
LEO - EML2	LEO	EML2	NTR	1100	5	12	3	3	4	3.43	900	0.3	0%
LEO - EML4/5	LEO	EML4/5	NTR	1101	5	13	3	3	4	3.97	900	0.3	0%
GTO - LEO	GTO	LEO	NTR	1102	6	5	3	3	1	2.50	900	0.3	0%
GTO - GEO	GTO	GEO	NTR	1103	6	7	3	3	1	1.83	900	0.3	0%
GTO - LTO	GTO	LTO	NTR	1104	6	8	3	3	1	0.68	900	0.3	0%
GTO - LLO	GTO	LLO	NTR	1105	6	10	3	3	4	1.54	900	0.3	0%
GTO - EML1	GTO	EML1	NTR	1106	6	11	3	3	3	1.27	900	0.3	0%
GTO - EML2	GTO	EML2	NTR	1107	6	12	3	3	4	0.93	900	0.3	0%
GTO - EML4/5	GTO	EML4/5	NTR	1108	6	13	3	3	4	1.47	900	0.3	0%
GEO - LEO	GEO	LEO	NTR	1109	7	5	3	3	1	4.33	900	0.3	0%
GEO - GTO	GEO	GTO	NTR	1110	7	6	3	3	1	1.83	900	0.3	0%
GEO - LTO	GEO	LTO	NTR	1111	7	8	3	3	1	2.51	900	0.3	0%
GEO - LLO	GEO	LLO	NTR	1112	7	10	3	3	4	2.05	900	0.3	0%
GEO - EML1	GEO	EML1	NTR	1113	7	11	3	3	3	1.38	900	0.3	0%
GEO - EML2	GEO	EML2	NTR	1114	7	12	3	3	4	1.47	900	0.3	0%
GEO - EML4/5	GEO	EML4/5	NTR	1115	7	13	3	3	4	1.71	900	0.3	0%
LTO - LEO	LTO	LEO	NTR	1116	8	5	3	3	1	3.18	900	0.3	0%
LTO - GTO	LTO	GTO	NTR	1117	8	6	3	3	1	0.68	900	0.3	0%
LTO - GEO	LTO	GEO	NTR	1118	8	7	3	3	1	2.51	900	0.3	0%
LTO - LLO	LTO	LLO	NTR	1119	8	10	3	3	3	0.86	900	0.3	0%
LTO - EML1	LTO	EML1	NTR	1120	8	11	3	3	2	0.58	900	0.3	0%
LTO - EML2	LTO	EML2	NTR	1121	8	12	3	3	3	0.35	900	0.3	0%
LTO - EML4/5	LTO	EML4/5	NTR	1122	8	13	3	3	3	0.69	900	0.3	0%
LTO - DTO	LTO	DTO	NTR	1123	8	14	3	4	200	1.69	900	0.35	0%

Figure B-5: Input spreadsheet for transportation arcs (cont'd). "TOF" stands for the time of flight and "IMF" stands for the inert mass ratio.

name	origin	destination	propellant	ID	origin ID	destination ID	origin cluster	destination cluster	TOF [days]	ΔV [km/s]	Isp [s]	IMF	aeroshell/TPS
LTO - NEO	LTO	NEO	NTR	1124	8	20	3	5	111	2.40	900	0.35	0%
LSP - LLO	LSP	LLO	NTR	1125	9	10	3	3	1	1.87	900	0.3	0%
LLO - LEO	LLO	LEO	NTR	1126	10	5	3	3	4	4.04	900	0.3	0%
LLO - GTO	LLO	GTO	NTR	1127	10	6	3	3	4	1.54	900	0.3	0%
LLO - GEO	LLO	GEO	NTR	1128	10	7	3	3	4	2.05	900	0.3	0%
LLO - LTO	LLO	LTO	NTR	1129	10	8	3	3	3	0.86	900	0.3	0%
LLO - LSP	LLO	LSP	NTR	1130	10	9	3	3	1	1.87	900	0.3	0%
LLO - EML1	LLO	EML1	NTR	1131	10	11	3	3	1	0.64	900	0.3	0%
LLO - EML2	LLO	EML2	NTR	1132	10	12	3	3	1	0.65	900	0.3	0%
LLO - EML4/5	LLO	EML4/5	NTR	1133	10	13	3	3	4	0.98	900	0.3	0%
EML1 - LEO	EML1	LEO	NTR	1134	11	5	3	3	3	3.77	900	0.3	0%
EML1 - GTO	EML1	GTO	NTR	1135	11	6	3	3	3	1.27	900	0.3	0%
EML1 - GEO	EML1	GEO	NTR	1136	11	7	3	3	3	1.38	900	0.3	0%
EML1 - LTO	EML1	LTO	NTR	1137	11	8	3	3	2	0.58	900	0.3	0%
EML1 - LLO	EML1	LLO	NTR	1138	11	10	3	3	1	0.64	900	0.3	0%
EML1 - EML2	EML1	EML2	NTR	1139	11	12	3	3	1	0.14	900	0.3	0%
EML1 - EML4/5	EML1	EML4/5	NTR	1140	11	13	3	3	4	0.33	900	0.3	0%
EML2 - LEO	EML2	LEO	NTR	1141	12	5	3	3	4	3.43	900	0.3	0%
EML2 - GTO	EML2	GTO	NTR	1142	12	6	3	3	4	0.93	900	0.3	0%
EML2 - GEO	EML2	GEO	NTR	1143	12	7	3	3	4	1.47	900	0.3	0%
EML2 - LTO	EML2	LTO	NTR	1144	12	8	3	3	3	0.35	900	0.3	0%
EML2 - LLO	EML2	LLO	NTR	1145	12	10	3	3	1	0.64	900	0.3	0%
EML2 - EML1	EML2	EML1	NTR	1146	12	11	3	3	1	0.14	900	0.3	0%
EML2 - EML4/5	EML2	EML4/5	NTR	1147	12	13	3	3	4	0.34	900	0.3	0%
EML4/5 - LEO	EML4/5	LEO	NTR	1148	13	5	3	3	4	3.97	900	0.3	0%
EML4/5 - GTO	EML4/5	GTO	NTR	1149	13	6	3	3	4	1.47	900	0.3	0%
EML4/5 - GEO	EML4/5	GEO	NTR	1150	13	7	3	3	4	1.71	900	0.3	0%
EML4/5 - LTO	EML4/5	LTO	NTR	1151	13	8	3	3	3	0.69	900	0.3	0%
EML4/5 - LLO	EML4/5	LLO	NTR	1152	13	10	3	3	4	0.98	900	0.3	0%
EML4/5 - EML1	EML4/5	EML1	NTR	1153	13	11	3	3	4	0.33	900	0.3	0%
EML4/5 - EML2	EML4/5	EML2	NTR	1154	13	12	3	3	4	0.34	900	0.3	0%
DTO - LTO	DTO	LTO	NTR	1155	14	8	4	3	200	1.69	900	0.35	0%
DTO - LDO	DTO	LDO	NTR	1156	14	15	4	4	1	0.66	900	0.3	0%
DTO - PTO	DTO	PTO	NTR	1157	14	16	4	4	1	0.40	900	0.3	0%
DTO - LMO	DTO	LMO	NTR	1158	14	18	4	4	2	1.10	900	0.3	0%
LDO - DTO	LDO	DTO	NTR	1159	15	14	4	4	1	0.66	900	0.3	0%
PTO - DTO	PTO	DTO	NTR	1160	16	14	4	4	1	0.40	900	0.3	0%
PTO - LPO	PTO	LPO	NTR	1161	16	17	4	4	1	0.55	900	0.3	0%
PTO - LMO	PTO	LMO	NTR	1162	16	18	4	4	1	0.70	900	0.3	0%
LPO - PTO	LPO	PTO	NTR	1163	17	16	4	4	1	0.55	900	0.3	0%
LMO - DTO	LMO	DTO	NTR	1164	18	14	4	4	2	1.10	900	0.3	0%
LMO - PTO	LMO	PTO	NTR	1165	18	16	4	4	1	0.70	900	0.3	0%
GC - LMO	GC	LMO	NTR	1166	19	18	4	4	1	4.10	900	0.3	0%
LEO - PAC	LEO	PAC	NTR	1167	5	3	3	6	1	0.01	900	0.3	40%
GTO - LEO	GTO	LEO	NTR	1168	6	5	3	3	1	0.23	900	0.3	40%
GEO - LEO	GEO	LEO	NTR	1169	7	5	3	3	1	2.06	900	0.3	40%
LLO - LEO	LLO	LEO	NTR	1170	10	5	3	3	4	1.31	900	0.3	40%
EML1 - LEO	EML1	LEO	NTR	1171	11	5	3	3	3	0.77	900	0.3	40%
EML2 - LEO	EML2	LEO	NTR	1172	12	5	3	3	4	0.33	900	0.3	40%
EML4/5 - LEO	EML4/5	LEO	NTR	1173	13	5	3	3	4	0.84	900	0.3	40%
LTO - LEO	LTO	LEO	NTR	1174	8	5	3	3	1	0.45	900	0.3	40%
DTO - PAC	DTO	PAC	NTR	1175	14	3	4	6	202	1.01	900	0.35	40%
DTO - LTO	DTO	LTO	NTR	1176	14	8	4	3	200	1.01	900	0.35	40%
LMO - GC	LMO	GC	NTR	1177	18	19	4	4	1	0.61	900	0.3	40%
NEO - PAC	NEO	PAC2	NTR	1178	20	4	5	7	32	1.75	900	0.35	40%
NEO - LTO	NEO	LTO	NTR	1179	20	8	5	3	30	1.75	900	0.35	40%
LEO - PAC	LEO	PAC2	NTR	1180	5	4	3	7	1	0.01	450	0.3	40%
LTO - DTO	LTO	DTO	NTR	1181	8	14	3	4	200	0.69	900	0.35	40%
DTO - PTO	DTO	PTO	NTR	1182	14	16	4	4	1	0.01	900	0.3	40%
DTO - LMO	DTO	LMO	NTR	1183	14	18	4	4	2	0.01	900	0.3	40%
PTO - LMO	PTO	LMO	NTR	1184	16	18	4	4	1	0.01	900	0.3	40%

Figure B-6: Input spreadsheet for transportation arcs (cont'd). "TOF" stands for the time of flight and "IMF" stands for the inert mass ratio.

name	body	type	ID	origin ID	destination ID	origin cluster	destination cluster
LEO	Earth	depot	1	5	5	3	3
LEO	Earth	tempStay	2	5	5	3	3
GTO	Earth	tempStay	4	6	6	3	3
GEO	Earth	depot	5	7	7	3	3
GEO	Earth	tempStay	6	7	7	3	3
LTO	Earth	tempStay	7	8	8	3	3
LLO	Moon	depot	8	10	10	3	3
LLO	Moon	tempStay	9	10	10	3	3
EML1	Earth/Moon	depot	10	11	11	3	3
EML1	Earth/Moon	tempStay	11	11	11	3	3
EML2	Earth/Moon	depot	12	12	12	3	3
EML2	Earth/Moon	tempStay	13	12	12	3	3
EML4/5	Earth/Moon	depot	14	13	13	3	3
EML4/5	Earth/Moon	tempStay	15	13	13	3	3
LDO	Deimos	depot	16	15	15	4	4
LDO	Deimos	tempStay	17	15	15	4	4
DTO	Deimos	tempStay	18	14	14	4	4
LPO	Phobos	depot	19	17	17	4	4
LPO	Phobos	tempStay	20	17	17	4	4
PTO	Phobos	tempStay	21	16	16	4	4
LMO	Mars	depot	22	18	18	4	4
LMO	Mars	tempStay	23	18	18	4	4
LSP	Moon	depot	24	9	9	3	3
LSP	Moon	ISRUO2	25	9	9	3	3
LSP	Moon	ISRUH2O	26	9	9	3	3
LSP	Moon	ISRUelec	27	9	9	3	3
GC	Mars	stay	28	19	19	4	4
GC	Mars	stayISRUO2	29	19	19	4	4
GC	Mars	stayISRUH2O	30	19	19	4	4
GC	Mars	stayISRUelec	31	19	19	4	4
GC	Mars	stayISRUmethane	32	19	19	4	4
NEO	NEO	stay	33	20	20	5	5
PAC	Earth	wait	34	3	3	6	6
PAC2	Earth	wait	35	4	4	7	7

Figure B-7: Input spreadsheet for holdover arcs.

Bibliography

[1] M. McKay, D. McKay, and M. Duke. Space Resources. NASA SP-509, 1992.

[2] A. Chepko, O. de Weck, W. Crossley, E. Santiago-Maldonado, and D. Linne. A Modeling Framework for Applying Discrete Optimization to System Architecture Selection and Application to In-Situ Resource Utilization. 12th AIAA/ISSMO Multidisciplinary Analysis and Optimization Conference, Victoria, Canada, 2008.

[3] P. Grogan. A Flexible, Modular Approach to Integrated Space Exploration Campaign Logistics Modeling, Simulation, and Analysis. Master's Thesis, Massachusetts Institute of Technology, Cambridge, MA, 2010.

[4] Massachusetts Institute of Technology. MIT Space Logistics Project URL: http://spacelogistics.mit.edu [cited May 25, 2013].

[5] T. Ishimatsu. *Generalized Multi-Commodity Network Flows: Case Studies in Space Logistics and Complex Infrastructure Systems.* PhD Thesis, Massachusetts Institute of Technology, Cambridge, MA, 2013.

[6] P. Abell, D. Korsmeyer, R. Landis, T. Jones, D. Adam, D. Morrison, L. Lemke, A. Gonzales, R. Gershman, T. Sweeter, L. Johnson, and E. Lu. Scientific exploration of near-Earth objects via the Orion Crew Exploration Vehicle. *Meteoritics and Planetary Science*, 44(12):1825–1836, 2009.

[7] Review of U.S. Human Spaceflight Plans Committee. Seeking a Human Spaceflight Program Worthy of a Great Nation. 2009.

[8] E. Capparelli, L. Delgado-Lopez, N. Bosanac, A. Burg, K. Ho, J. Kluger, S. Langston, V. Lo Gatto, O. Mansurov, P. Nizenkov, A. Vrolijk, L. Zea, and J. Battat. Evaluating International Collaboration for Human Exploration beyond LEO. IAA Space Exploration Conference, Washington, D.C., 2014.

[9] Antarctic Heritage Trust. Sir Ernest Shackleton's British Antarctic (Nimrod) Expedition 1907 - 1909 URL: http://www.nzaht.org/AHT/HistoryRoyds/ [cited May 31, 2013].

[10] Eagle Engineering Inc. Conceptual Design of a Lunar Oxygen Pilot Plant: Lunar Base Systems Study. 1988.

[11] G. Sanders and M. Duke. NASA In-Situ Resource Utilization (ISRU) Capability Roadmap Executive Summary. 2005.

[12] G. Sanders, W. Larson, R. Sacjsteder, and A. Mclemore. NASA In-Situ Resource Utilization (ISRU) Project - Development and Implementation. AIAA Space 2008 Conference and Exposition, San Diego, CA, 2008.

[13] G. Sanders, K. Romig, W. Larson, R. Johnson, D. Rapp, K. Johnson, K. Sacksteder, D. Linne, P. Curreri, M. Duke, B. Blair, L. Gertsch, D. Boucher, E. Rice, L. Clark, E. McCullough, and R. Zubrin. Results from the NASA Capability Roadmap Team for In-Situ Resource Utilization (ISRU). International Lunar Conference, Toronto, Canada, 2008.

[14] J. Howell, J. Mankins, and J. Fikes. In-Space Cryogenic Propellant Depot Stepping Stone. International Astronautical Congress, Fukuoka, Japan, 2005.

[15] W. Notardonato. Active Control of Cryogenic Propellants in Space. *Cryogenics*, 52(4-6):236–242, 2012.

[16] M. Liggett. Space-Based LH2 Propellant Storage System: Subscale Ground Testing Results. *Cryogenics*, 33(4):438–442, 1993.

[17] K. Ho, K. Gerhard, A. Nicholas, A. Buck, and J. Hoffman. On-Orbit Depot Architectures Using Contingency Propellant. *Acta Astronautica*, 96:217–226, 2014.

[18] S. Gunn. Design of Second-Generation Nuclear Thermal Rocket Engines. AIAA/SAE/ASME/ASEE 26th Joint Propulsion Conference, Orlando, FL, 1990.

[19] M. Turner. *Rocket and Spacecraft Propulsion: Principles, Practice and New Developments.* Springer, 2008.

[20] B. Drake. Human Exploration of Mars Design Reference Architecture 5.0. NASA/SP 2009-566, 2009.

[21] American Institute of Aeronautics and stronautics. AIAA Space Logistics Technical Committee URL:
https://info.aiaa.org/tac/smg/sltc [cited March 6, 2013].

[22] National Aeronautics and Space Administration. International Space Station Assembly - Past Flights URL:
http://www.nasa.gov/mission_pages/station/structure/iss_assembly.html [cited May 20, 2013].

[23] National Aeronautics and Space Administration. Environmental Control and Life Support (ECLS) Integrated Roadmap Development. 2011.

[24] D. Smitherman and G. Woodcock. Space Transportation Infrastructure Supported by Propellant Depot. AIAA Space 2011 Conference and Exposition, Long Beach, CA, 2011.

[25] T. Taylor, W. Kistler, and B. Citron. On-Orbit Fuel Depot Deployment, Management and Evolution Focused on Cost Reduction. AIAA Space 2009 Conference and Exposition, Passadena, CA, 2009.

[26] G. Woodcock. Logistics Support of Lunar Base. *Acta Astronautica*, 17(7):717–738, 1988.

[27] A. Charania and D. DePasquale. Economic Analysis of a Lunar In-Situ Resource Utilization (ISRU) Propellant Services Market. International Astronautical Congress, Hyderabad, India, 2007.

[28] F. Zeagler and B. Kutter. Evolving a Depot-Based Space Transportation Architecture. AIAA Space 2010 Conference and Exposition, Anahelm, CA, 2010.

[29] F. Chandler, D. Bienhoff, J. Cronick, and G. Grayson. Propellant Depots for Earth Orbit and Lunar Exploration. AIAA Space 2007 Conference and Exposition, Long Beach, CA, 2007.

[30] M. Baine, G. Grush, and E. Hurlbert. An Open Exploration Architecture Using an L-1 Space Propellant Depot. SpaceOps 2010 Conference, Huntsville, AL, 2010.

[31] S. Schreiner, L. Sibille, J. Dominguez, J. Hoffman, G. Sanders, and A. Sirk. Development of a Molten Regolith Electrolysis Reactor Model for Lunar In-Situ Resource Utilization. 8th Symposium on Space Resource Utilization, Kissimmee, FL, 2015.

[32] M. Hecht. MOXIE and Mars 2020 (How to Produce Oxygen using Local Mars Resources. Presentation, The Massachusetts Space Grant Consortium.

[33] A. Muscatello, R. Mueller, G. Sanders, and W. Larson. Phobos and Deimos Sample Collection and Prospecting Missions for Science and ISRU. Concepts and Approaches for Mars Exploration, Houston, TX, 2012.

[34] E. Cardiff. Volatile Extraction and In Situ Resource Utilization for the Moon Applied to Near Earth Objects. Presentation at Lunar Exploration Analysis Group, 2012.

[35] O. de Weck and D. Simchi-Levi. Haughton-Mars Project Expedition 2005. Final Report, NASA/TP 2006-214196, 2006.

[36] S. Shull, E. Gralla, O. de Weck, a. Siddiqi, and R. Shishko. The Future of Asset Management for Human Space Exploration: Supply Classification and an Interplanetary Supply Chain Management Database. AIAA Space 2006 Conference and Exposition, San Jose, CA, 2006.

[37] C. Taylor, M. Song, D. Klabjan, O. de Weck, and D. Simchi-Levi. Modeling Interplanetary Logistics: A Mathematical Model for Mission Planning. SpaceOps 2006 Conference, Rome, Italy, 2006.

[38] C. Taylor, M. Song, D. Klabjan, O. de Weck, and D. Simchi-Levi. A Mathematical Model for Interplanetary Logistics. SOLE 2006, Dallas, TX, 2006.

[39] E. Gralla, S. Shull, O. de Weck, G. Lee, and R. Shishko. A Modeling Framework for Interplanetary Supply Chains. AIAA Space 2006 Conference and Exposition, San Jose, CA, 2006.

[40] E. Gralla, S. Shull, O. de Weck, G. Lee, and R. Shishko. A Modeling Framework for Interplanetary Supply Chains. AIAA Space 2006 Conference and Exposition, San Jose, CA, 2006.

[41] O. de Weck, D. Simchi-Levi, R. Shishko, J. Ahn, E. Gralla, D. Klabjan, J. Mellein, S. Shull, A. Siddiqi, B. Bairstow, and G. Lee. SpaceNet v1.3 User's Guide. NASA/TP 2007-214725, 2007.

[42] O. de Weck, E. Jordan, G. Lee, P. Grogan, T. Ishimatsu, and A. Siddiqi. SpaceNet 2.5 User's Guide. 2009.

[43] O. de Weck, E. Jordan, G. Lee, P. Grogan, T. Ishimatsu, and A. Siddiqi. SpaceNet 2.5 Quick Start Tutorial. 2009.

[44] Massachusetts Institute of Technology Strategic Engineering Research Group. SpaceNet URL:
http://spacenet.mit.edu [cited March 6, 2013].

[45] O. de Weck, N. Armar, P. Grogan, A. Siddiqi, G. Lee, E. Jordan, and R. Shishko. A Flexible Architecture and Object-oriented Model for Space Logistics Simulation. AIAA Space 2009 Conference and Exposition, Pasadena, CA, 2009.

[46] P. Grogan, H. Yue, and O. de Weck. Space Logistics Modeling and Simulation Analysis using SpaceNet: Four Application Cases. AIAA Space 2011 Conference and Exposition, Long Beach, CA, 2011.

[47] H. Yue. Propulsive and Logistical Feasibility of Alternative Future Human-Robotic Mars Exploration Architectures. Master's Thesis, Massachusetts Institute of Technology, Cambridge, MA, 2011.

[48] P. Grogan, C. Lee, and O. de Weck. Comparative Usability Study of Two Space Logistics Analysis Tools. AIAA Space 2011 Conference and Exposition, Long Beach, CA, 2011.

[49] C. Taylor. *Integrated Transportation System Design Optimization*. PhD Thesis, Massachusetts Institute of Technology, Cambridge, MA, 2007.

[50] K. Ho, J. Green, and O. de Weck. Integrated Framework for the Design of Crewed Space Habitats and their Supporting Logistics System. AIAA Space 2012 Conference and Exposition, Pasadena, CA, 2012.

[51] K. Ho, J. Green, and O. de Weck. Improved Concurrent Optimization Formulation of Crewed Space Habitats and Their Supporting Logistics Systems. AIAA Space 2013 Conference and Exposition, San Diego, CA, 2013.

[52] K. Ho, J. Green, and O. de Weck. Concurrent Design of Scientific Crewed Space Habitats and Their Supporting Logistics System. *Journal of Spacecraft and Rockets*, 51(1):76–85, 2013.

[53] D. Arney and A. Wilhite. Modeling Space System Architectures with Graph Theory. *Journal of Spacecraft and Rockets*, 51(5):1413–1429, 2014.

[54] R. Ahuja, T. Magnanti, and J. Orlin. *Network Flows – Theory, Algrithims, and Applications*. Prentice Hall, 1993.

[55] D. Phillips and A. Garcia-Diaz. *Fundamentals of Network Analysis*. Prentice Hall, 1981.

[56] G. Bhaumik. *Optimum Operating Policies of a Water Distribution System with Losses*. PhD Thesis, The University of Texas at Austin, Austin, TX, 1973.

[57] R. Crum. Cash Management in the Multinational Firm: A Constrained Generalized Network Approach. 1977.

[58] Y. Kim. An Optimal Computational Approach to the Analysis of a Generalized Network of Copper Refining Process. Joint ORSA/TIMS/AIIE Conference, Atlantic City, NJ, 1973.

[59] A. Geoffrion and G. Graves. Multicommodity Distribution System Design by Bender's Decomposition. *Management Science*, 20:822–844, 1974.

[60] B. Vaidyanathan, K. Jha, and R. Ahuja. Multicommodity Network Flow Approach to the Railroad Crew-Scheduling Problem. *IBM Journal of Research and Development*, 51(3-4):325–344, 2007.

[61] A. Assad. Multicommodity Network Flows - A Survey. *Network*, 8:37–91, 1978.

[62] L. Ford and D. Fulkerson. Constructing Maximal Dynamic Flows from Static Flows. *Operations Research*, 6:419–433, 1958.

[63] S. Lovetskii and I. Melamed. Dynamic Flows in Networks. *Automation and Remote Control*, 48(11):1417–1434, 1987.

[64] J. Aronson. A Survey of Dynamic Network Flows. *Annals of Operations Research*, 20:1–66, 1989.

[65] J. Bookbinder and S. Sethi. The Dynamic Transportation Problem: A Survey. *Naval Research Logistics Quarterly*, 27(1):65–87, 1980.

[66] E. Kohler, K. Langkau, and M. Skutella. Time-Expanded Graphs for Flow-Dependent Transit Times. 10th Annual European Symposium, Rome, Italy, 2002.

[67] M. Silver and O. de Weck. Time-Expanded Decision Network: A Framework for Design Evolvable Complex Systems. *Systems Engineering*, 10(2):167–188, 2007.

[68] A. Hall, S. Hippler, and M. Skutella. Multicommodity Flows over Time: Efficient Algorithms and Complexity. *Theoretical Computer Science*, 379:387–404, 2007.

[69] L. Fleischer and M. Skutella. The Quickest Multicommodity Flow Problem. 9th International IPCO Conference, Cambridge, MA, 2002.

[70] M. Gross and M. Skutella. Generalized Maximum Flows over Time. 9th International Workshop, WAOA 2011, Cambridge, MA, 2011.

[71] J. Erickson. Algorithms. 2011.

[72] B. Dean. Shortest Paths in FIFO Time-Dependent Networks: Theory and Algorithms. 2004.

[73] B. Kotnyek. An Annotated Overview of Dynamic Network Flows. Technical Report, Institut National de Recherche en Informatique et en Automatique, 2003.

[74] L. Fleischer and J. Sethuraman. Efficient Algorithms for Separated Continuous Linear Programs: The Multicommodity Flow Problem with Holding Costs and Extensions. *Mathematics of Operations Research*, 30(4):916–938, 2005.

[75] M. Pullan. An Algorithm for a Class of Continuous Linear Programming Problems. *SIAM Journal on Control and Optimization*, 31(6):1558–1577, 1993.

[76] M. Pullan. Forms of optimal solutions for separated continuous linear programs. *SIAM Journal on Control and Optimization*, 33(6):1952–1977, 1995.

[77] M. Pullan. A Study of General Dynamic Network Programs with Arc Time-Delays. *SIAM Journal on Control and Optimization*, 7(4):889–912, 1997.

[78] A. Philpott and M. Craddock. An Adaptive Discretization Algorithm for a Class of Continuous Network Programs. *Networks*, 26(1):1–11, 1995.

[79] S. Haschemi and E. Nasrabadi. On Solving Continuous-Time Dynamic Network Flows. *Journal of Global Optimization*, 53(3):497–524, 2012.

[80] O. de Weck, R. de Neufville, and M. Chaize. Staged Deployment of Communications Satellite Constellations in Low Earth Orbit. *Journal of Aerospace Computing, Information, and Communication*, 1:119–136, 2004.

[81] D. Miller, R. Sedwick, and K. Hartman. Evolutionary Growth of Mission Capability Using Distributed Satellite Sparse Apertures: Application to NASA's Soil Moisture MISSION (EX-4). 2001.

[82] R. Hettich and K. Kortanek. Semi-Infinite Programming: Theory, Methods, and Applications. *SIAM Review*, 35(3):380–429, 1993.

[83] F. Harary. *Graph Theory*. Westview Press, 1994.

[84] D. Rogers, R. Plante, R. Wong, and J. Evans. Aggregation and Disaggregation Techniques and Methodology in Optimization. *Operations Research*, 39(4):553–582, 1991.

[85] B. Donahue and M. Cupples. Comparative Analysis of Current NASA Human Mars Mission Architectures. *Journal of Spacecraft and Rockets*, 38(5):745–751, 2001.

[86] NASA. NASA Facts: Space Launch System.

[87] F. Landau and J. Longuski. Human Exploration of Mars via Earth-Mars Semicyclers. *Journal of Spacecraft and Rockets*, 44(1):203–210, 2007.

[88] R. Humble, G. Henry, and W. Larson. *Space Propulsion Analysis and Design*. McGraw-Hill, 1995.

[89] D. Street and A. Wilhite. A Scalable Orbital Propellant Depot Design. Masters Project Report, Space Systems Design Lab, Georgia Institute of Technology, 2006.

[90] NASA. NASA Mars Exploration URL: http://mars.nasa.gov/programmissions/science/goal4/ [cited December 25, 2014].

[91] H. Price, A. Hawkins, and T. Radcliffe. Austere Human Missions to Mars. AIAA Space 2009 Conference and Exposition, Pasadena, CA, 2009.

[92] Discovery News. Russia and Europe to Send Man to Mars? URL: http://news.discovery.com/space/russia-and-europe-to-send-man-to-mars-110818.htm [cited December 25, 2014]. 2009.

[93] S. Anthony. SpaceX says it will put humans on Mars by 2026, almost 10 years ahead of NASA URL:
http://www.extremetech.com/extreme/184640-spacex-says-it-will-put-humans-on-mars-by-2026-almost-10-years-ahead-of-nasa [cited December 25, 2014].

[94] S. Do, K. Ho, S. Schreiner, A. Owens, and O. de Weck. An Independent Assessment of the Technical Feasibility of the Mars One Mission Plan. International Astronautical Congress, Toronto, Canada, 2014.

[95] B. Drake. Human Exploration of Mars Design Reference Architecture 5.0 Addendum. NASA/SP 2009-566-ADD, 2009.

[96] B. Drake. Human Exploration of Mars Design Reference Architecture 5.0 Addendum 2. NASA/SP 2009-566-ADD2, 2014.

[97] K. Ho, O. de Weck, J. Hoffman, and R. Shishko. Dynamic modelling and optimization for space logistics using time-expanded networks. *Acta Astronautica*, 105(2):428–443, 2014.

[98] R. Landis, D. Korsmeyer, P. Abell, and D. Adamo. A Piloted Orion Flight Mission to a Near-Earth Object: A Feasibility Study. AIAA Space 2007 Conference and Exposition, Long Beach, CA, 2007.

[99] A. Fujiwara, J. Kawaguchi, D. Yeomans, M. Abe, T. Mukai, T. Okada, J. Saito, H. Yano, M. Yoshikawa, D. Scheeres, O. Barnouin-Jha, A. Cheng, H. Demura, R. Gaskell, N. Hirata, H. Ikeda, T. Kominato, H. Miyamoto, A. Nakamura, R. Nakamura, S. Sasaki, and K. Uesugi. The rubble-pile asteroid Itokawa as observed by Hayabusa. *Science*, 312:1330–1334, 2006.

[100] E. Smith. A Manned Flyby Mission to [433] Eros. Northrup Space Laboratories, Hawthorne, CA, 1966.

[101] C. Culbert. Human Space Flight Architecture Team (HAT) Overview. 2011.

[102] C. Culbert and S. Vangen. Human Space Flight Architecture Team (HAT) Technology Planning. 2012.

[103] B. Obama. Remarks by the President on Space Exploration in the 21st Century. John F. Kennedy Space Center, Merritt Island, FL, April 2010.

[104] R. Entriken. A Parallel Decomposition Algorithm for Staircase Linear Programs. Technical Report SOL 88-21, Systems Optimization Laboratory, Stanford University.

[105] J. Birge, C. Donohue, D. Holmes, and O. Svintsitski. A Parallel Implementation of the Nested Decomposition Algorithm for Multistage Stochastic Linear Programs. *Mathematical Programming*, 75:327–352, 1996.

[106] N. Armar. Cargo Revenue Management for Space Logistics. Master's Thesis, Massachusetts Institute of Technology, Cambridge, MA, 2009.

[107] Delta-V Map of the Solar System URL:
http://i.imgur.com/WGOy3qT.png [cited August 15, 2014].

[108] H. Oberth. *Ways to Spaceflight.* translated from German in NASA TT F-622, 1929.